

Overview of heteronuclear 3- and 4-D NMR

(not complete)

goal:

you should understand the basic building blocks and be able to judge whether certain experiments can be applied to your protein

practical aspects:

how do I characterize my protein?

how do I get an idea about T₂?

concepts:

INEPT transfer

how do you calculate transfer efficiencies?

constant time evolution, semi-constant time

basic pulse sequences:

backbone assignment, side chain assignment, 3-D and 4-D

NOESYs

additional embellishments:

sensitivity enhancements, deuteration, TROSY, water flip-back

Advanced Course “Multidimensional NMR in Solution”

James Cook University in Cairns, QLD, 16-20 August 2010

Stephan Grzesiek

Biozentrum, University of Basel

Klingelbergstr. 70 CH-4056 Basel, Switzerland

e-mail: stephan.grzesiek@unibas.ch

<http://www.biozentrum.unibas.ch/~grzesiek/>

Copyright: This material is available for further use, distribution and modification under the condition of acknowledgement of the original author and the indication of the distributor. No distributor is allowed to restrict its further redistribution. That is to say, proprietary modifications are not allowed.

1.	CAN MY PROTEIN BE STUDIED BY 2-4D NMR?	1
1.1	INEPT TRANSFER EFFICIENCY	2
1.2	TYPICAL T ₂ S AND J _S	3
1.3	HOW DO I GET AN IDEA ABOUT T ₂ : THE 1-1 ECHO EXPERIMENT	4
2.	BASIC PULSE SEQUENCES	7
2.1	HNCO	8
2.2	CONSTANT TIME EVOLUTION	9
2.3	ESTIMATION OF SIGNAL TO NOISE RATIO IN HNCO	10
2.4	HNCA, HCACO AS DERIVATIVES OF THE HNCO	11
2.5	FURTHER ON: HN(CA)HA, HN(CA)CO, HN(CO)CA	17
3.	THE CA RESOLUTION PROBLEM	19
3.1	CBCA(CO)NH	21
3.2	AMINO ACID TYPE DETERMINATION FROM CB-CA FREQUENCIES	23
3.3	HBHA(CO)NH: THE SEMICONSTANT TIME EVOLUTION	27
3.4	CBCANH vs. HNCACB.....	30
3.5	HN(CO)CACB, (H)CC(CO)NH TOCSY, ETC.....	33
4.	H-C CORRELATION SPECTRA	33
4.1	HCCH-COSY AND HCCH-TOCSY	33
4.2	PRACTICAL ASPECTS OF HC CORRELATION SPECTRA: ALIASING, BASE LINE, PHASING	38
5.	3D NOESYS AND TOCSY	42
6.	4D NOESYS	44
7.	IMPROVEMENTS OF BASIC SEQUENCES	51
7.1	DEUTERATION	51
7.2	SENSITIVITY ENHANCEMENT	53
7.3	TROSY.....	54
7.4	CRINEPT	57
7.5	WATER FLIP-BACK	58
8.	OTHER PRACTICAL THINGS	60
8.1	REPRODUCIBILITY OF CHEMICAL SHIFTS	60
8.2	PERPENDICULAR STRIP PLOTS	61
8.3	HOW MANY DIMENSIONS DOES ONE REALLY NEED?	62
8.4	REDUCED DIMENSIONALITY.....	63
9.	LISTS OF BASIC EXPERIMENTS FOR ASSIGNMENTS	64
10.	EXERCISES AND SOLUTIONS	66

Suggested Reading

- Cavanagh, W. J. Fairbrother, A.G. Palmer, N.J. Skelton, Protein NMR Spectroscopy, Academic Press, San Diego, 1996/2006. Good introductory book for the modern, homonuclear and heteronuclear protein NMR techniques.
- Sattler, M., Schleucher, J., Griesinger, C. Prog. NMR Spectroscopy (1999), 34, 93-158
- Bax, Grzesiek, Acc. Chem. Res. (1993), 26, 131

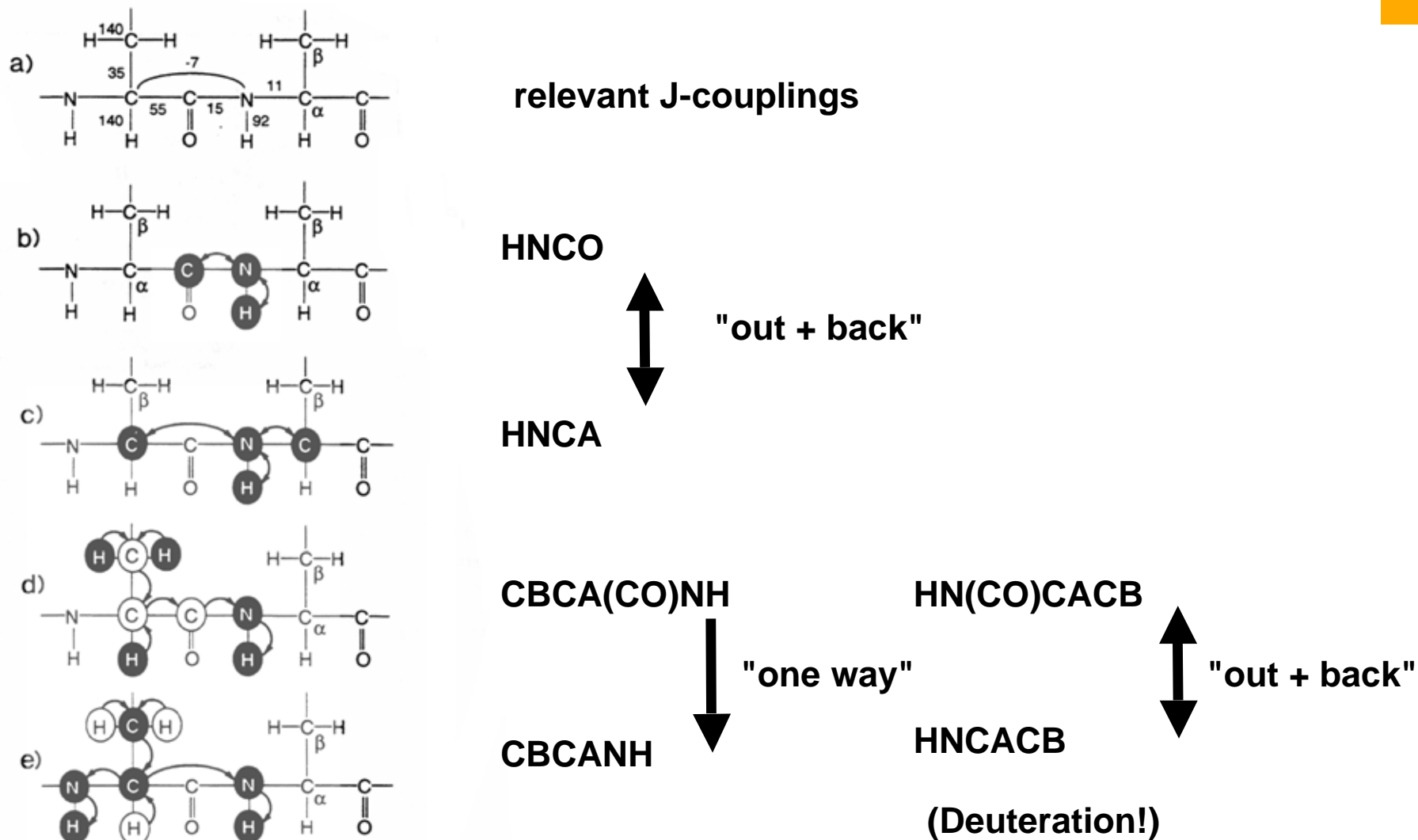
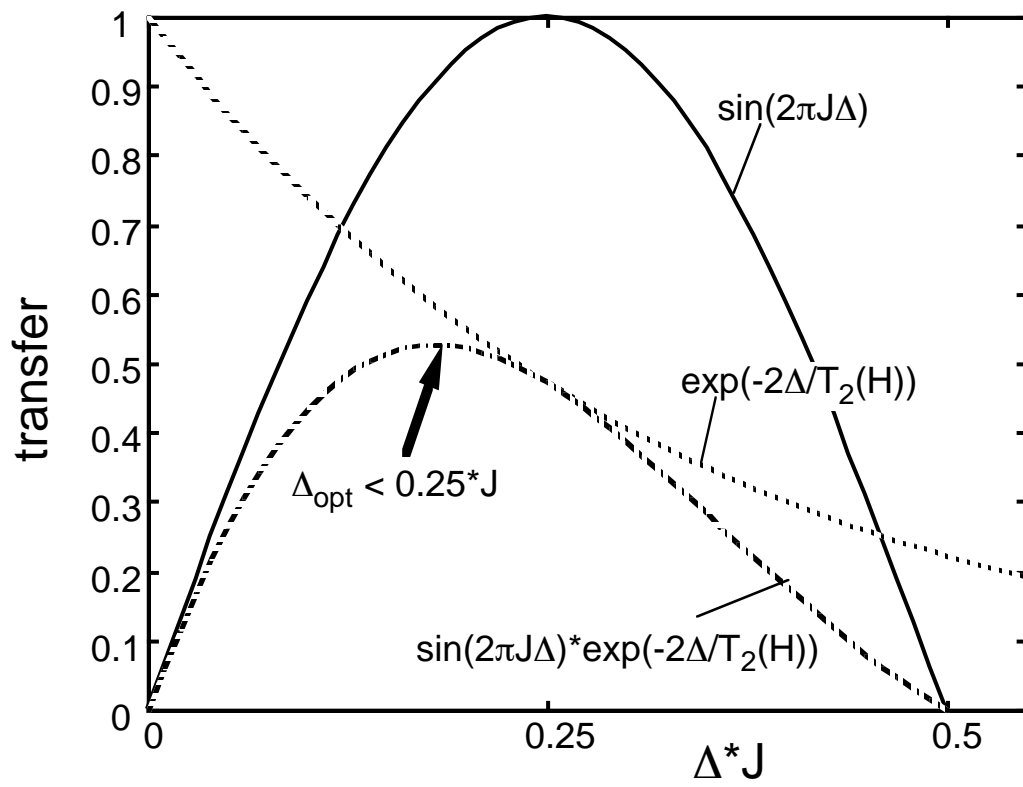
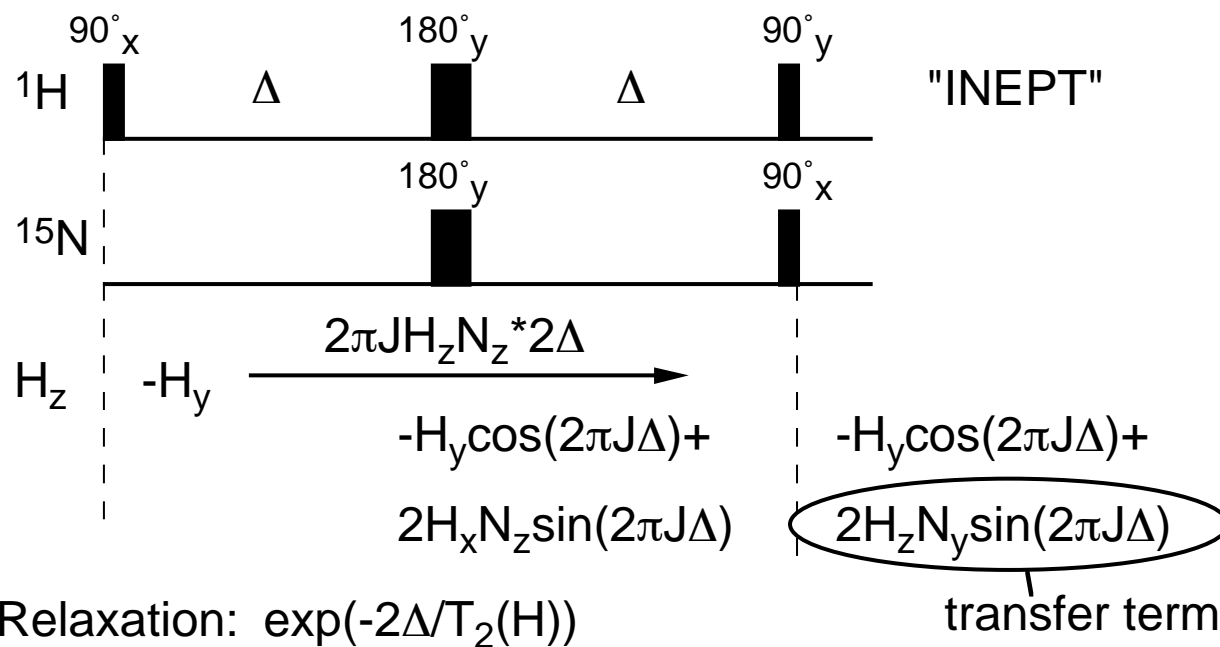


Figure 4. (a) A dipeptide segment of a protein backbone with the approximate values for the J couplings which are essential for the assignment procedure in isotopically enriched proteins. (b–e) Schematic diagrams of the nuclei that are correlated in the (b) HNCO, (c) HNCA, (d) HBHA(CBCACO)NH, and (e) CBCANH experiments. Nuclei for which the chemical shift is measured in the 3D experiment are marked by solid circles. Nuclei involved in the magnetization transfer pathway, but not observed, are marked by open circles. Magnetization transfer in these experiments is marked by curved solid lines, and the direction of the transfer is marked by arrows.

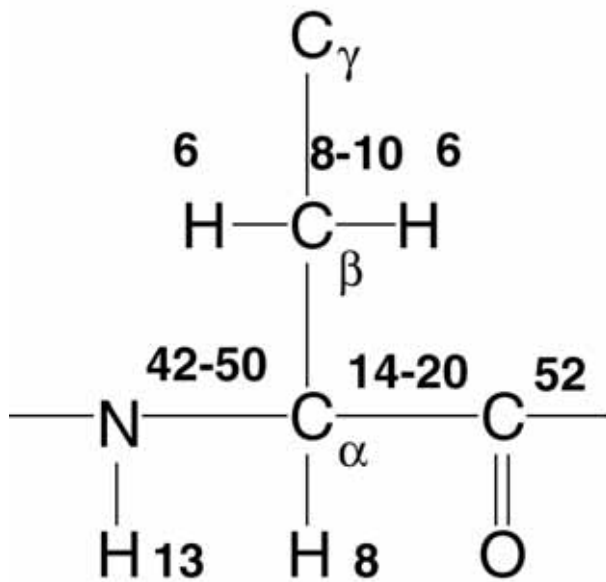
Bax, Grzesiek, *Acc. Chem. Res.* **26**, 131 (1993)

Sattler, Schleucher, Griesinger, *PROG. NMR SPECT.* **34**, 93, (1999)

Salzmann et al., *JACS*, **121**, 844, (1999)



$$\Delta_{\text{opt}} = \frac{1}{2\pi J} \text{atan } \pi J T_2$$



slow tumbling limit:

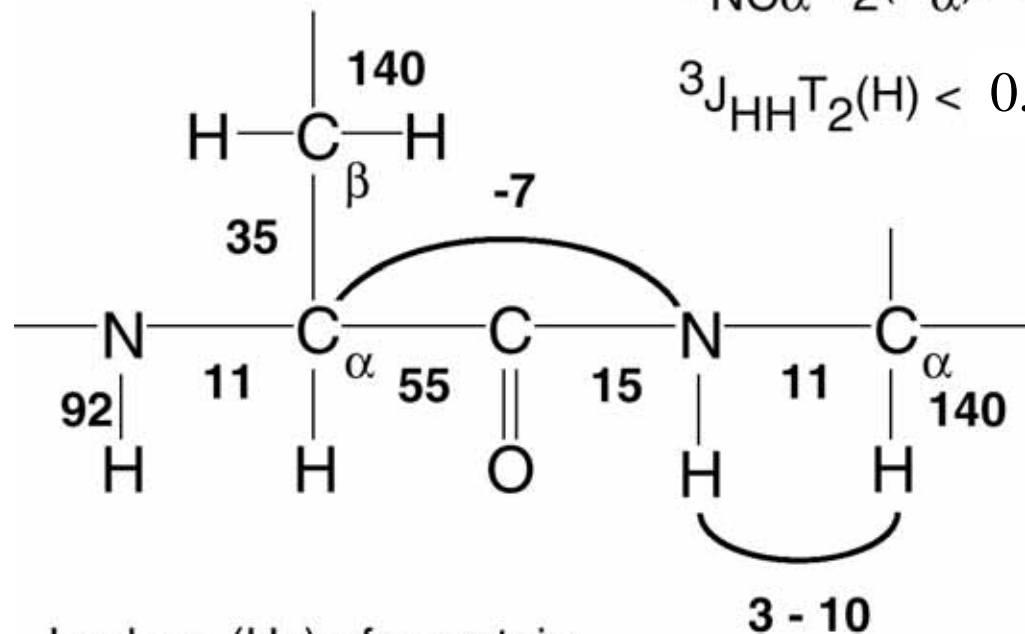
$$1/T_2 \sim J(0) \sim \tau_c \sim \text{MWT}$$

Typical T_2 -values (ms) for a ($\tau_c \sim 15$ ns) protein
(MWT ~ 30 kDa)

$J T_2 \ll 0.5 \Rightarrow$ no efficient transfer

$$^1J_{NC\alpha} T_2(C\alpha) = 0.15 \text{ !! for } 30 \text{ kDa}$$

$$^3J_{HH} T_2(H) < 0.08 \text{ ! for } 30 \text{ kDa}$$



J-values (Hz) of a protein

3 - 10

Can my protein be studied by 2D/3D/4D NMR?

$$\Phi = x, y, -x, -y$$

$$\text{Rec} = x, -x, x, -x$$



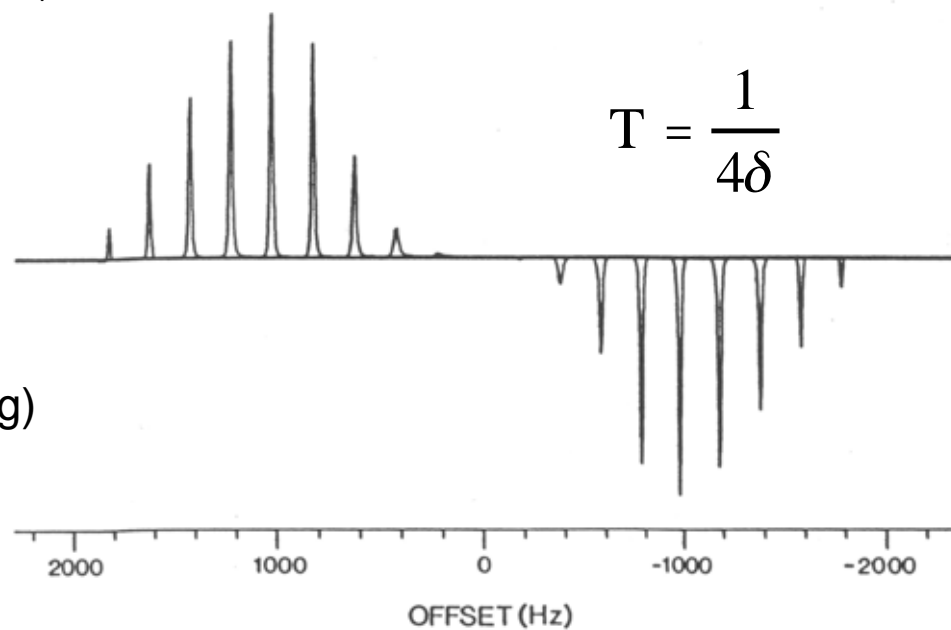
No labels available:

1D in H₂O

T₂ H^N from 1-1 echo

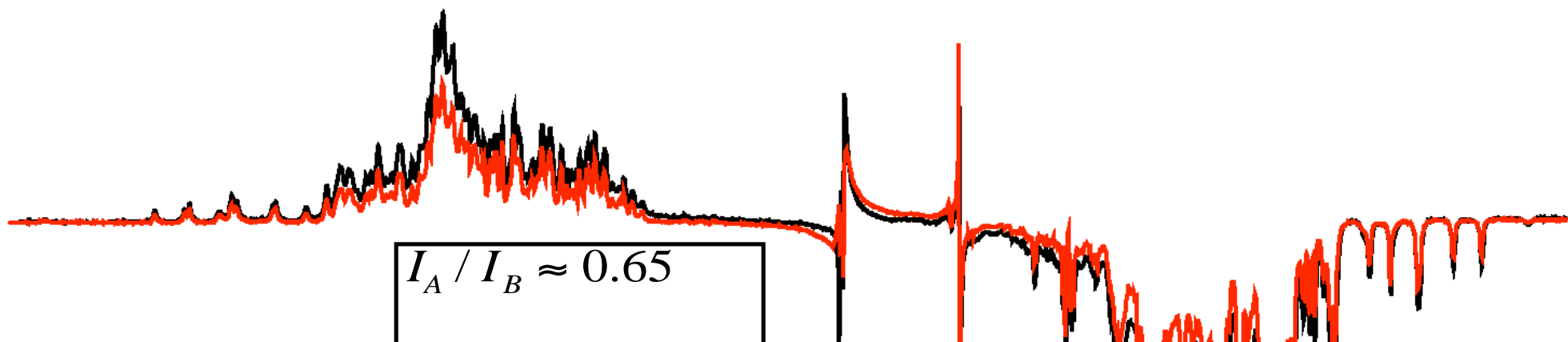
Sklenar + Bax J.M.R. 74, 469-79 (1987)

SPIN-ECHO WATER SUPPRESSION



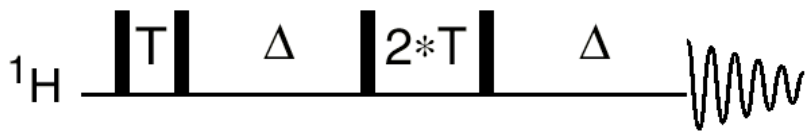
(no J_{HNHA} dephasing)

1D-oneone experiment - NEF 308K

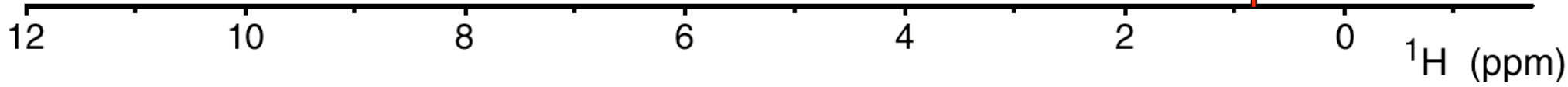


$$I_A / I_B \approx 0.65$$
$$T_2 = \frac{2(\Delta_A - \Delta_B)}{\ln(I_A / I_B)}$$
$$T_2 = 13 \text{ ms}$$

$\Delta_A = 0.1 \text{ ms}$
 $\Delta_B = 2.9 \text{ ms}$



$T = 85 \mu\text{s @ } 600 \text{ MHz}$



J. Biomol. NMR 3, 121-6, 1993

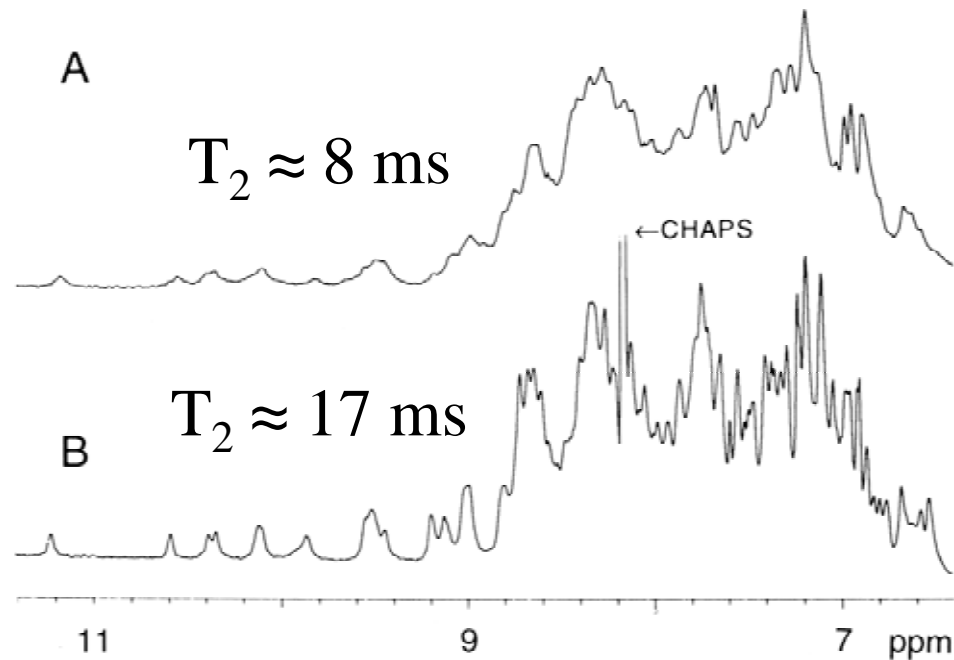


Fig. 1. Amide region of 0.8 mM calcineurin B at 35 °C, pH 4.9, in the (A) absence and (B) presence of 18 mM CHAPS. The position of the very intense amide proton resonance of CHAPS (8.13 ppm) is marked.

$$\tau_c [ns] \approx \frac{1}{5T_2 [s]}$$

$$T_2 = 30 \text{ ms} \Rightarrow \tau_c = 6.6 \text{ ns}$$

Structure determination feasible

Without deuteration:

if $T_2 \geq 12 \text{ ms}$, $\tau_c \leq 15 \text{ ns}$,

MWT < 30 kDa

With deuteration:

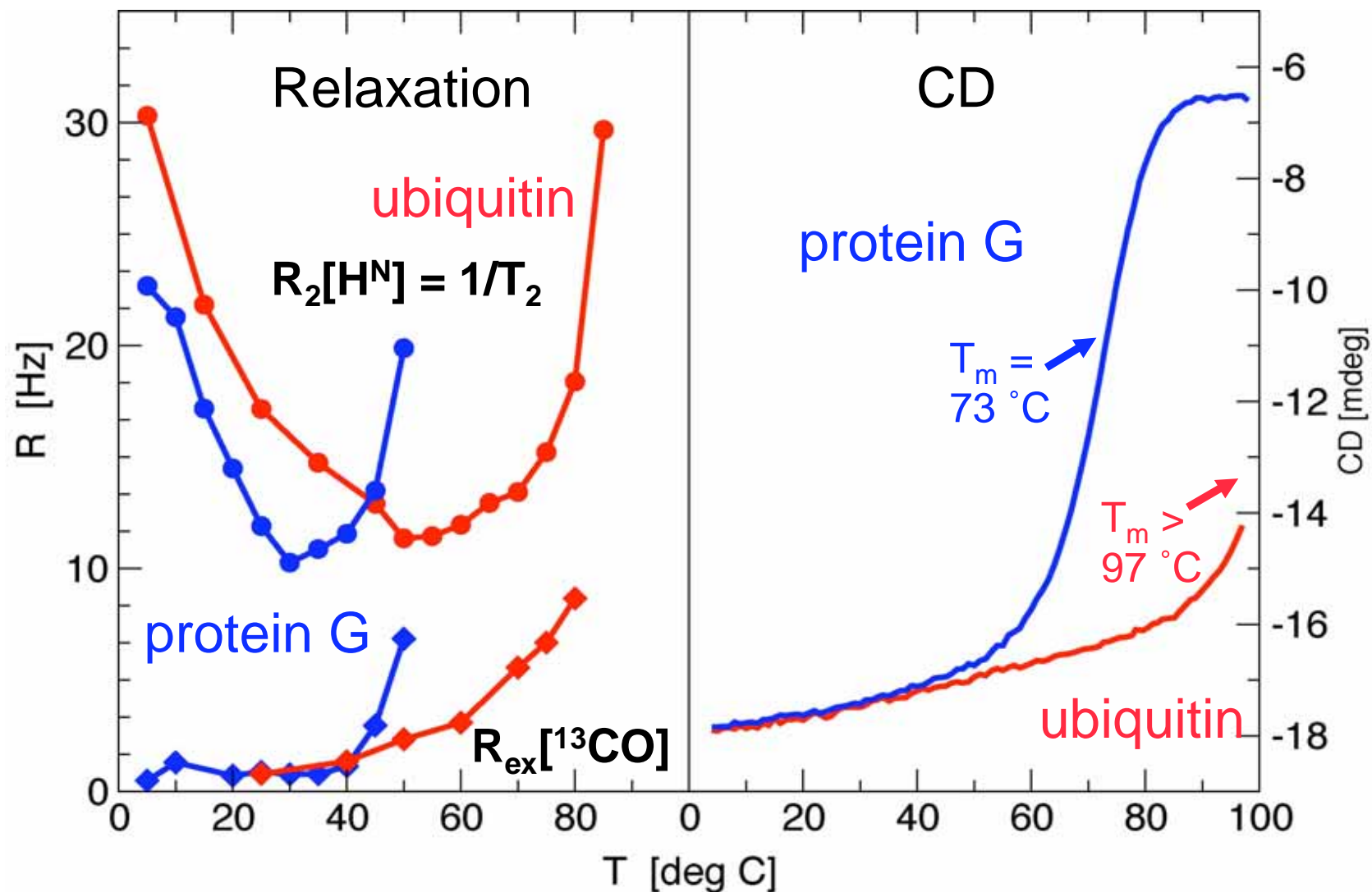
tertiary structures $\leq 60\text{-}80 \text{ kDa}$

secondary structures $\leq 110 \text{ kDa}$

resolved H-N TROSYs < 900 kDa

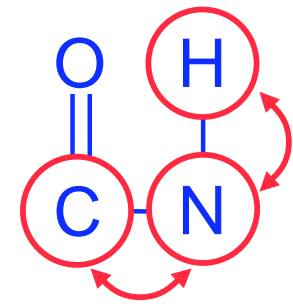
$$\tau_c [ns] \sim \frac{1}{2} MWT [kDa] \quad @ 20^\circ C$$

ubiquitin (pH 4.6) vs. protein G (pH 5.8)

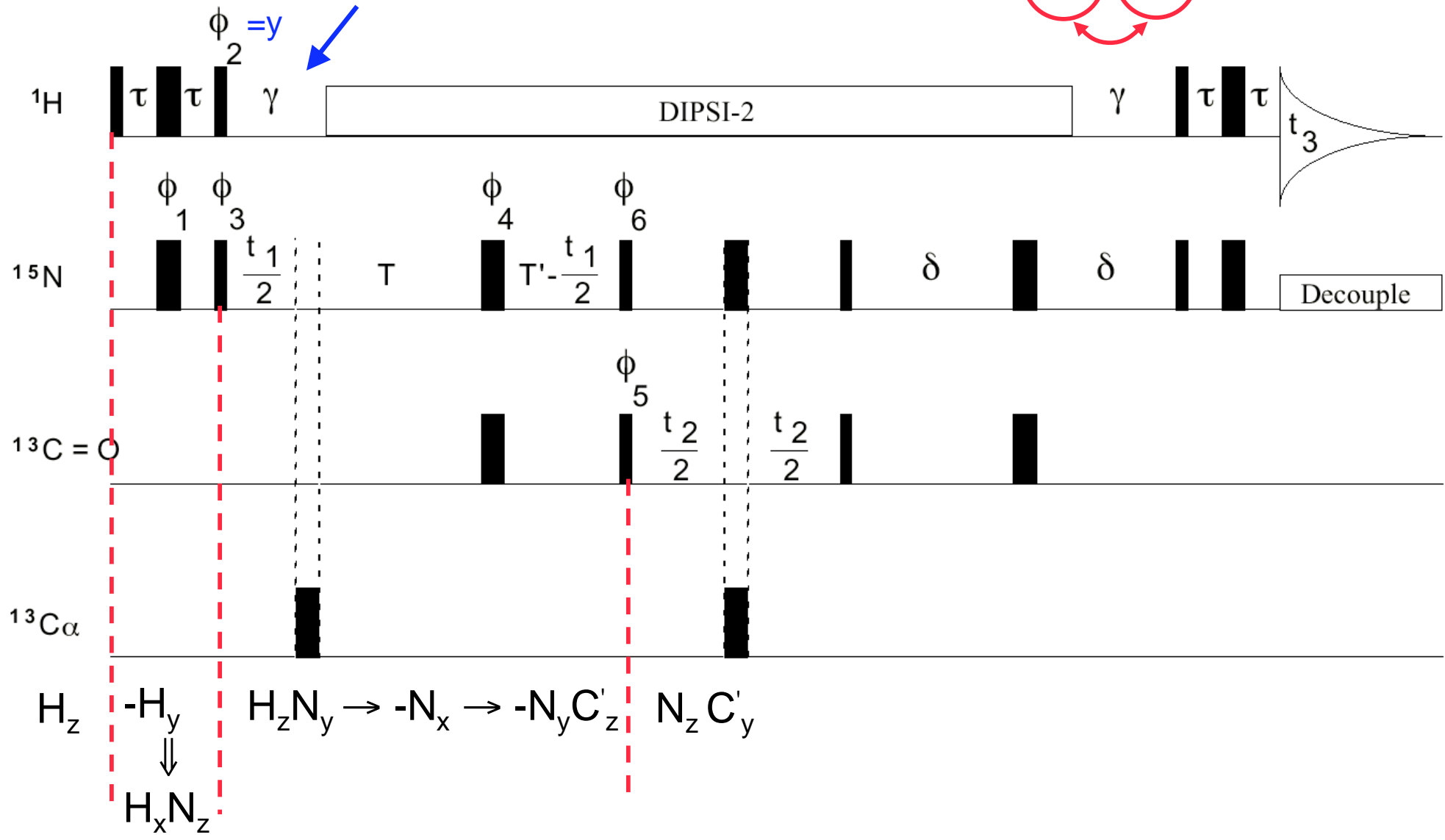


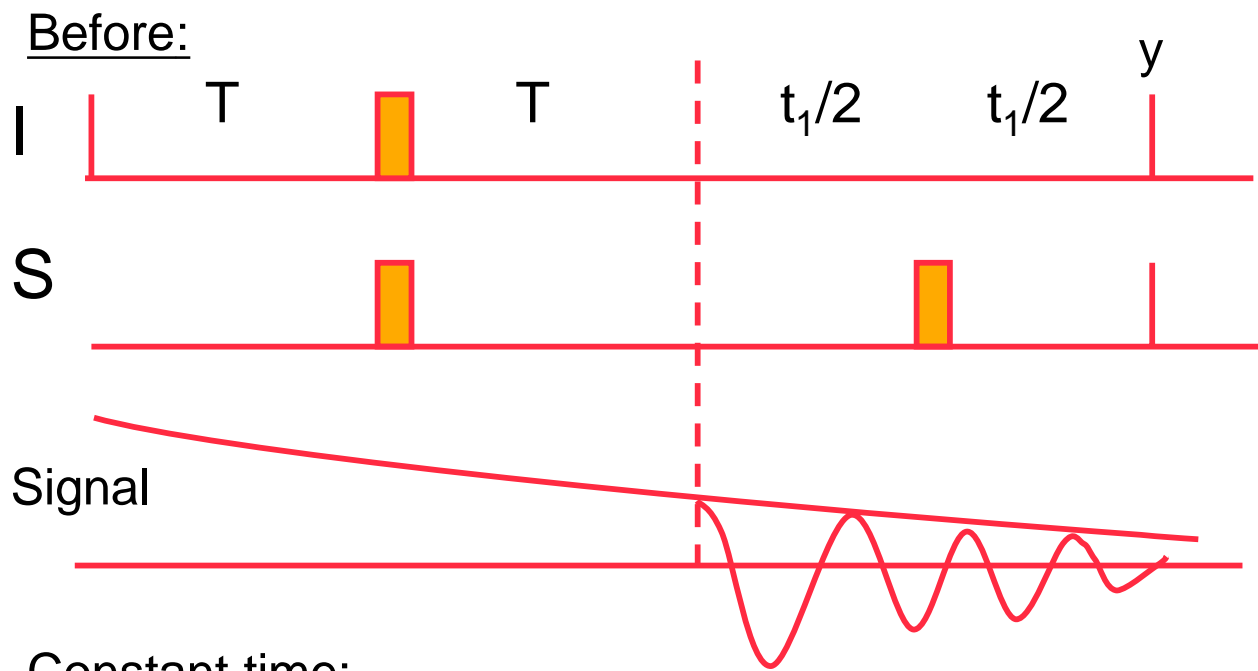
Unfolding affects T_2 long before the melting transition

Strohmeier, Cordier, Heerklotz, Grzesiek unpublished

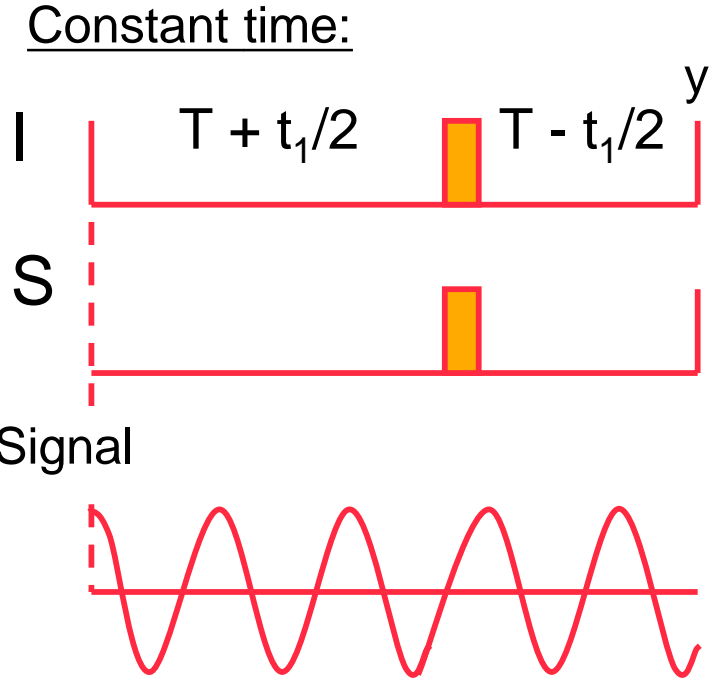


$H_z N_y \rightarrow -N_x$ for improved $^{15}N T_2$





Constant time evolution



J - dephasing time :

$$T + \frac{t_1}{2} + T - \frac{t_1}{2} = 2T$$

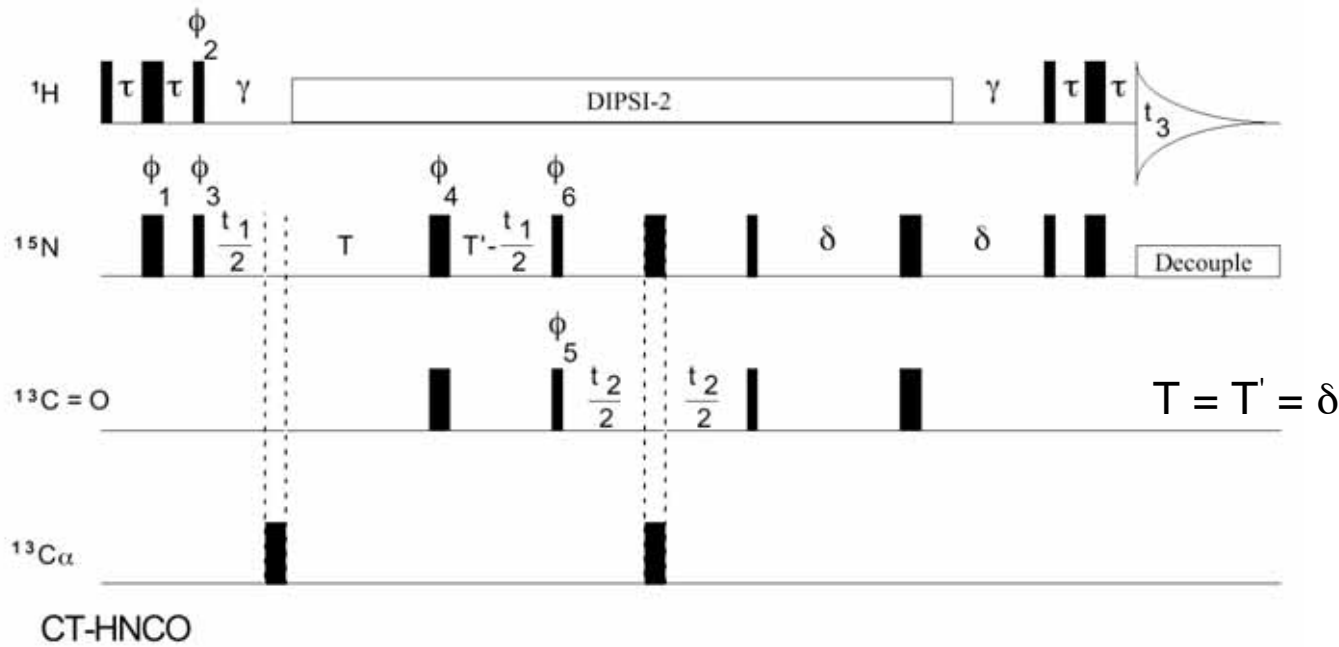
chemical shift evolution :

$$T + \frac{t_1}{2} - \left(T - \frac{t_1}{2} \right) = t_1$$

- + no additional relaxation during t_1
- maximal t_1 limited by $2T$ ($\sim 1/2J$)

$$I_z \xrightarrow{J I_z S_z \cdot 2T} -I_y \xrightarrow{\delta^I I_z \cdot t_1} 2I_x S_z \cos \delta^I t_1 + 2I_y S_z \sin \delta^I t_1$$

Estimate S/N



3D vs. 2D

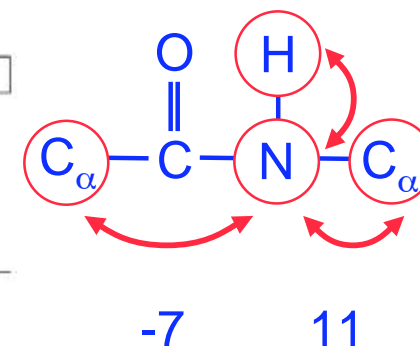
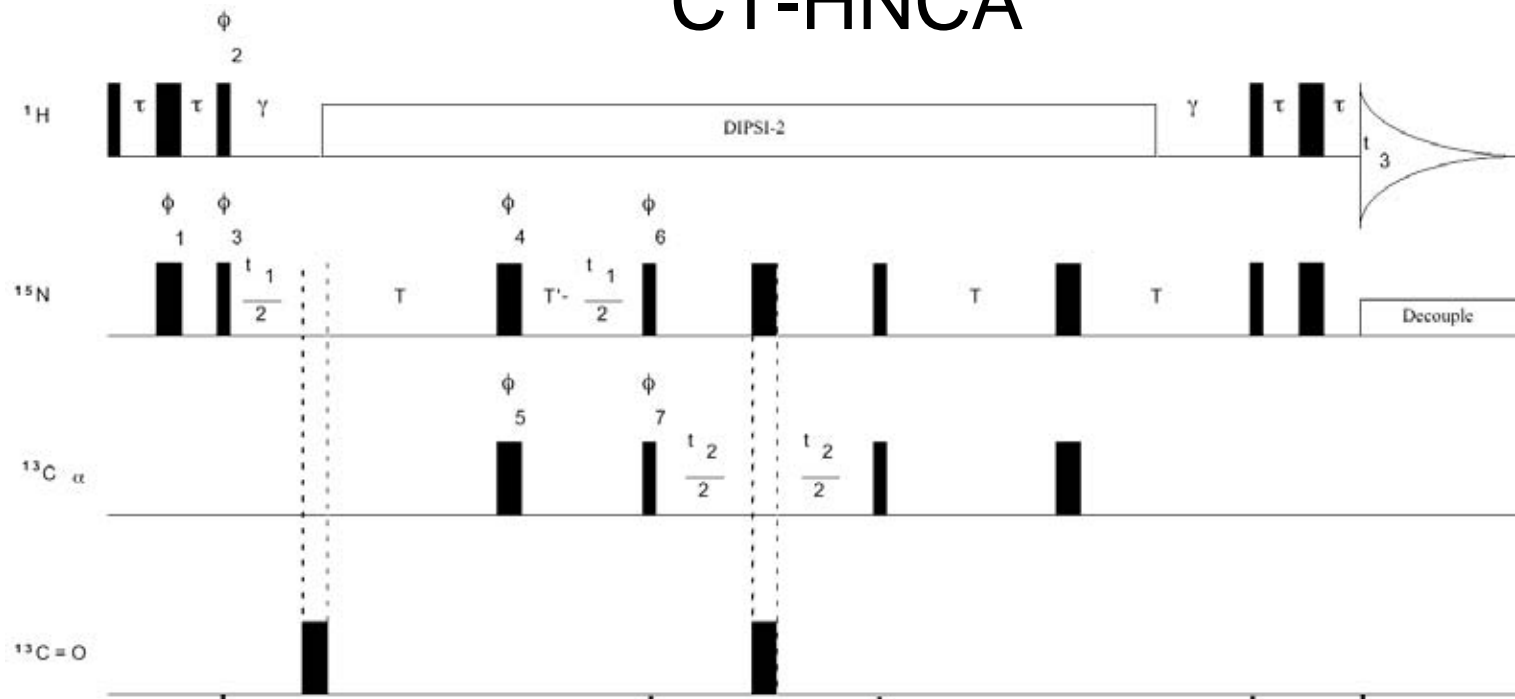
$$T_2(N) = 42 \text{ ms}; \quad J_{NC'} = 15 \text{ Hz}$$

$$S/N = \sin^2(2\pi J_{NC'} \delta) \cdot \exp^2(-2\delta/T_2(N)) \cdot \frac{S/N(\text{HSQC})}{\sqrt{2}}; \quad \text{optimal } \delta = 11.5 \text{ ms} < \frac{1}{4J_{NC'}} = 16.7 \text{ ms}$$

$$\frac{S/N(\text{HNCO})}{S/N(\text{HSQC})} = \frac{1}{\sqrt{2}} \cdot 0.26 = 0.18$$

$$\frac{S/N(\text{HSQC})}{S/N(1D)} = \frac{1}{\sqrt{2}} \sin^2(2\pi J_{H_N} \tau) \cdot \exp^2(-2\tau/T_2(H_N)) = 0.35; \quad \frac{S/N(\text{HNCO})}{S/N(1D)} = 0.18 * 0.35 = 0.065 = \frac{1}{15}$$

CT-HNCA



$${}^1J_{NC\alpha} = 11 \text{ Hz}; \quad {}^2J_{NC\alpha} = -7 \text{ Hz}; \quad 2T = 22 \text{ ms}; \quad T_{2N} = 42 \text{ ms}$$

$${}^1J : \sqrt{S/N} \sim \sin 2\pi \overset{0.69}{JT} \cdot \cos 2\pi \overset{0.88}{JT} \cdot \overset{0.59}{\exp\left(-\frac{2T}{T_{2N}}\right)} = 0.36$$

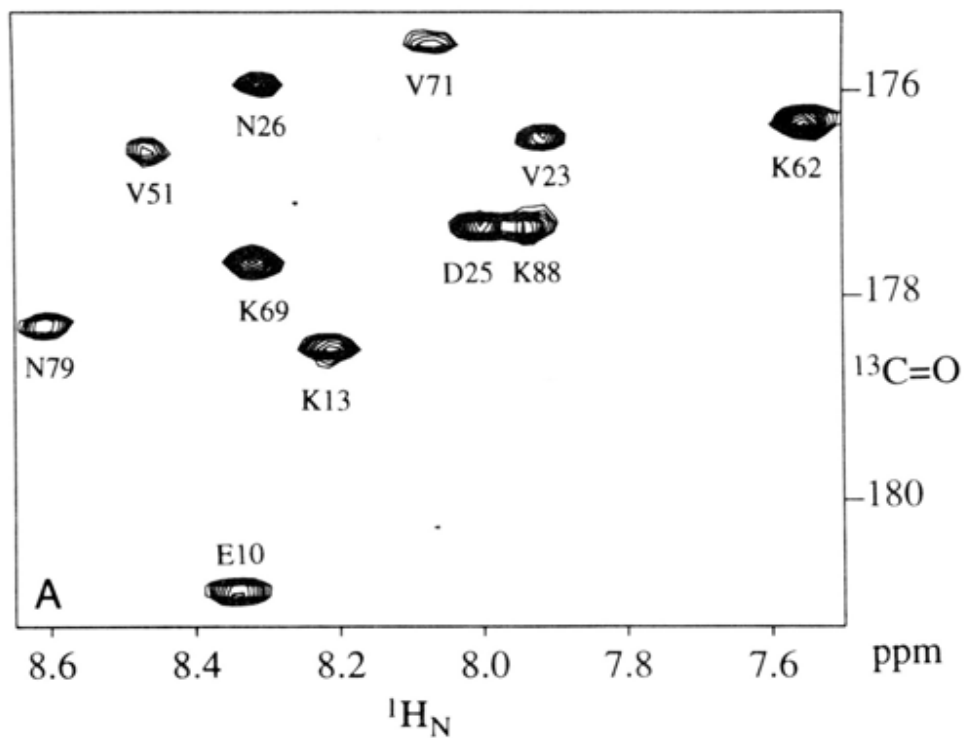
$${}^2J : \sqrt{S/N} \sim \sin 2\pi \overset{0.47}{JT} \cdot \cos 2\pi \overset{0.72}{JT} \cdot \overset{0.59}{\exp\left(-\frac{2T}{T_{2N}}\right)} = 0.20$$

$$\frac{S/N(\text{HNCA})}{}^1J \frac{0.36^2}{\sqrt{2}} = 0.09 \hat{=} \frac{\text{HNCO}}{2}$$

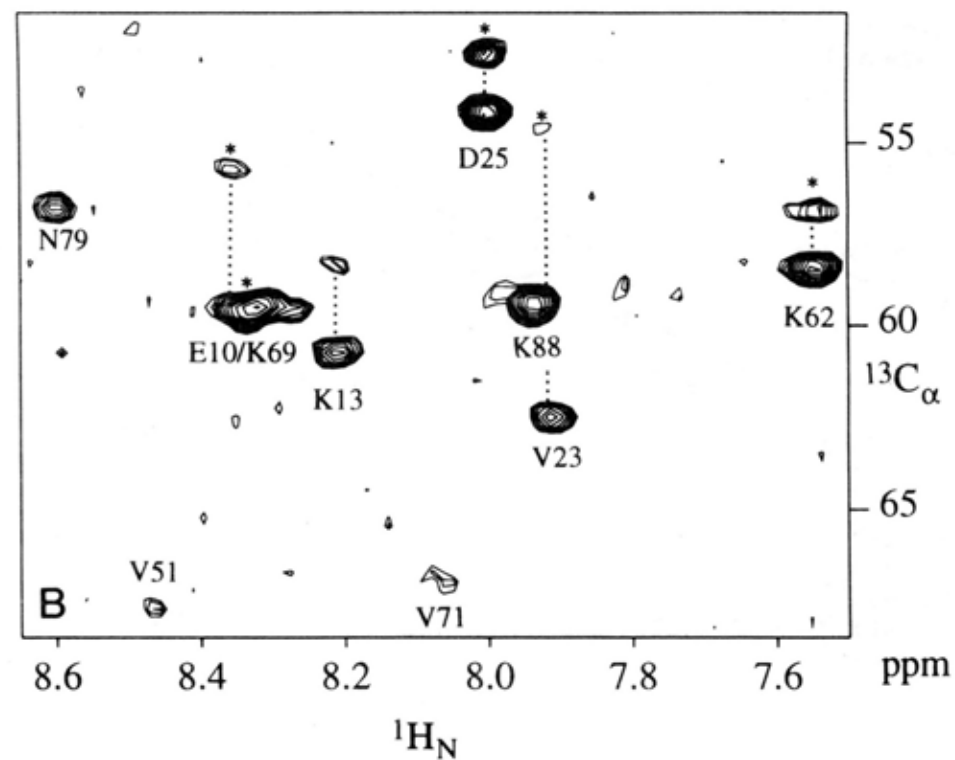
$$= \frac{{}^2J 0.20^2}{\sqrt{2}} = 0.028 \hat{=} \frac{\text{HNCO}}{7}$$

Interferon- γ (31.4 kDa)

HNCO



HNCA

 $^{15}\text{N} = 118.9$ ppm

Ikura, Kay, Bax

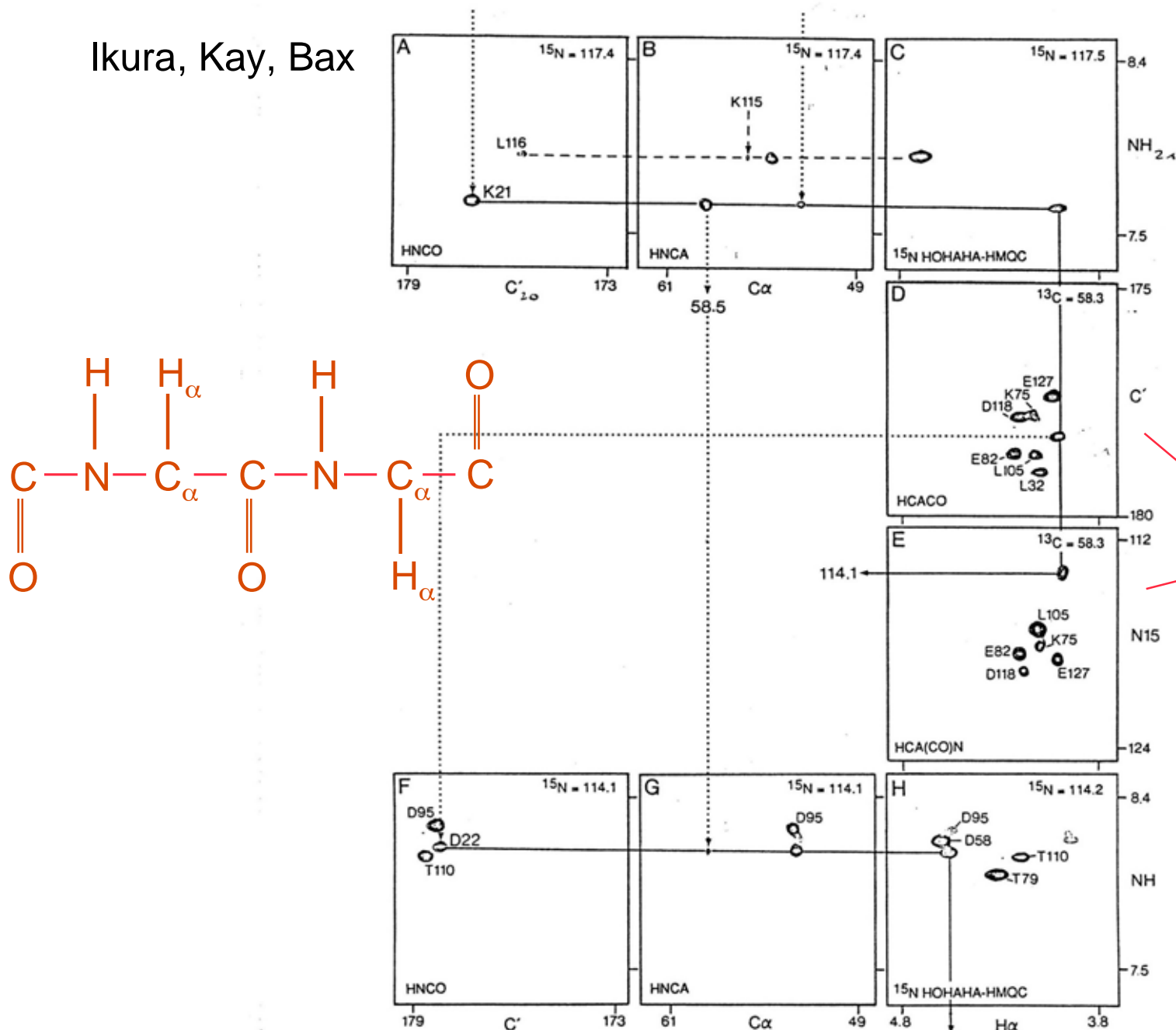
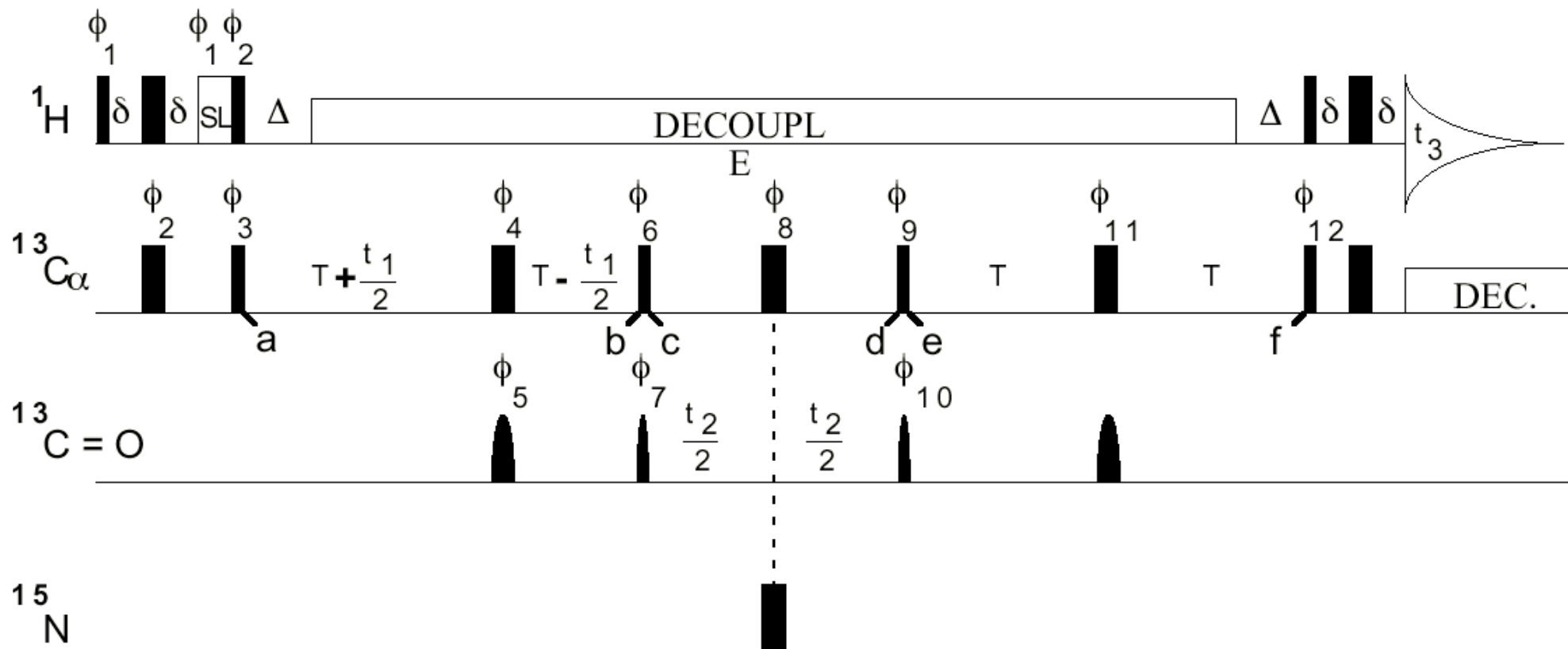


FIGURE 3: Selected regions of slices from five separate 3D NMR experiments discussed in the text. These regions illustrate the J correlation between Lys-21 and Asp-22. Solid and dotted lines trace the connectivity patterns for these two residues. Broken lines correspond to parts of the connectivity patterns observed for other residues. Slices A–C are taken at the Lys-21 ^{15}N chemical shift. Slices D and E are taken at the Lys-21 C^{α} shift, observed in B. Slices F–H are taken at the ^{15}N frequency of Asp-22, as measured in E. The analysis of the connectivity patterns is discussed in the text. No base-line correction or any other cosmetic procedures were used for any of the 3D spectra.

HCACO: Ikura et al. Biochemistry 29, 4659 (1990)

Powers et al. J. Magn. Res. 89, 496 (1990)



$$S/N \text{ (vs. 1D)} = \exp(-4\delta/T_{2\text{H}\alpha}) \cdot \exp(-4T/T_{2\text{C}\alpha}) \cdot \sin^2(2\pi J_{\text{C}\alpha\text{C}'}T) \cdot \cos^2(2\pi J_{\text{C}\alpha\text{C}\beta}T) / 2 = 0.039$$

$$= \text{HNCO} / 1.5 \text{ BUT ALSO DIFFERENT RELAXATION DURING } t_3!$$

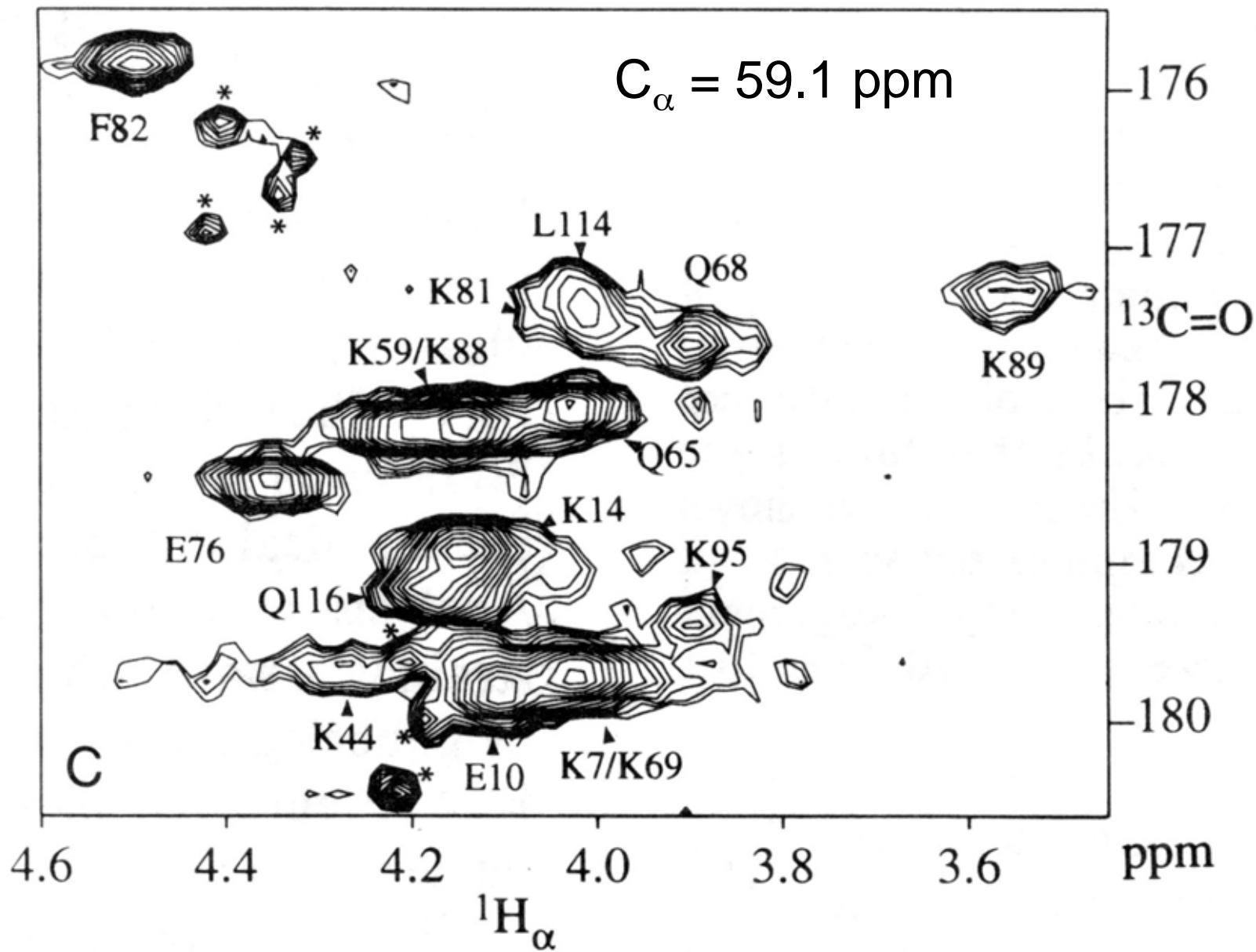
$$[\sin(2\pi J_{\text{C}\alpha\text{H}\alpha}\delta) = 1]$$

E- and D-sidechains

Grzesiek + Bax, J. Magn. Reson. B 102, 103 (1993)

Löhr + Rüterjans, J. Magn. Reson. B 109, 80 (1995)

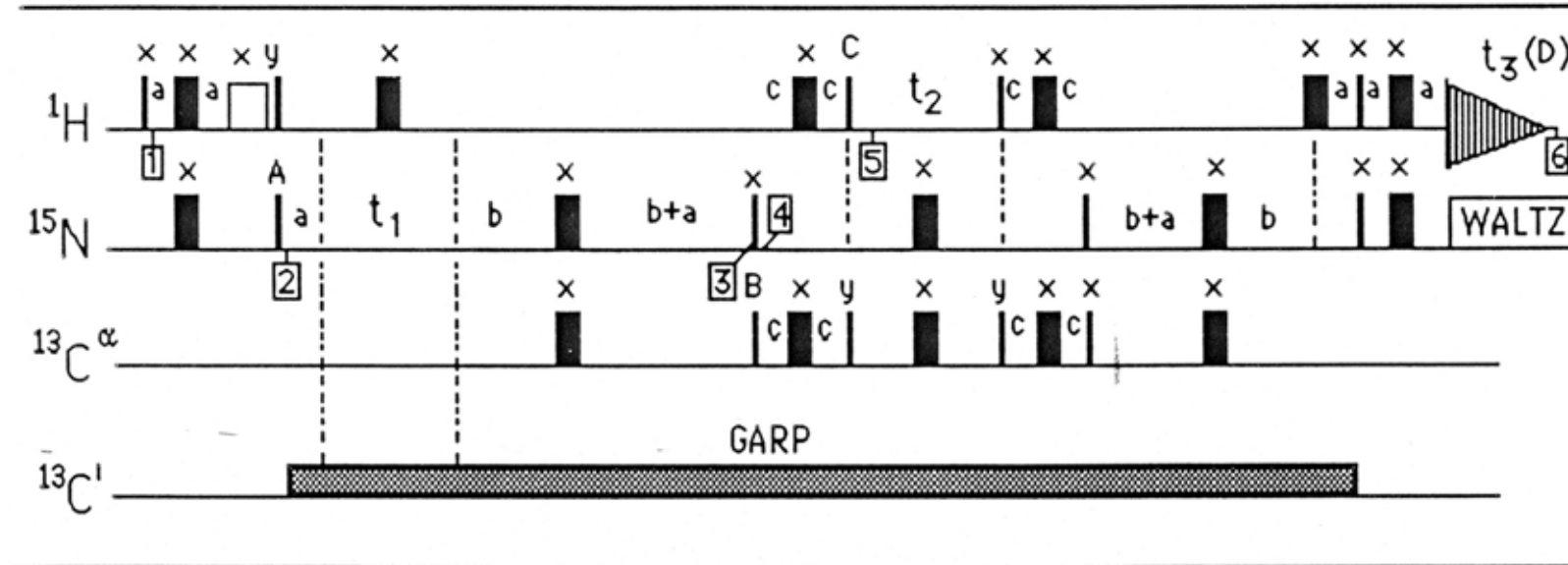
HCACO of Interferon - γ



A new 3D HN(CA)HA experiment for obtaining fingerprint H^N-H^α cross peaks in ^{15}N - and ^{13}C -labeled proteins

Robert T. Clubb^{a,b}, V. Thanabal^a and Gerhard Wagner^{a,*}

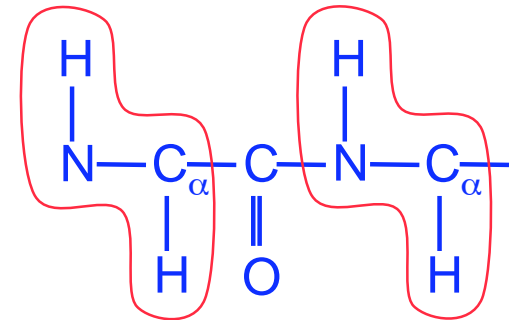
Journal of Biomolecular NMR, 2 (1992) 203–210



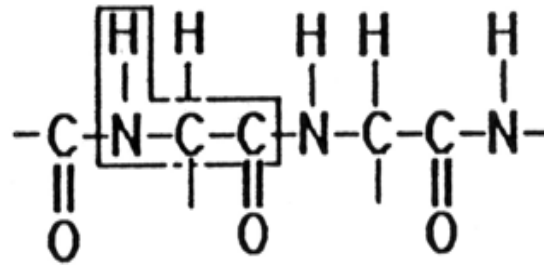
$$S/N = (\text{HNCA}) * \exp(-4c / T_{2C\alpha}) * \cos^2(2\pi J_{C\alpha C\beta}) = (\text{HNCA}) * 0.58 = 0.017$$

$$= \text{HNCO} / 3.4$$

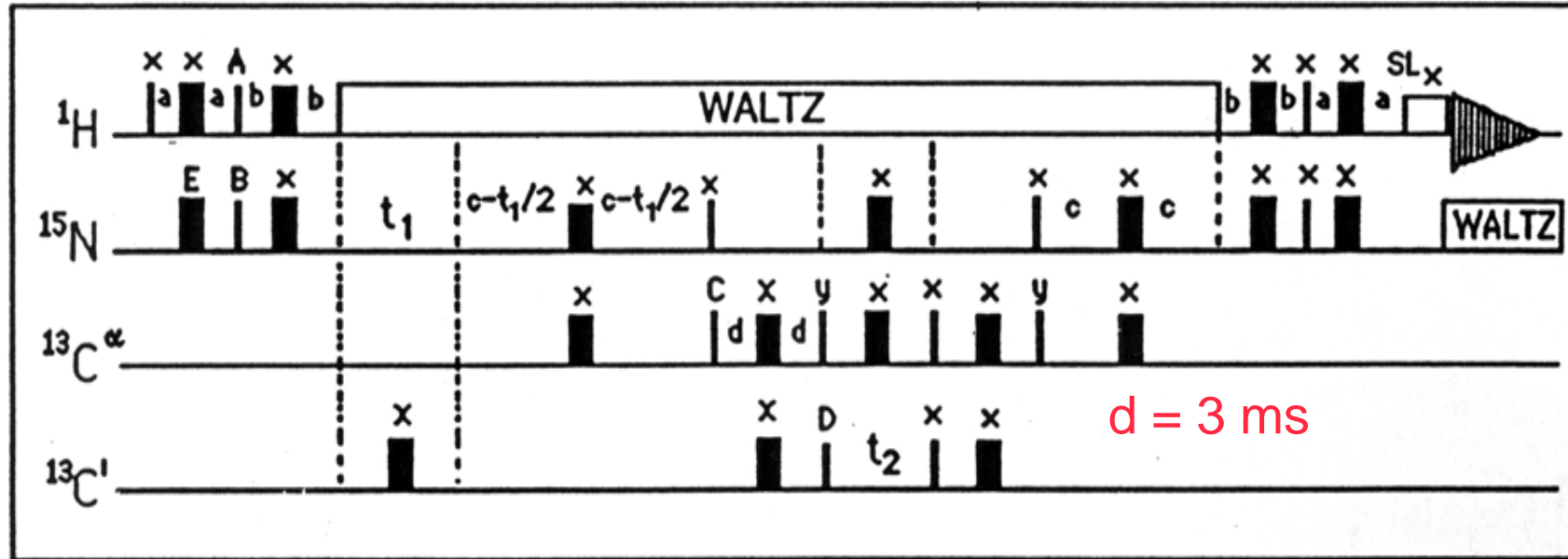
HN(COCA)HA: Clubb + Wagner, J. Biomol. NMR 2, 389 (1992)



HN(CA)CO Clubb, Thanabal, Wagner, J. Magn. Reson. 97, 213-217 (1992)



HN(CA)CO



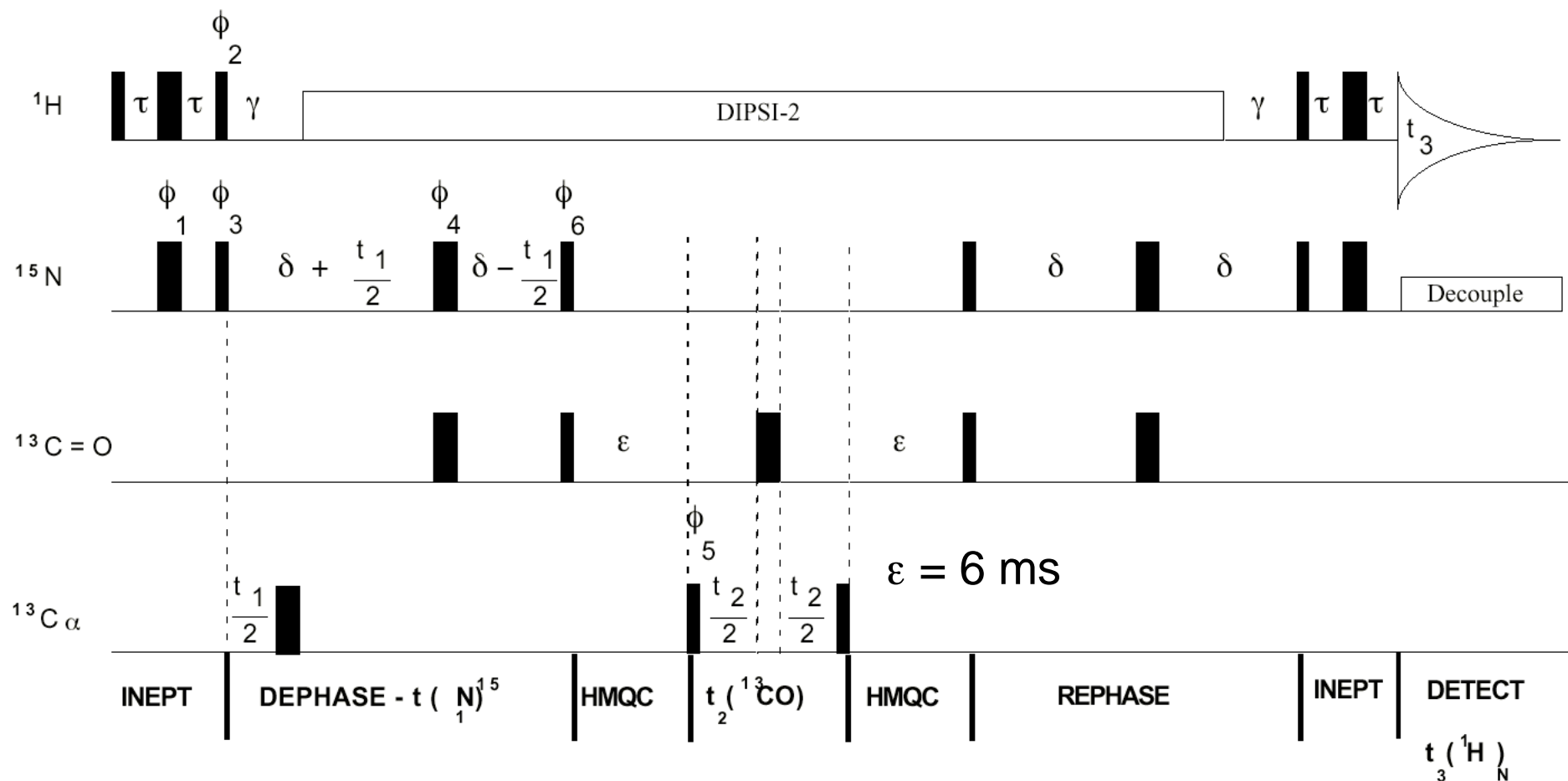
$$S/N = (\text{HNCA}) \cdot \exp\left(-\frac{4d}{T_{2C\alpha}}\right) \cdot \cos^2(2\pi d J_{C\alpha C\beta}) \cdot \sin^2(2\pi d J_{C\alpha C'}) =$$

$$= (\text{HNCA}) * 0.20 = 5.8 \cdot 10^{-3} = \text{HNCO}/10$$

works well for deuterated proteins!

Engelke + Rüterjans, J. Magn. Res. B, 109, 318 (1995)

HN(CO)CA

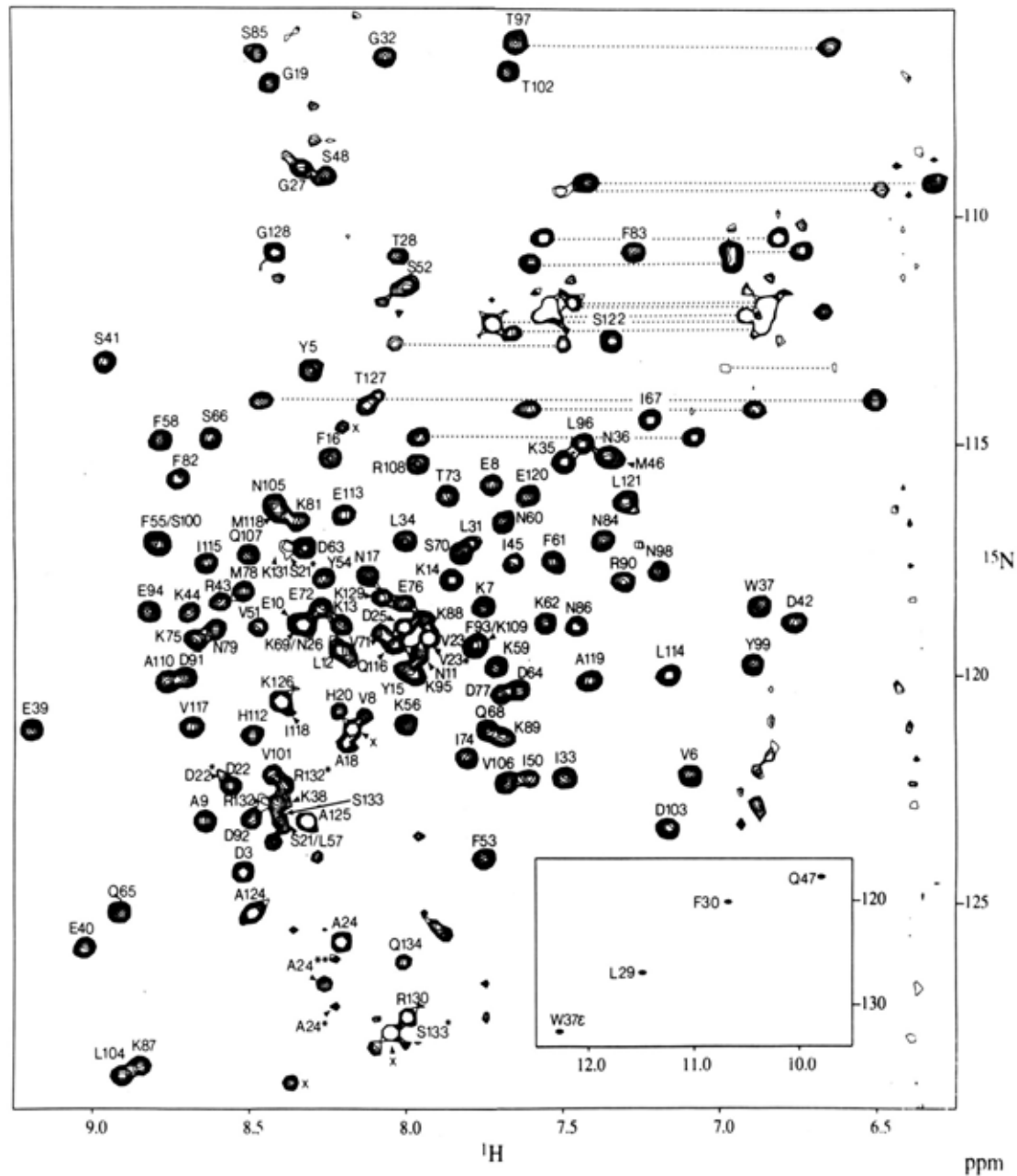


$$\begin{aligned}
 \text{S/N} &= (\text{HNCO}) \cdot \exp(-2\varepsilon/T_2(\text{CO})) \cdot \sin^2(\pi\varepsilon J_{\text{C}\alpha}) \\
 &= \text{HNCO} \cdot 0.58 = 0.034
 \end{aligned}$$

J. Magn. Reson. 96, 432 (1992)

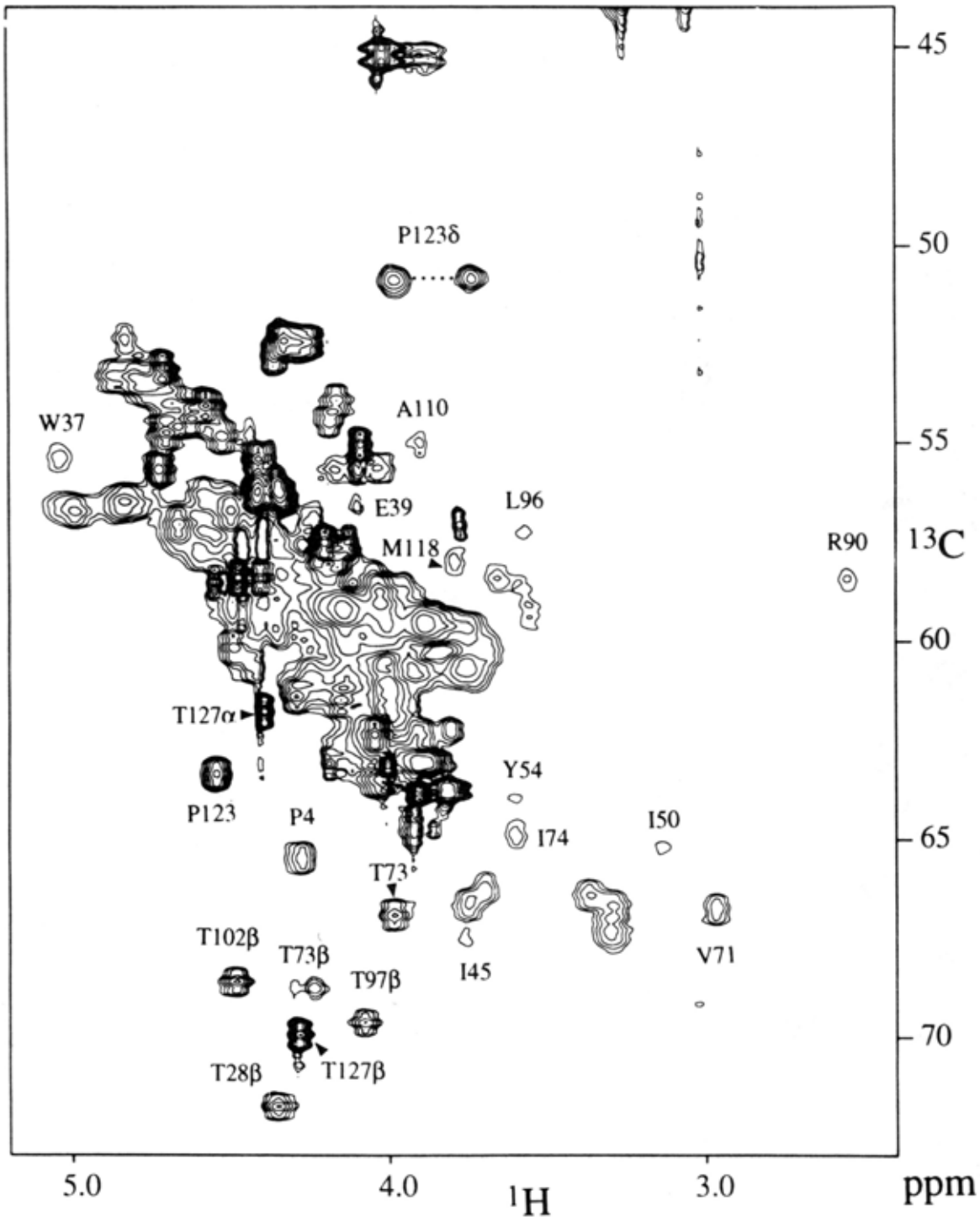
problem with CO
relaxation at high
fields:

$$1/T_2 \sim \text{CSA}^2 B^2 \tau_c$$

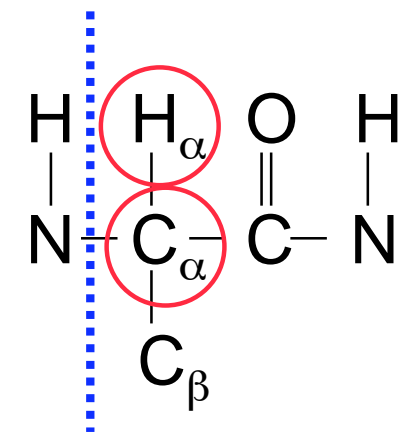


Interferon- γ 31 kDa

FIGURE 1: Resolution-enhanced 2D ^1H - ^{15}N HSQC spectrum of IFN- $\gamma\Delta 10$, labeled uniformly with ^{15}N (>95%), recorded at 600-MHz ^1H frequency. Cross peaks connected by dotted lines correspond to Gln and Asn side chain NH_2 groups. Cross peaks marked "x" were only observed in the ^{15}N (>95%)-labeled sample and not in the $^{15}\text{N}/^{13}\text{C}$ -labeled samples. R132* and S133* correspond to protein that terminates at S133. Asterisks for residues S21–D25 correspond to a minor conformer.

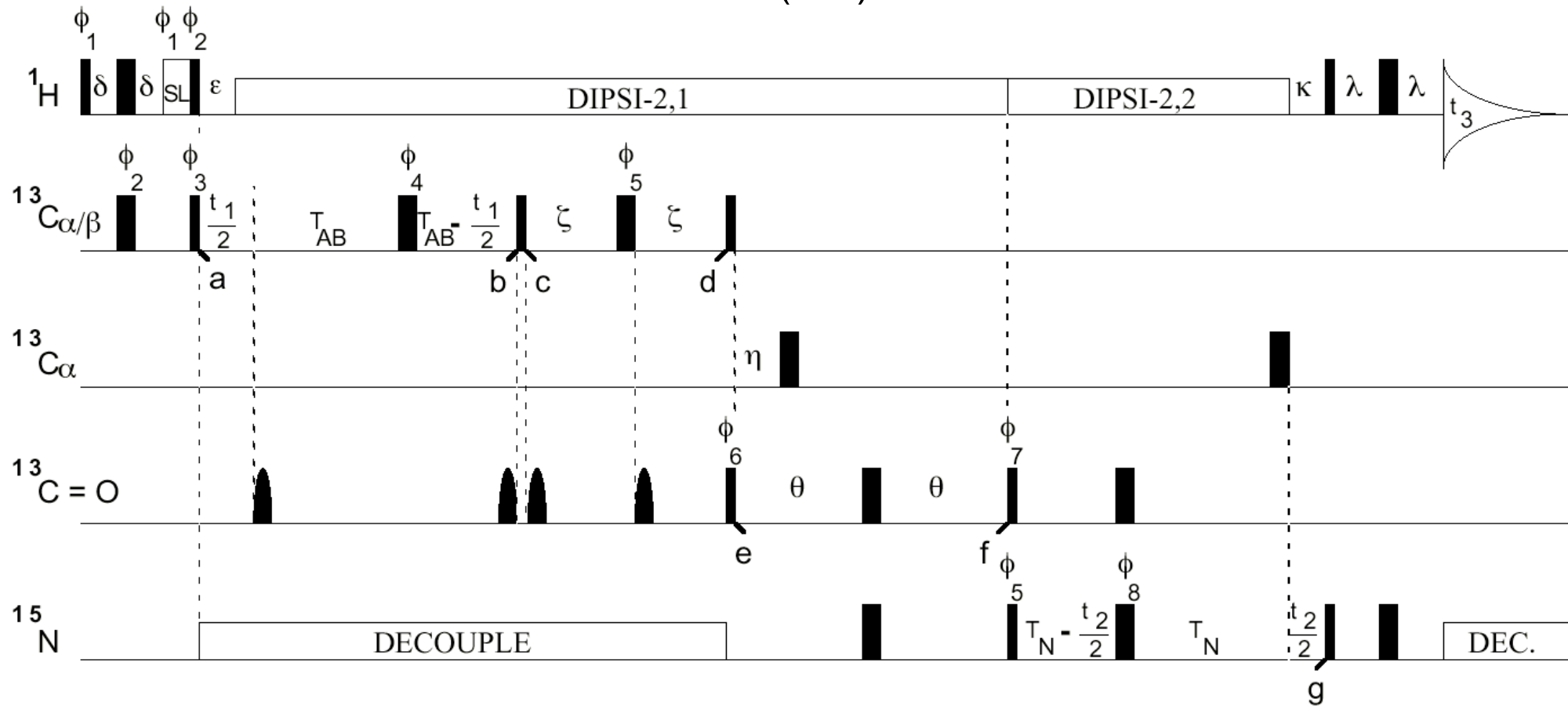


H_α-C_α-Spectrum of Human Interferon-γ

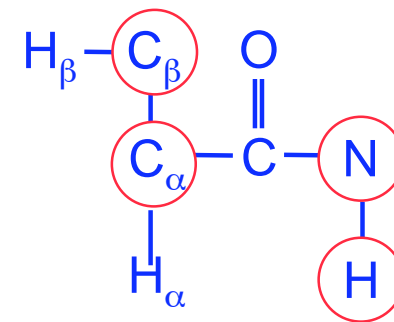


weak J-connection
in backbone

CBCA(CO)NH



$$\begin{aligned}
 S/N = & e^{-3/6} e^{-6.6/8} e^{-7.4/14} e^{-22.4/52} e^{-22/42} e^{-4.5/13} \cdot \sin(2\pi J_{H\beta C\beta} \delta) \cdot \\
 & \cdot \sin(2\pi J_{C\alpha C\beta} T_{AB}) \cdot \cos(2\pi J_{C\beta C\gamma} T_{AB}) \cdot \sin(2\pi J_{C\alpha C\beta} \zeta) \\
 & \cdot \sin(2\pi J_{C\alpha C} \zeta) \cdot \sin(2\pi J_{C'N} \theta) \cdot \sin(2\pi J_{C'N} T_N) \\
 & \cdot \sin(2\pi J_{HN} \lambda) \sim 0.09 - 0.17 * HNCO
 \end{aligned}$$



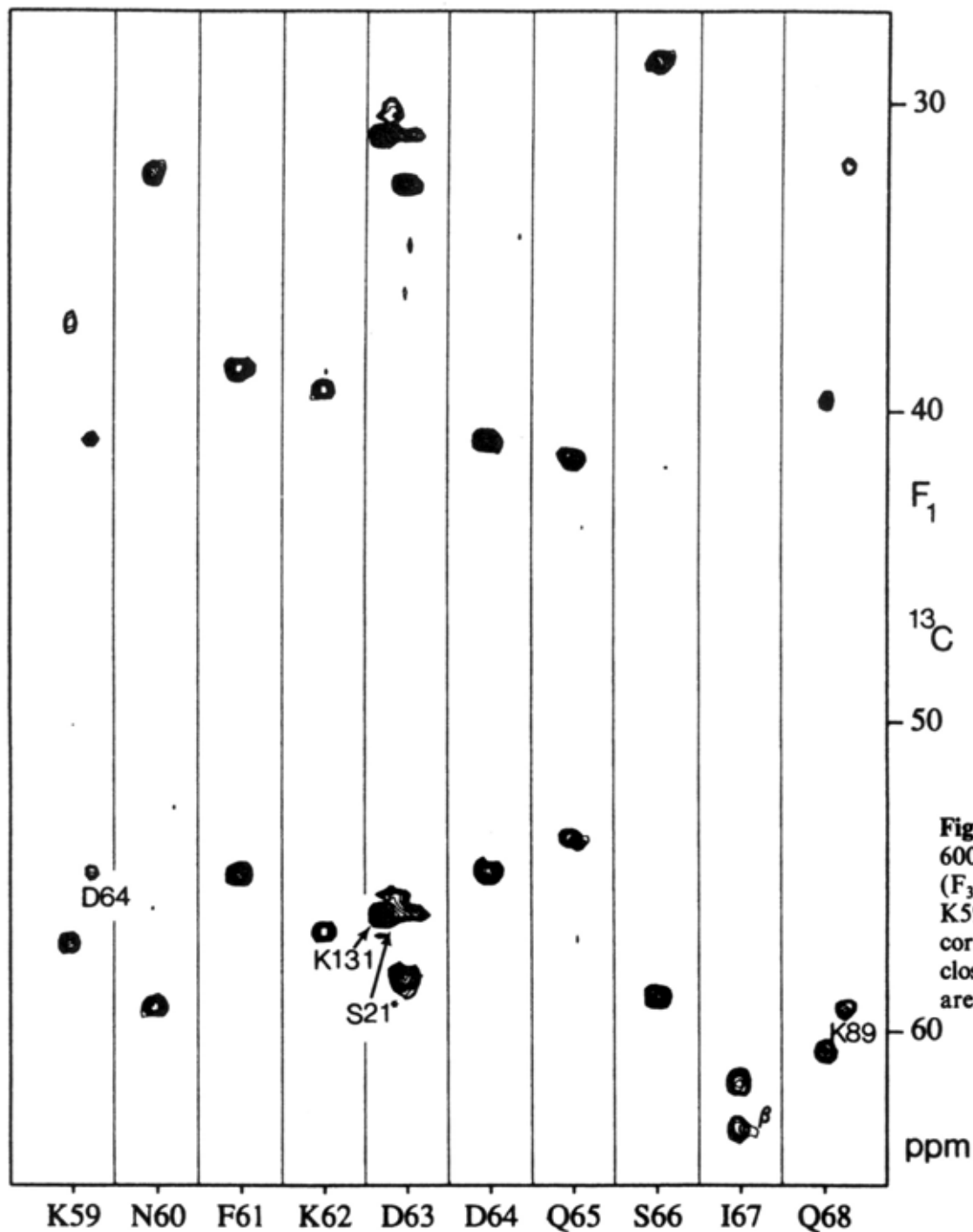
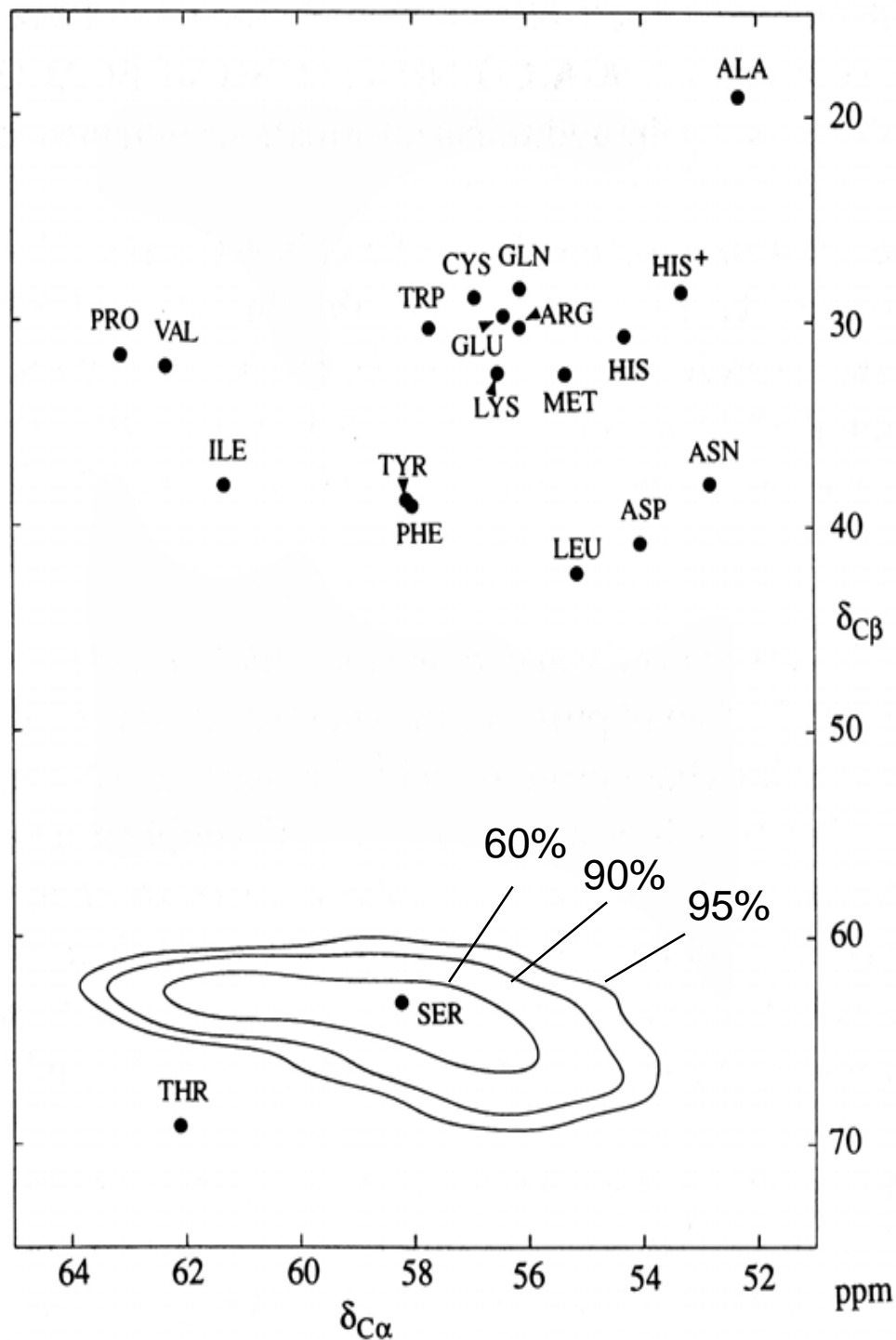
CBCA(CO)NH of Interferon- γ 

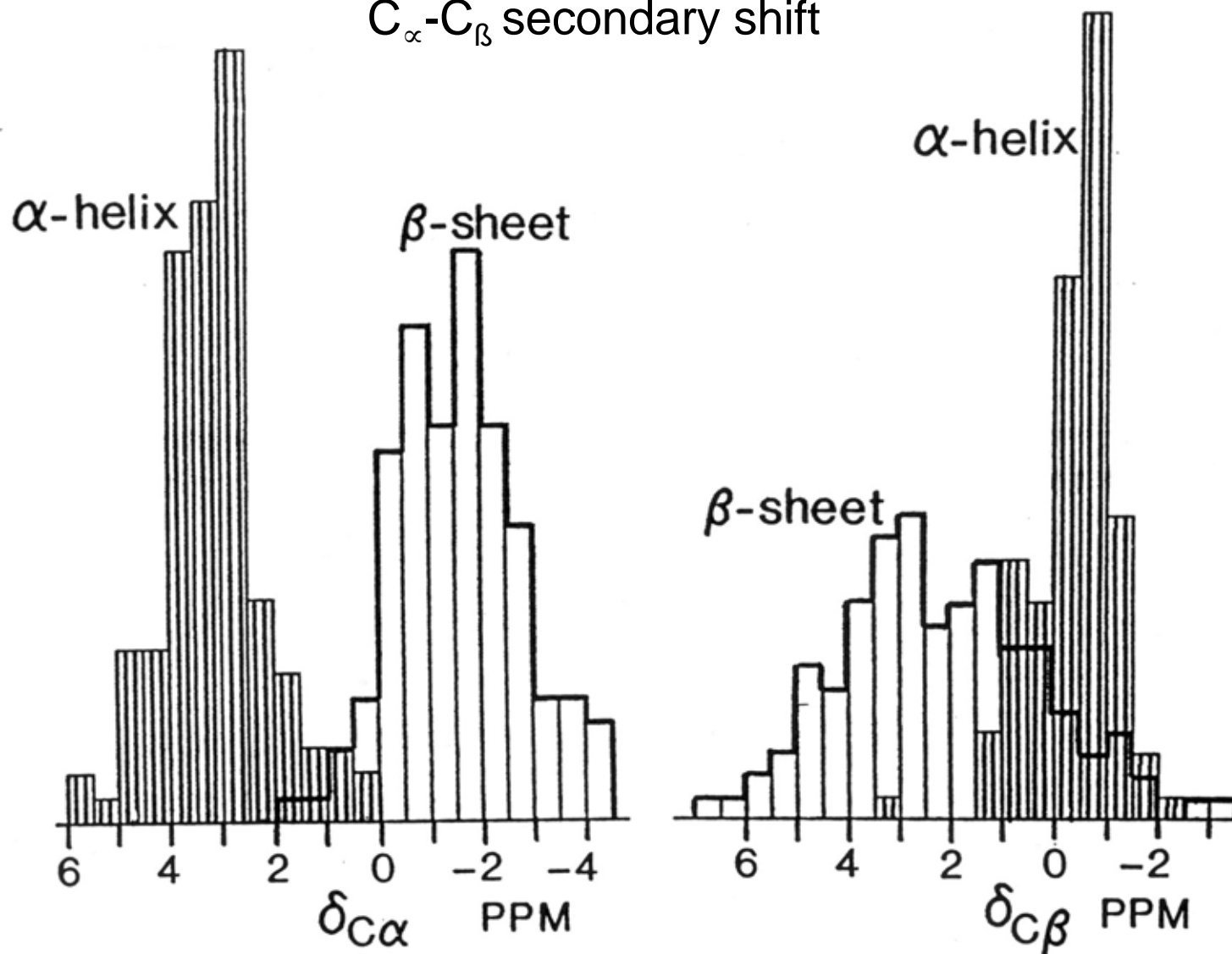
Figure 2. F_1 (C_α , C_β) strips for residues K59–Q68, taken from the 600-MHz 3D CBCA(CO)NH spectrum of interferon- γ at the $^1\text{H}/^{15}\text{N}$ (F_3/F_2) frequencies of their amides. In the leftmost strip, the amide of K59 correlates with C_α and C_β of F58. Also visible in this strip is the correlation for the amide of D64 (which has a ^1H – ^{15}N correlation very close to that of K59) to the C_α and C_β of D63. These latter correlations are observed with much higher intensity in the sixth strip.

Amino acid type determination in
the sequential assignment
procedure of uniformly $^{13}\text{C}/^{15}\text{N}$ -
enriched proteins

J. Biomol. NMR 3, 1993, 185-204



C_{α} - C_{β} secondary shift



Spera + Bax, J. Am. Chem. Soc. 113, 5490, (1991)

De Dios et al., SCIENCE 260, 1491 (1993) (theoretical calculation)

TALOS database <http://spin.niddk.nih.gov/bax/software/TALOS>.

Uniqueness of C_{α} - C_{β} shift pairs

TABLE 1
OVERLAP INTEGRALS BETWEEN THE C^{α} AND C^{β} CHEMICAL SHIFT DISTRIBUTIONS FOR THE NATURAL AMINO ACIDS^a

TYPE											<N> N ₉₅		
ALA													
ALA	99.91										1.00	1	
SER	99.78										1.00	1	
THR	99.78										1.00	1	
ASP	LEU	PHE	TYR	ASN									
ASP	37.22	19.51	16.22	15.46	8.24						2.51	5	
LEU	41.75	21.88	15.19	14.01	5.15						2.26	5	
PHE	28.48	28.28	15.65	12.41	10.36						2.67	5	
PRO	44.94	41.57	3.20	2.77	2.58						2.02	5	
ILE	41.13	23.02	22.61	5.07	3.06	2.41					2.24	6	
TYR	28.63	28.43	16.02	11.89	9.61	2.67					2.67	6	
HIS*	33.59	18.82	12.35	11.75	9.46	7.37	3.23				2.98	7	
VAL	41.93	38.78	4.99	3.28	3.12	1.92	1.72				2.27	7	
ARG	16.40	15.47	12.67	12.63	12.53	9.46	8.90	7.37			4.20	8	
ASN	55.94	12.38	7.13	6.57	5.21	4.95	2.34	1.50			2.57	8	
TRP	18.81	14.53	13.63	11.40	10.91	9.92	9.33	6.51			4.16	8	
GLN	20.10	17.11	14.39	11.59	11.26	11.15	6.96	4.26			3.79	8	
CYS	17.64	15.92	15.02	13.47	10.69	10.32	6.17	5.49	4.72			3.99	9
GLU	16.35	15.42	14.76	11.85	11.77	11.71	7.05	5.79	4.60			4.13	9
HIS	19.04	14.66	13.70	11.14	10.56	9.45	8.32	7.00	5.43			4.14	9
MET	21.73	18.75	11.79	11.46	9.50	9.37	6.77	4.61	2.77			3.90	9
LYS	23.11	19.94	13.40	10.38	8.18	6.59	6.18	3.41	2.75	2.71	ASN	3.88	10

^aProbabilities are listed in % that, given the C^{α} and C^{β} frequency distributions of a certain amino acid type i, one could also assign to it an amino acid type j. The entries in the rows have been ordered according to decreasing probabilities, and only the most likely are listed, so that the sum of their probabilities is at least 95%. Also listed is the mean number, <N>, and the 95% number, N₉₅, of the choices as defined in the text.

TABLE 2
AMINO ACID TYPE PROBABILITIES FOR THE C^α AND C^β CHEMICAL SHIFT PAIRS OF RESIDUES 11–14^a
OF INTERFERON- γ

Spin system		$\delta_{C\alpha}$	$\delta_{C\beta}$	ARG ^b	ASN	ASP	ILE	LEU	LYS	MET	PHE	PRO	TRP	TYR	VAL
I	(Asn ¹¹)	56.40	37.98	0.0	53.7	3.9	1.3	0.9	2.4	0.1	18.0	0.0	0.2	19.0	0.4
II	(Leu ¹²)	58.25	41.94	0.0	0.0	10.2	11.6	56.0	0.0	0.0	11.3	0.0	0.0	11.0	0.0
III	(Lys ¹³)	60.74	32.51	0.8	0.0	0.0	0.1	0.0	28.1	5.9	0.0	25.3	4.0	0.0	35.3
IV	(Lys ¹⁴)	59.38	32.35	3.7	0.0	0.0	0.0	0.0	43.6	28.4	0.0	4.0	5.8	0.0	9.0

^a Labeled as spin systems I, II, III, and IV.

^b Only amino acid types that have a probability of at least 2% for one of the four spin systems are listed.

TABLE 3
PROBABILITY OF PRIMARY SEQUENCE POSITIONS FOR STRETCHES OF J-CONNECTED RESIDUES,
LISTED IN TABLE 2^a

Strands of length 2:

I + II		II + III		III + IV	
43.8	Asn ¹¹ – Leu ¹²	26.3	Leu ¹² – Lys ¹³	17.8	Val ⁸⁰ – Lys ⁸¹
14.7	Phe ³⁰ – Leu ³¹	26.3	Leu ³⁴ – Lys ³⁵	17.8	Val ⁶ – Lys ⁷
8.8	Asn ⁶⁰ – Phe ⁶¹	6.8	Ile ⁵⁰ – Val ⁵¹	14.2	Lys ¹³ – Lys ¹⁴
8.6	Asn ⁹⁸ – Tyr ⁹⁹	6.5	Tyr ⁵ – Val ⁶	14.2	Lys ⁸⁷ – Lys ⁸⁸
3.2	Asp ¹⁰³ – Leu ¹⁰⁴	6.0	Asp ²² – Val ²³	14.2	Lys ⁸⁸ – Lys ⁸⁹

Strands of length 3:

I + II + III		II + III + IV	
76.7	Asn ¹¹ – Leu ¹² – Lys ¹³	79.2	Leu ¹² – Lys ¹³ – Lys ¹⁴
15.5	Asn ⁶⁰ – Phe ⁶¹ – Lys ⁶²	19.5	Tyr ⁵ – Val ⁶ – Lys ⁷
5.5	Tyr ⁵⁴ – Phe ⁵⁵ – Lys ⁵⁶		

Strands of length 4:

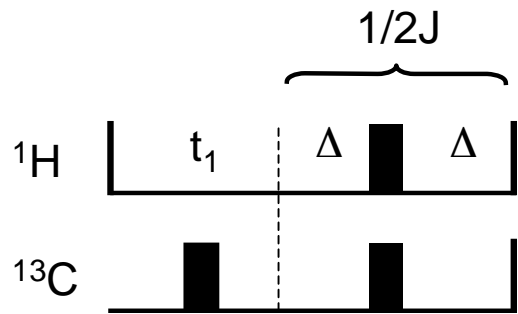
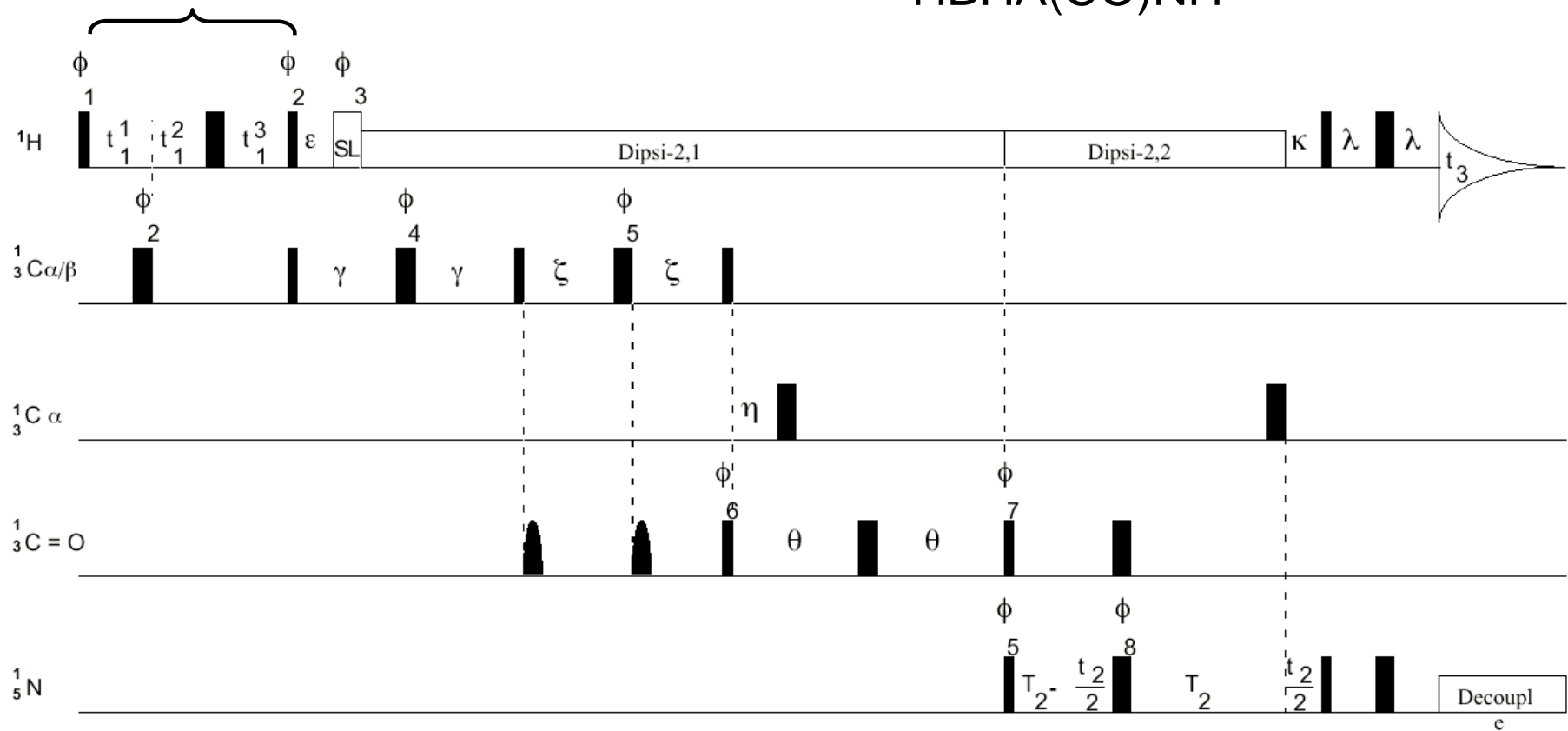
I + II + III + IV	
100.0	Asn ¹¹ – Leu ¹² – Lys ¹³ – Lys ¹⁴

^a The probability for locating stretches of length 2, 3, and 4, which can be generated from spin systems I–IV of Table 2, in the primary sequence of interferon- γ are calculated according to Eq. 20. The positions in the primary sequence have been ordered according to decreasing probabilities. The five most probable positions are listed, if their probability exceeds 1%.

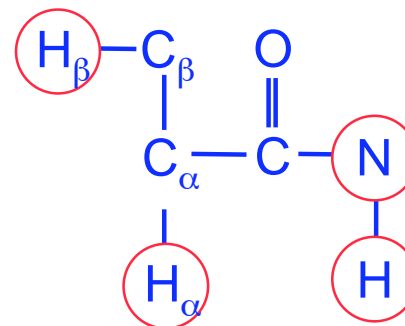
program seqprob available
@ <http://www.biozentrum.unibas.ch/~grzesiek/>

Semi-constant time

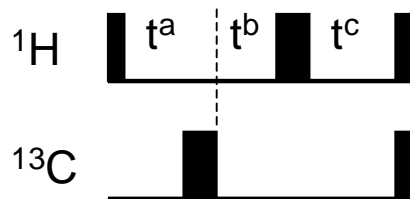
HBHA(CO)NH



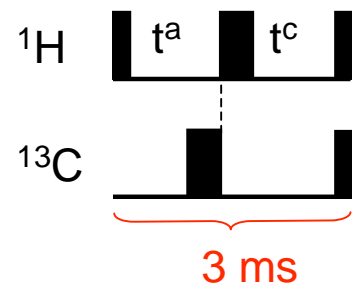
(old)



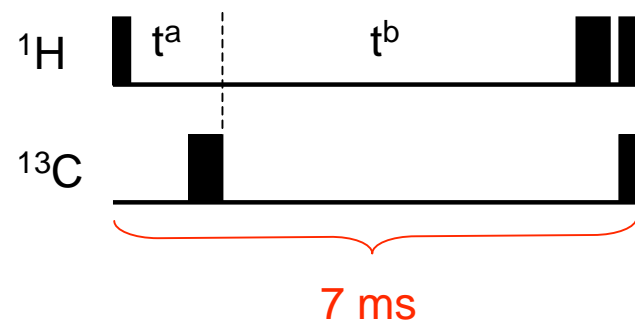
Semi constant time



acquisition start:



acquisition end:



chem. shift evolution: $t^a + t^b - t^c$

$$\Rightarrow 1/\text{sw} = \Delta t^a + \Delta t^b - \Delta t^c$$

J-dephasing: $t^a - t^b + t^c \sim 1/(2J) = \text{constant}$

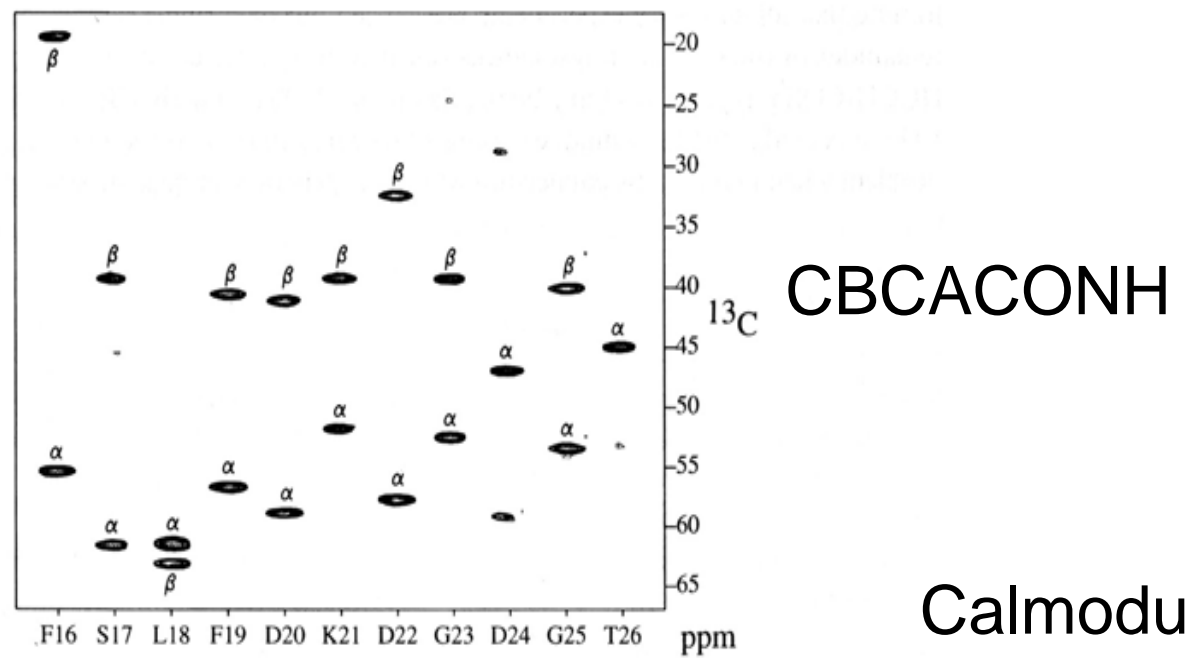
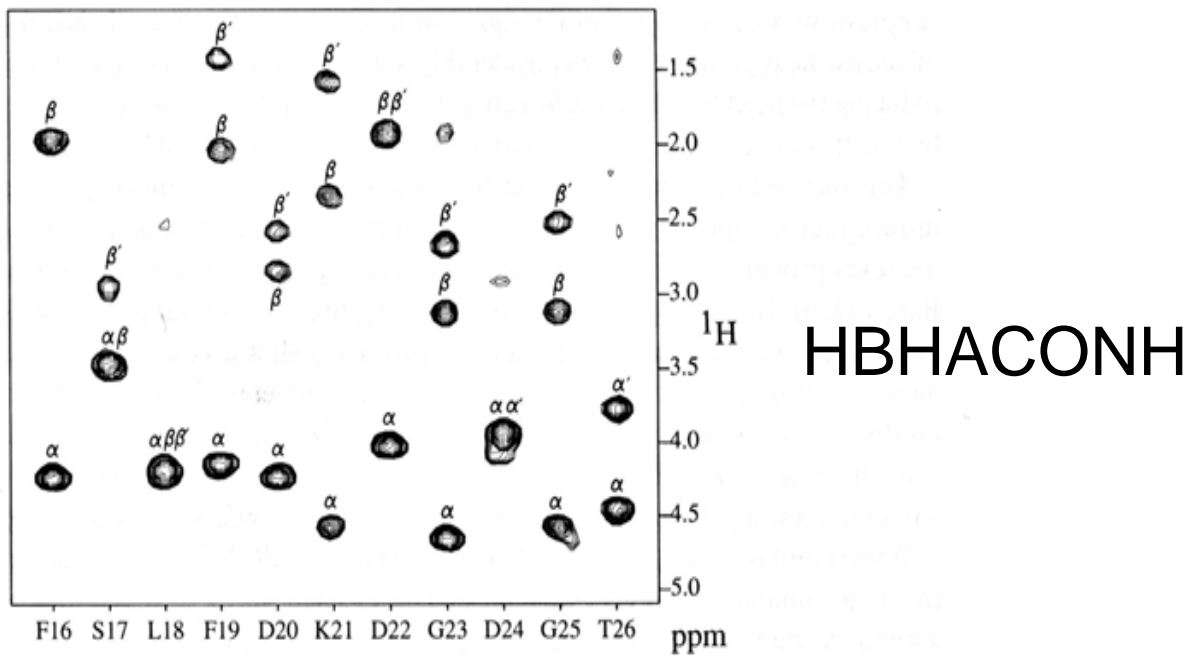
$$\Rightarrow \Delta t^a - \Delta t^b + \Delta t^c = 0$$

chem. shift evolution: 0

J-dephasing: $0.8/(2J)$

chem. shift evolution: $t_{\text{aq}} = t^a + t^b$

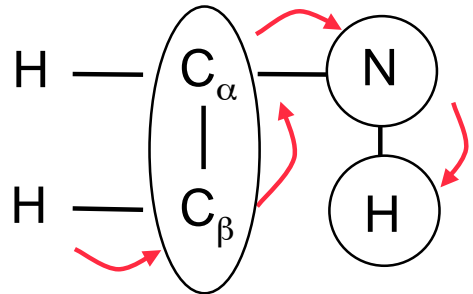
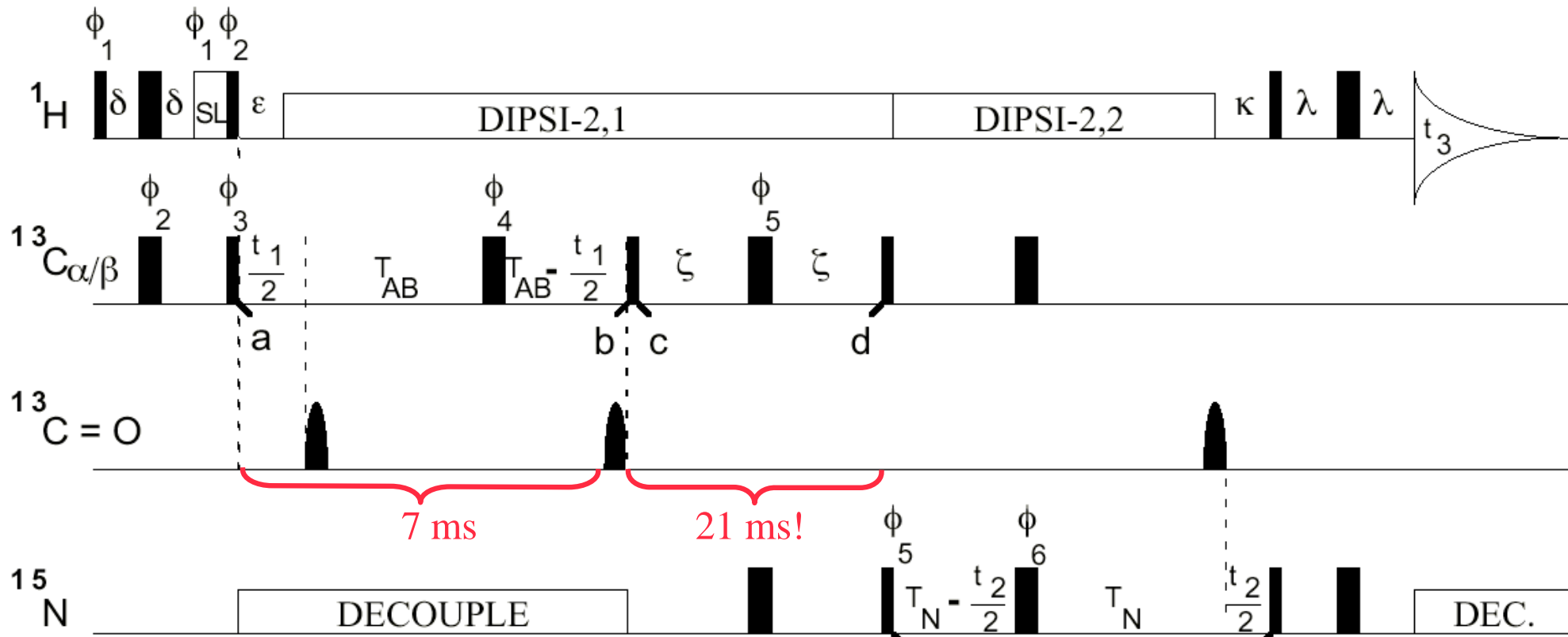
J-dephasing: $1/(2J)$



Calmodulin + M13 (20 kDa)

Fig. 4. Strip plot of the correlations observed for the amides of residues Phe¹⁶-Thr²⁶ of the calmodulin-peptide complex. Each amide correlates (A) with the H^α and H^β of the preceding residue or (B) with the corresponding C^α and C^β frequencies. Resonances which are not marked by α or β correspond to correlations to amide ¹H-¹⁵N pairs that are close in frequency to the one for which the strip has been selected.

CBCANH, J. Mag. Reson. 99, 201 (1992)



"one way"

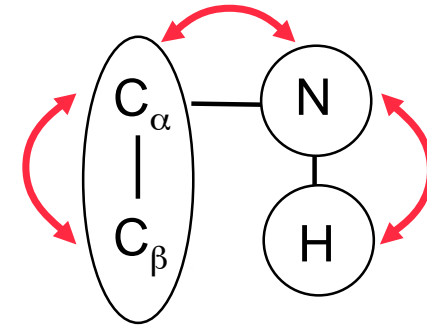
$S/N = \text{HNCO} * (0.03-0.06)$

"out + back"

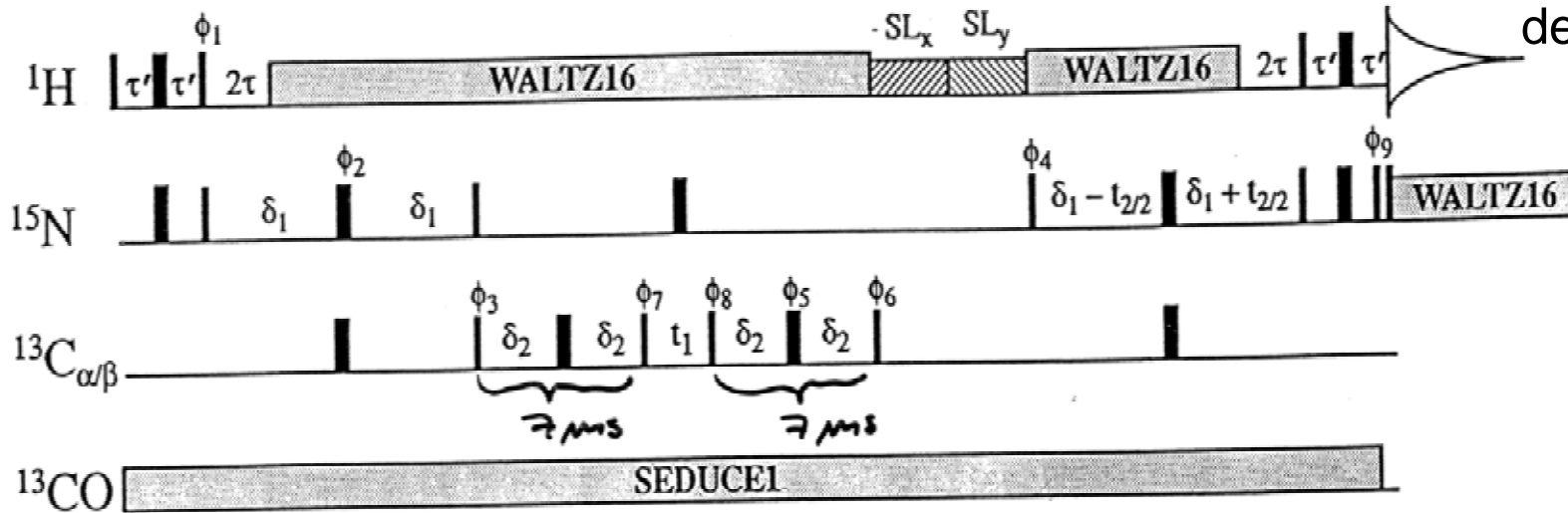
HNCACB

JOURNAL OF MAGNETIC RESONANCE, Series B 101, 201-205 (1993)

MICHAEL WITTEKIND AND LUCIANO MUELLER

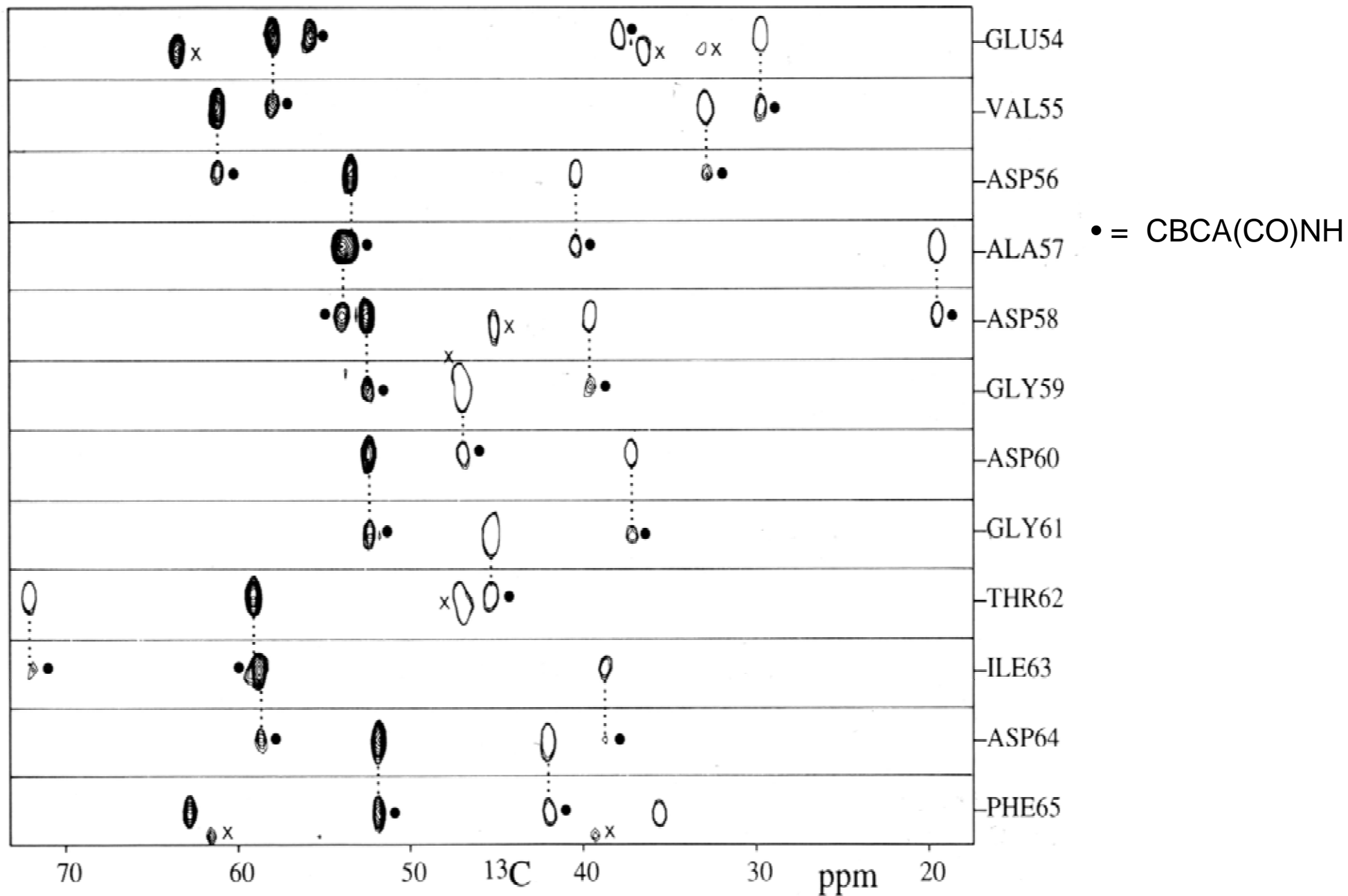


works also with deuterated proteins

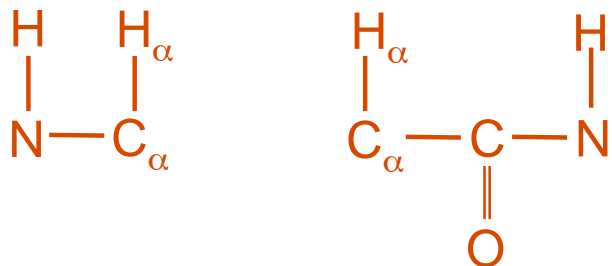


$$S/N = \text{HNCO} * 0.09$$

CBCANH of CaM/M13 ~ 20 kDa



4D HNCAHA, HN(CO)CAHA



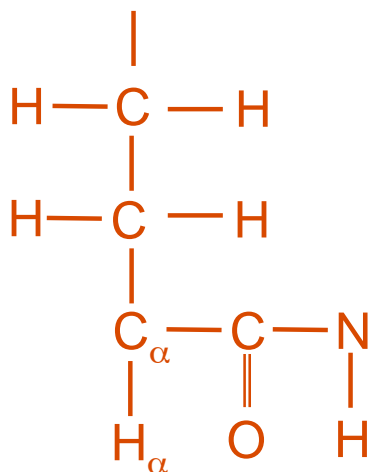
Boucher + Laue, J. Am. Chem. Soc. 114, 2262 (1992)

Olejniczak + al., J. Magn. Reson. 100, 444 (1992)

Kay et al., J. Magn. Reson. 98, 443 (1992)

...

Sidechain C-C-TOCSY to (CO)NH



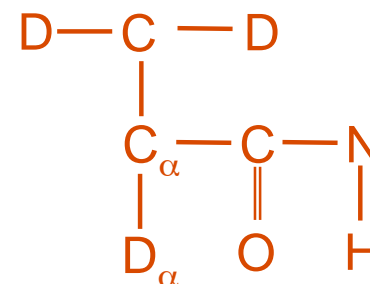
Logan et al., FEBS Lett. 314, 413 (1992)

Montelione et al., JACS, 114, 10974 (1992)

Grzesiek et al., J. Magn. Reson. B 101, 114 (1993)

HN(CO)CACB

(out + back, deuteration!)

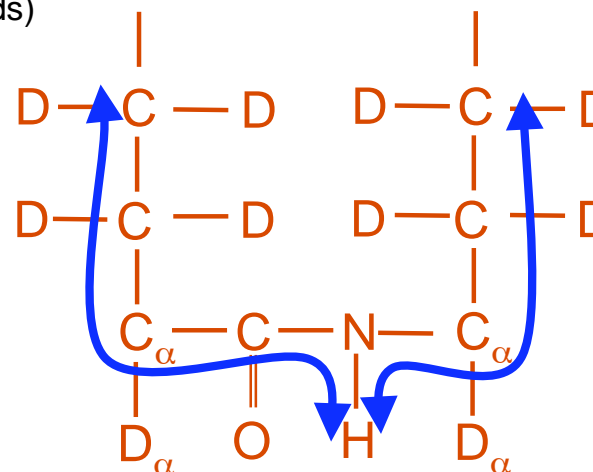


Yamazaki et al. (1994), JACS, 116, 11655.

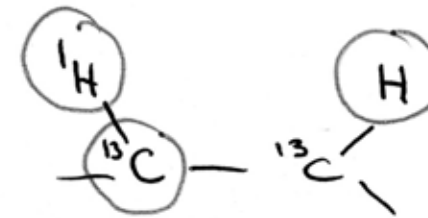
Salzmann et al., JACS, 1999, 121, 844

Sidechain C-C-TOCSY from CANH

(out + back, deuteration!, carbonyl relaxation at high fields)



Löhr and Rüterjans, J. Magn. Reson. 156, 10 (2002)



HCCH - COSY

Practical Aspects of Proton-Carbon-Carbon-Proton Three-Dimensional Correlation Spectroscopy of ^{13}C -Labeled Proteins

AD BAX, G. MARIUS CLORE, PAUL C. DRISCOLL, ANGELA M. GRONENBORN, MITSUHIKO IKURA, AND LEWIS E. KAY

Laboratory of Chemical Physics, NIDDK, National Institutes of Health, Bethesda, Maryland 20892

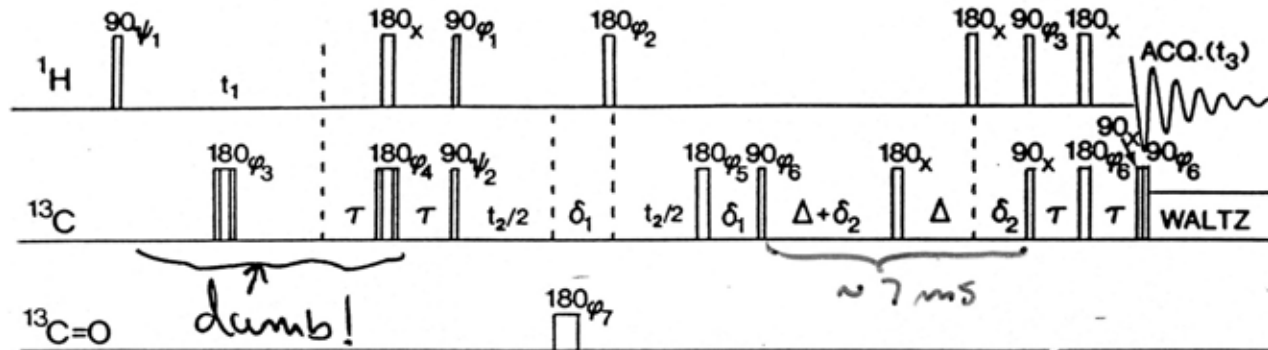


FIG. 1. Pulse sequence of the HCCH 3D experiment. For adequate suppression of artifacts, the sequence requires a 16-step phase cycle: $\phi_1 = y, -y$; $\phi_2 = 4(x), 4(y), 4(-x), 4(-y)$; $\phi_3 = 8(x), 8(-x)$; $\phi_4 = 2(x), 2(-x)$; $\phi_5 = 2(x), 2(y), 2(-x), 2(-y)$; $\phi_6 = 4(x), 4(-x)$; $\phi_7 = 8(x), 8(y)$; Acq. = $2(x, -x, -x, x), 2(-x, x, x, -x)$. The ^{13}C carrier is positioned in the center of the aliphatic region and the $180^\circ_{\phi_7}$ carbonyl pulse is generated by means of a DANTE sequence. The $180^\circ_{\phi_3}$ and $180^\circ_{\phi_4}$ pulses are of the composite type $(90^\circ_x 180^\circ_y 90^\circ_x)$. Quadrature in the F_1 and F_2 dimensions is obtained with the TPPI-States method (19), using $\psi_1 = 16(x), 16(y)$; $\psi_2 = 32(x), 32(y)$. Each time t_1 is incremented, the receiver reference phase and ψ_1 are also incremented by 180° . Each time t_2 is incremented the receiver phase and ψ_2 are also incremented by 180° . Data obtained for $\psi_1 = x, y$ and $\psi_2 = x, y$ are stored separately and processed as complex data.

HCCH-COSY

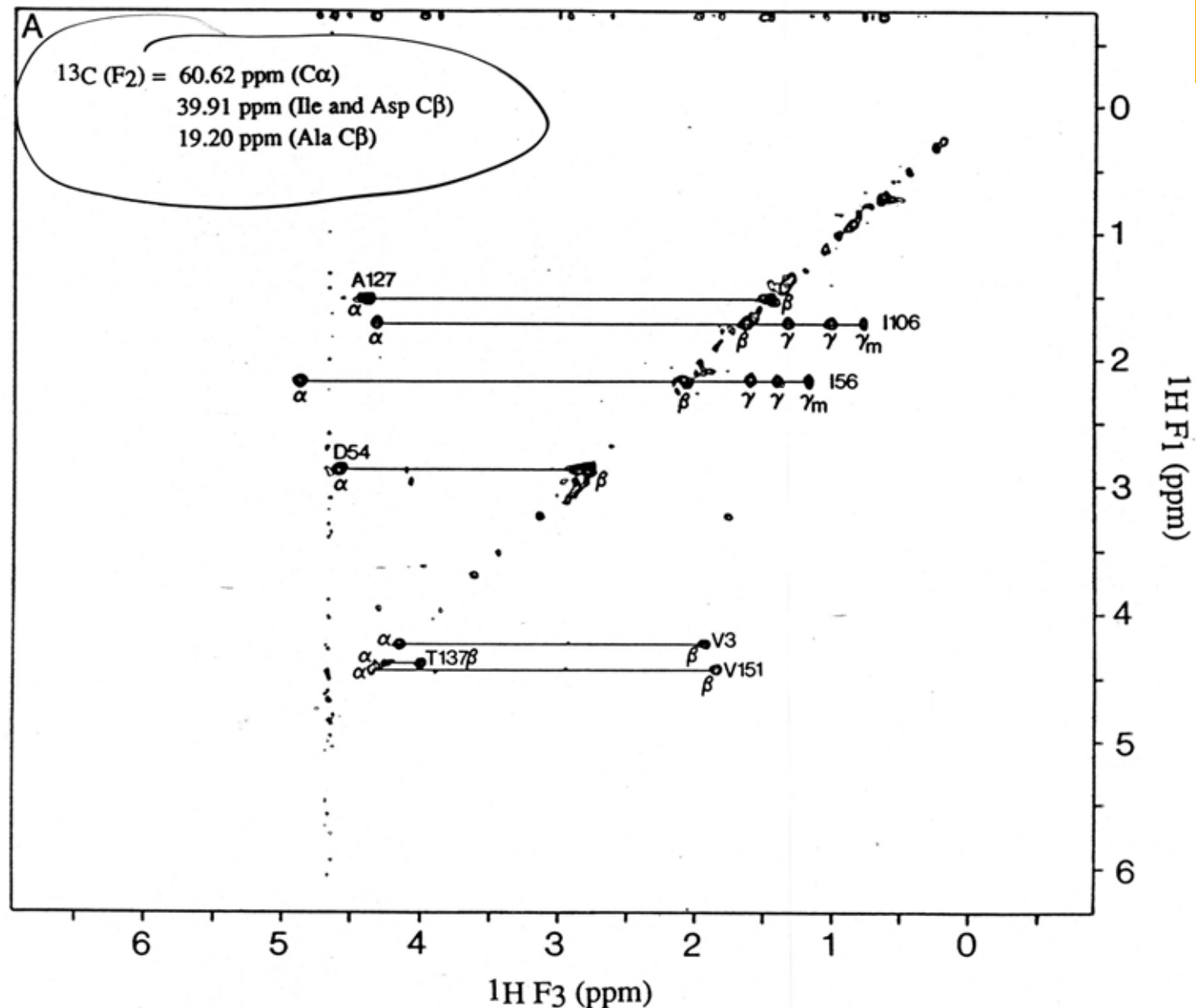
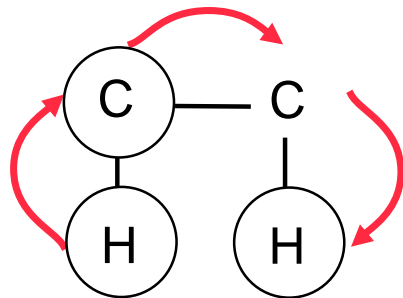
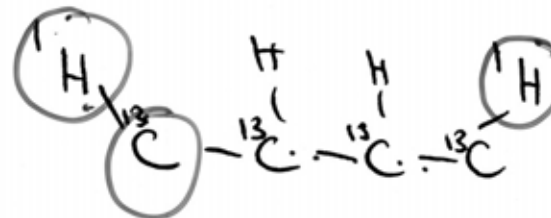


FIG. 2. F_1 , F_3 slices of the 3D HCCH spectrum of interleukin- 1β , recorded at 600 MHz. Because of extensive folding utilized in the F_2 dimension, each slice corresponds to three ^{13}C chemical shifts, indicated in each panel. Separation between slices in the F_2 dimension is 0.32 ppm (48 Hz). Diagonal resonances correspond to one-bond correlations between $^{13}\text{C} (F_2)$ and $^1\text{H} (F_1 = F_3)$ chemical shifts; cross peaks originate from magnetization transfer to protons that are geminal or vicinal with respect to the protons on the diagonal.

HCCH - TOCSY



¹H-¹H Correlation via Isotropic Mixing of ¹³C Magnetization, a New Three-Dimensional Approach for Assigning ¹H and ¹³C Spectra of ¹³C-Enriched Proteins

AD BAX, G. MARIUS CLORE, AND ANGELA M. GRONENBORN

Fesik et al. JACS 112, 886 (1990)

Kay et al. (gradient-enhanced H₂O) J. Magn. Reson. B 101, 333 (1993)

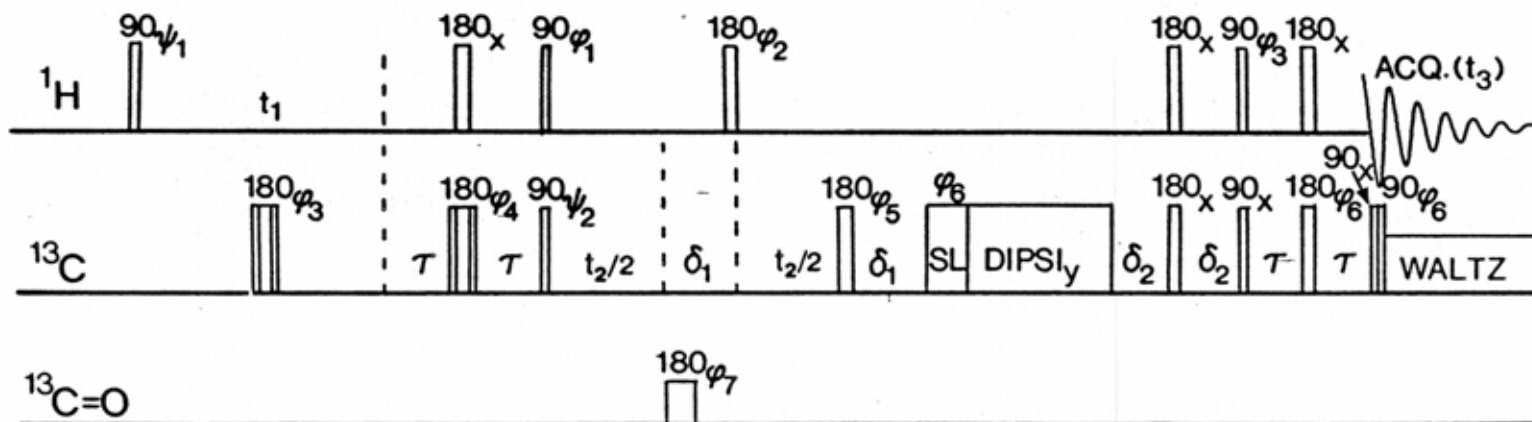
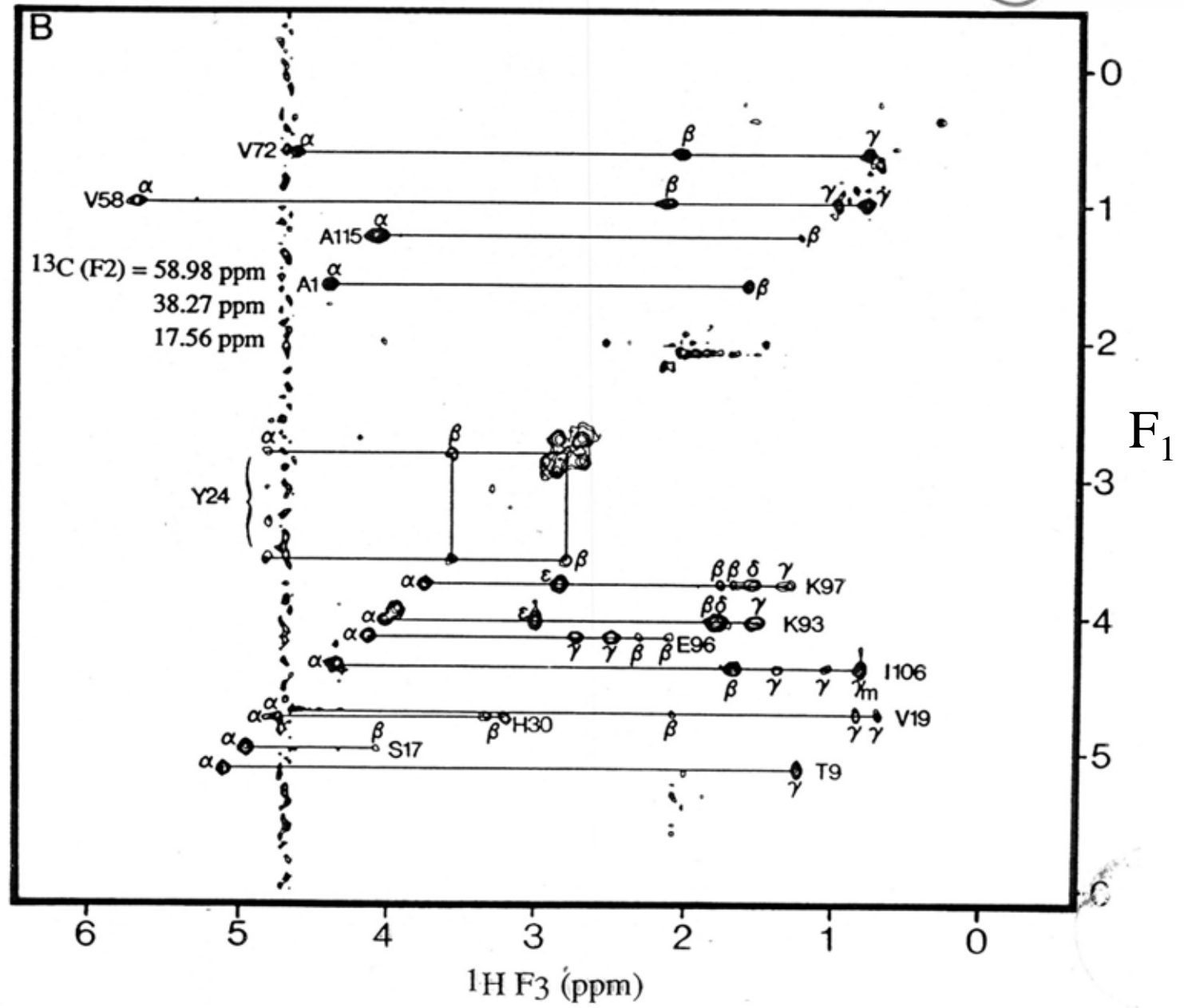
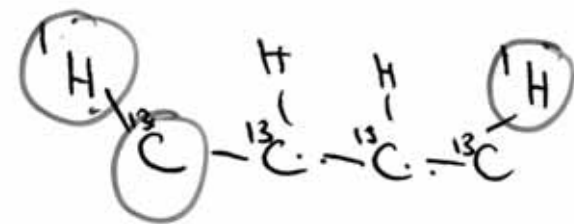


FIG. 1. Pulse scheme of the HCCH-TOCSY experiment. The delays τ are set to $1/(4J_{CH})$, 1.5 ms in practice. The delays δ_1 and δ_2 are set to $\sim 1/(6J_{CH})$, 1.1 ms in practice, to permit net magnetization transfer to and from methine, methylene, and methyl resonances in the same experiment (20). The phase cycling

HC(C)H-TOCSY



Aliasing and baselines

JOURNAL OF MAGNETIC RESONANCE 91, 174–178 (1991)

Removal of F_1 Baseline Distortion and Optimization of Folding in Multidimensional NMR Spectra

AD BAX, MITSUHIKO IKURA, LEWIS E. KAY, AND GUANG ZHU

The effective sampling delay in a multidimensional experiment usually can be calculated in a straightforward manner. For example, in the NOESY experiment,

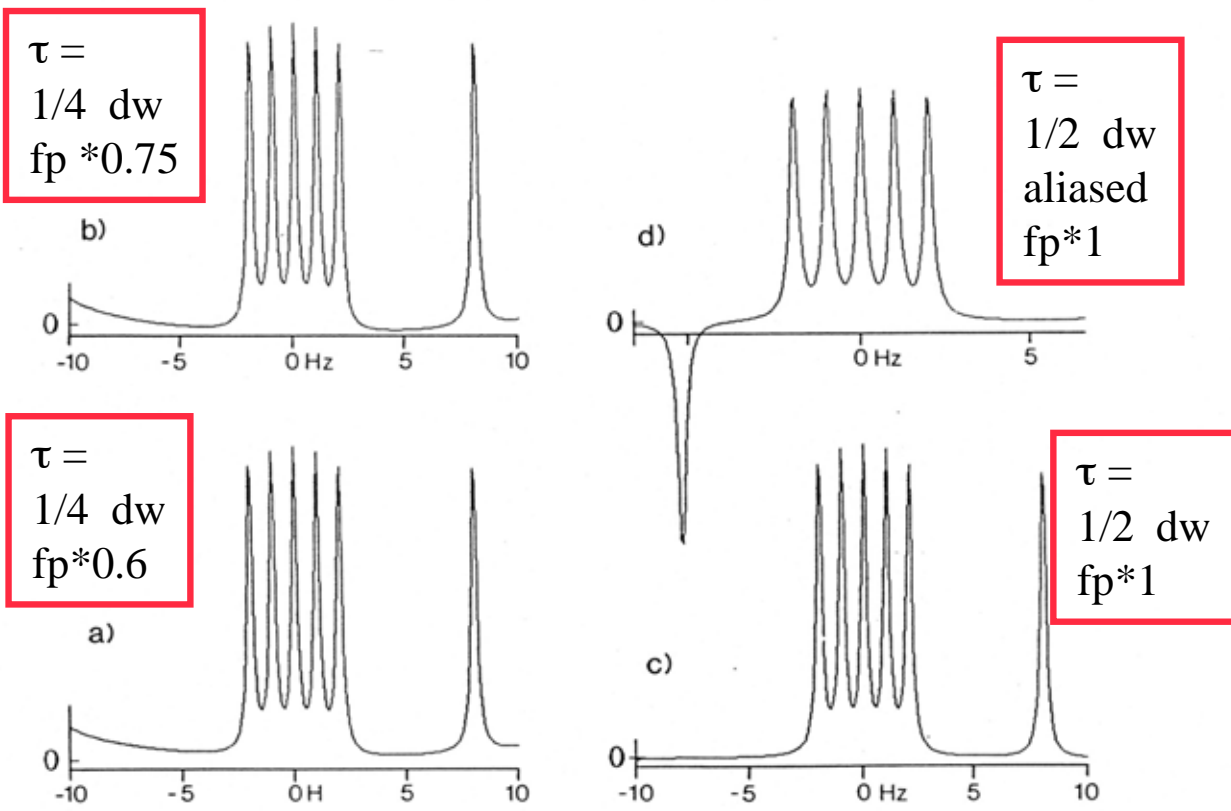
$$90^\circ - t_1 - 90^\circ - T_{\text{mix}} - 90^\circ - \text{Acq.}(t_2),$$

the sampling delay, τ , in the t_1 dimension is given by (10)

$$\tau = 4\tau_{90}/\pi + t_1(0), \quad [1]$$

where τ_{90} is the duration of the 90° pulse, the $t_1(0)$ is the programmed duration for the first t_1 increment (usually $< 2 \mu\text{s}$). For the HMQC experiment,

Flat baselines only for $\tau = 0, 1/2, 1 \text{ dw}$



Zhu et al. (1993),
J. Magn. Reson. A105, 219

FIG. 1. (a, b) Simulated spectra obtained by Fourier transformation of data with an initial sampling delay of one-quarter dwell time. For (a), multiplication of the first data point by 0.75 has been used, for (b) the scaling factor was 0.6. For both (a) and (b) the linear phase correction was 90° across the spectrum. (c) Spectrum obtained for a sampling delay equal to one-half dwell time, with no scaling of the first data point.

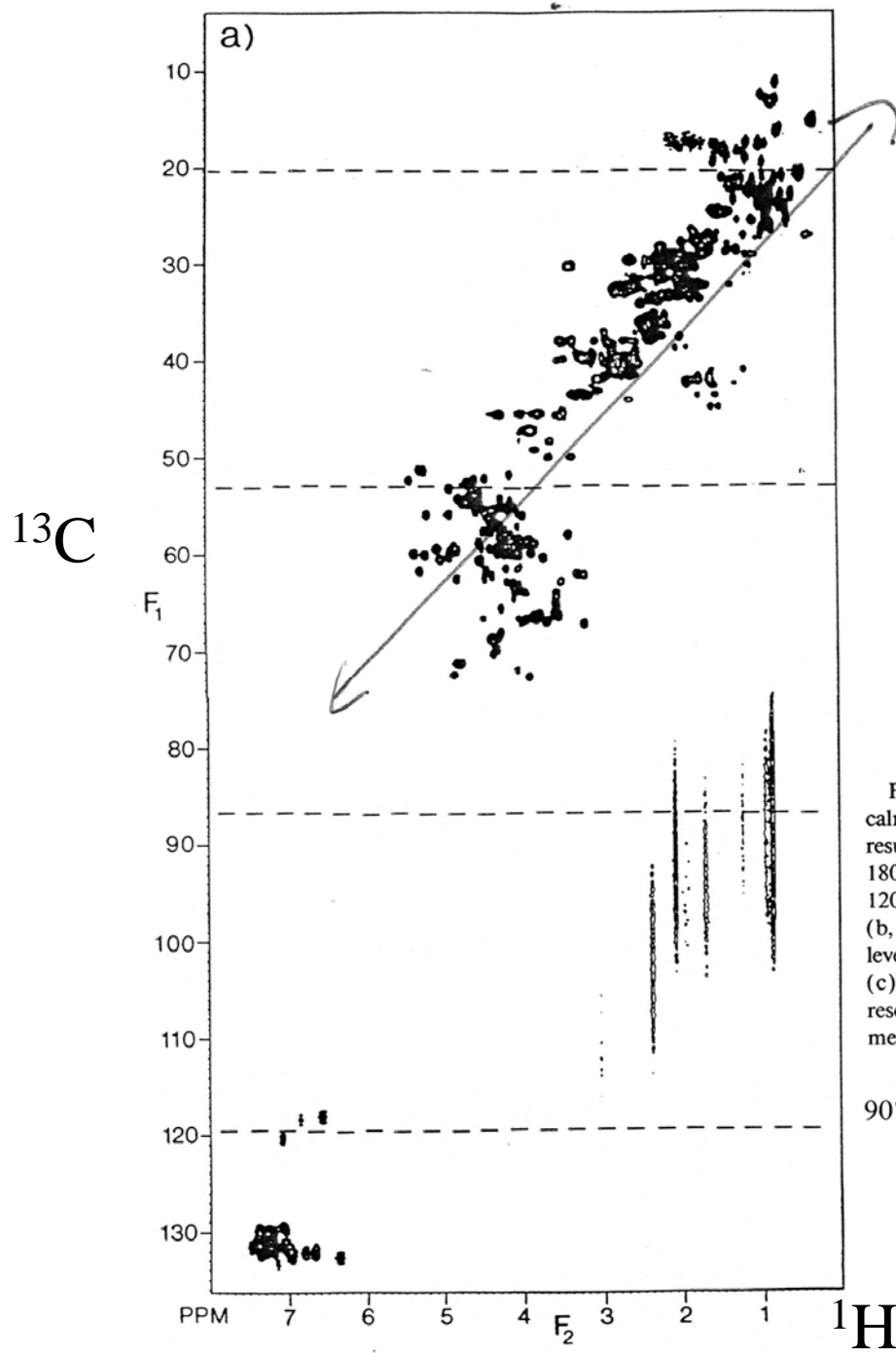


FIG. 2. Heteronuclear multiple-quantum correlation (HMQC) spectra of uniformly ¹³C-enriched (95%) calmodulin in D₂O, recorded at 500 MHz. (a) Regular correlation spectrum, using a *t*₁ increment of 60 μs, resulting in a 132 ppm spectral window in the *F*₁ dimension. The ¹³C 90° pulse width was 40 μs, the ¹H 180° pulse width was 48 μs, and the first *t*₁ duration was set to 20 μs, giving an effective first *t*₁ duration of 120 μs. The broken lines indicate where aliasing occurs when the *F*₁ spectral window is narrowed fourfold. (b, c) HMQC spectrum recorded under identical conditions, but with a *t*₁ increment of 240 μs. (b) Positive levels, corresponding to nonaliased resonances and resonances that have been aliased twice in the *F*₁ dimension. (c) Negative levels, corresponding to resonances that have been aliased once. Because of the relatively strong resolution enhancement digital filtering used in both the *F*₁ and the *F*₂ dimensions, the relatively narrow methyl resonances show an “overenhanced” lineshape, resulting in the lobes marked “x” in (b, c).

$$90^\circ(^1\text{H}) - 1/(2J_{\text{XH}}) - 90^\circ(\text{X}) - t_1/2 - 180^\circ(^1\text{H}) - t_1/2 - 90^\circ(\text{X}) - 1/(2J_{\text{XH}}) - \text{Acq.}(t_2)$$

$$90^\circ(^1\text{H}) - 1/(2J_{\text{XH}}) - 90^\circ(\text{X}) - t_1/2 - 180^\circ(^1\text{H}) -$$

$$t_1/2 - 90^\circ(\text{X}) - 1/(2J_{\text{XH}}) - \text{Acq.}(t_2),$$

NOTES

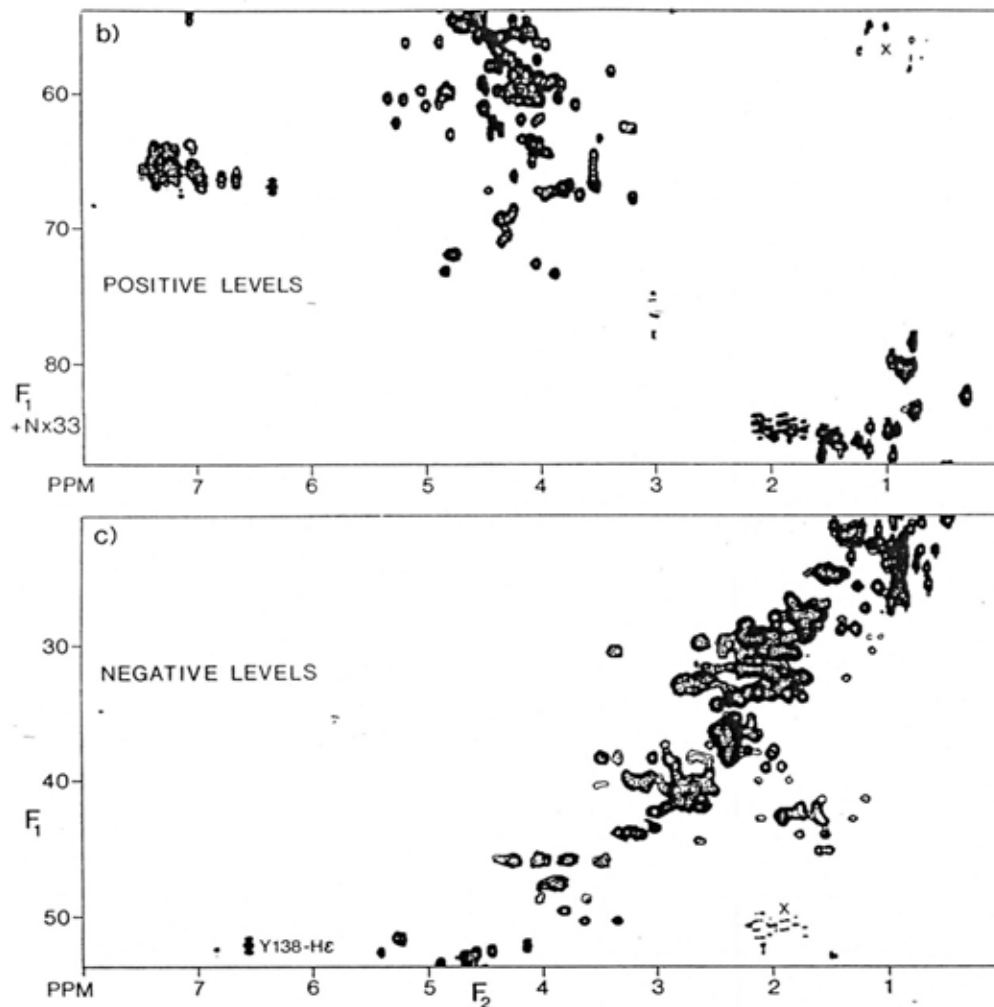


FIG. 2—Continued

Linear (ϕ_1) + constant (ϕ_0) phase correction:

$$\phi_1 = \tau/\Delta t_1 * 360^\circ; \phi_0 = -\phi_1/2$$

E.g. HMQC:

$$\tau = t_1(0) + 4 * p_{90}(\text{X})/\pi + p_{180}(\text{H})$$

where $\tau_{90\text{X}}$ is the duration of a $90^\circ(\text{X})$ pulse and $\tau_{180\text{H}}$ is the ^1H 180° pulse width. If data are acquired in the States format (7), the linear phase correction, ϕ_1 , needed in the F_1 dimension is given by

$$\phi_1 = \tau/\Delta t_1 \times 360^\circ, \quad \phi_0 = -\frac{1}{2} \phi_1 \quad [3]$$

where Δt_1 is the dwell time in the t_1 dimension (t_1 increment). Thus, if sampling is delayed by exactly half a dwell time, a 180° linear phase correction is needed across the spectrum. As a consequence, resonances that have been aliased appear with opposite phase (4), facilitating separation of aliased and nonaliased resonances. This is illustrated in Fig. 1d, where the spectral width has been narrowed down by 33% relative to the spectrum of Fig. 1c. The most upfield resonance now appears aliased and with opposite phase at the lowfield side of the spectrum.

Frequently, extensive aliasing can be used without risking overlap (and cancellation) of aliased and nonaliased resonances, especially for heteronuclear experiments that

Some simple rules for getting flat baselines and good phases (RSH, States-TPPI):

- Flat baselines are only achieved from normal FT, if $t_{\text{initial}} = 0, 0.5 \text{ DW}, \text{ or } 1 \text{ DW}$. [Don't use anything else unless you know what you are doing. t_{initial} is the time for chemical shift evolution for the first digitized data point. For the calculation of t_{initial} , an initial or final 90-degree pulse (that converts z- into transverse magnetization or vice versa) is counted as $2/\pi \cdot \text{pulse length}$.]
- the first order phase correction (phc1) is $\pm t_{\text{initial}}/\text{DW} \cdot 360^\circ$ (\pm depends on program convention). For initial delays of 0, 0.5 DW, and 1 DW, this corresponds to (\pm) $0^\circ, 180^\circ, 360^\circ$ first order phase corrections.
- the contribution to the zero order phase correction from chemical shift evolution is: $\text{phc0} = -1/2 \cdot \text{phc1}$.
- other effects can contribute to the zero order phase correction. Such effects are e.g. Bloch-Siegert phase shifts and hardware phase shifts in the directly detected dimension. These effects should not contribute to the first order phase correction.
- In the case of $\text{phc1} = 0^\circ, 180^\circ, 360^\circ$, the first data point must be multiplied by 0.5, 1.0, and 1.0 respectively, in order to get a flat baseline at value zero.
- In the case of $\text{phc1} = 360^\circ, t_{\text{initial}} = \text{DW}$, a constant baseline correction must be applied after the FT. [Some information was lost (the integral over the spectrum is set to zero) because data sampling started too late. This information is restored by the baseline correction procedure.]

^{15}N (^{13}C) - separated 3D-NOESY-HMQC/HSQC

Fesik + Zuiderweg J.Magn. Reson. (1988), 78, 588

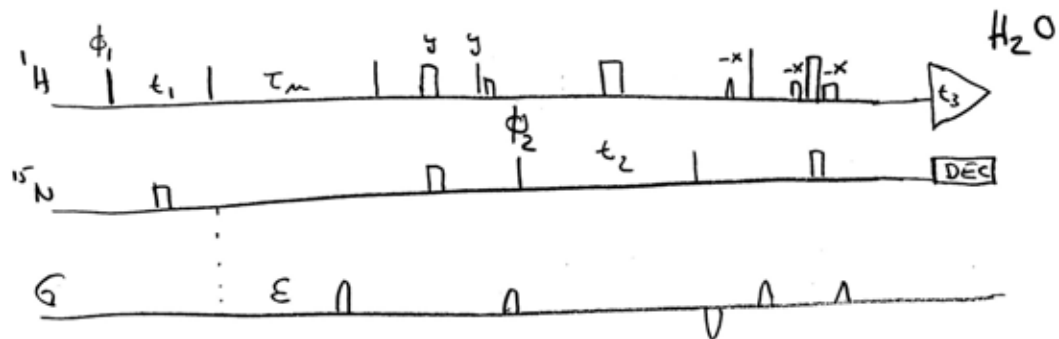
Marion et al. JACS (1989), 111, 1515

Ikura et al. J.Magn. Reson. (1990), 86, 204

Zuiderweg et al. J.Magn. Reson. (1990), 86, 210

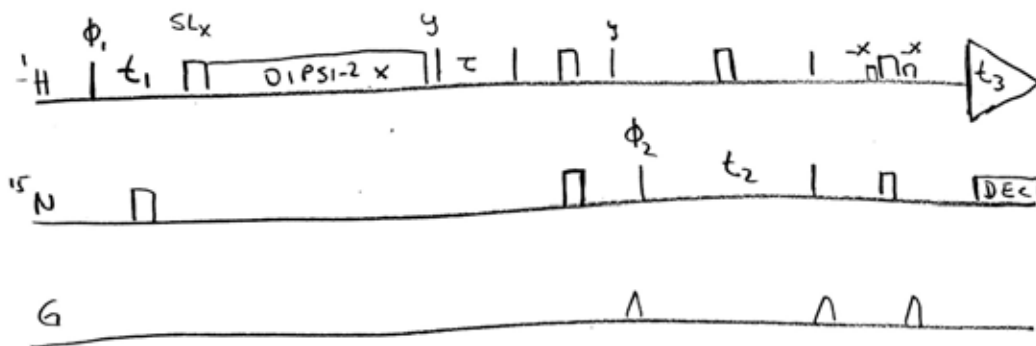
^{15}N - separated 3D HOHAHA ($\text{H}_\text{N}(\text{i})$, $\text{N}(\text{i})$, $\text{H}_\alpha(\text{i})$)

Marion et al. Biochemistry (1989), 28, 6150



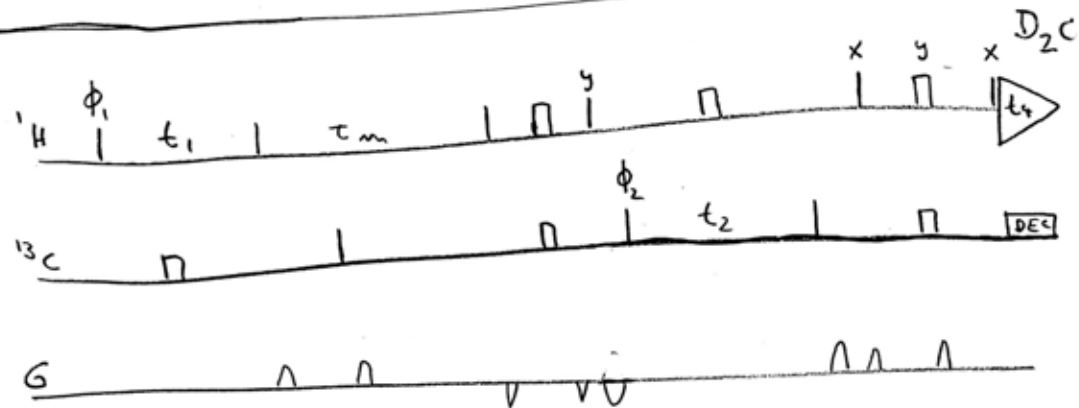
3D ^{15}N -edited NOESY HSQC with water flipback
Lippens et al. J. Biomol NMR 5, 327 (1993)

3D ^{15}N – NOESY



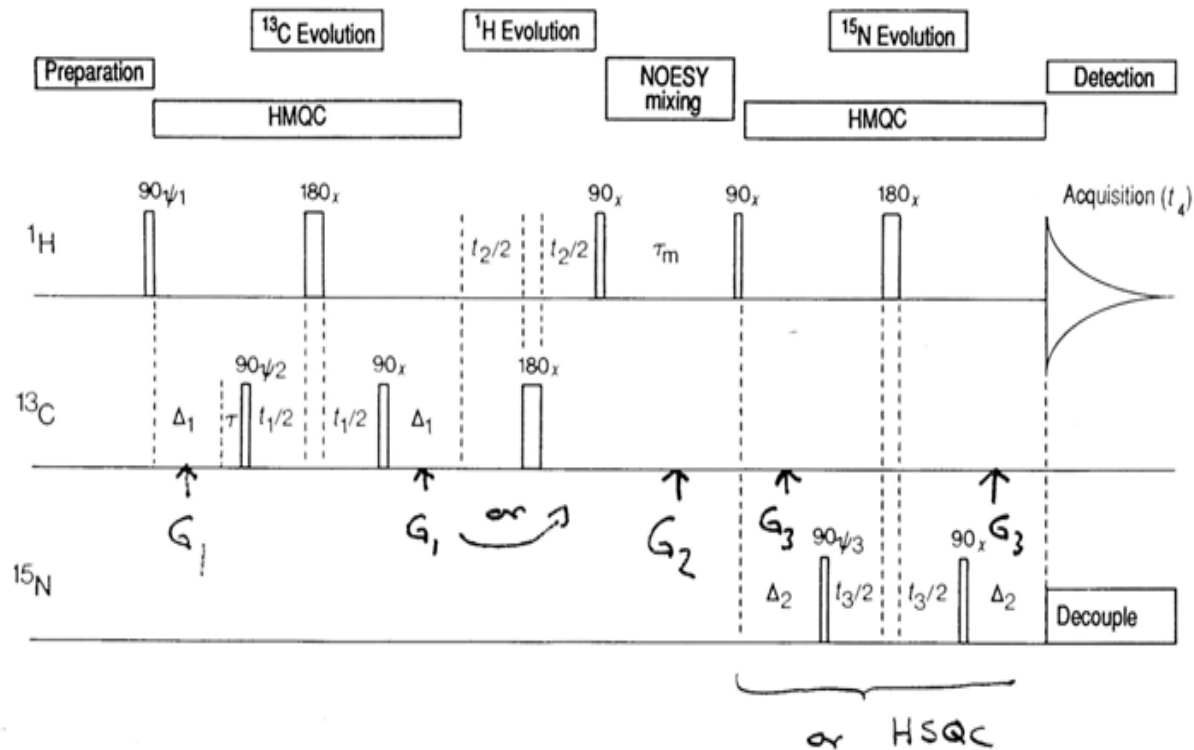
3D ^{15}N -edited HOHAHA - HSQC

3D ^{15}N – HOHAHA



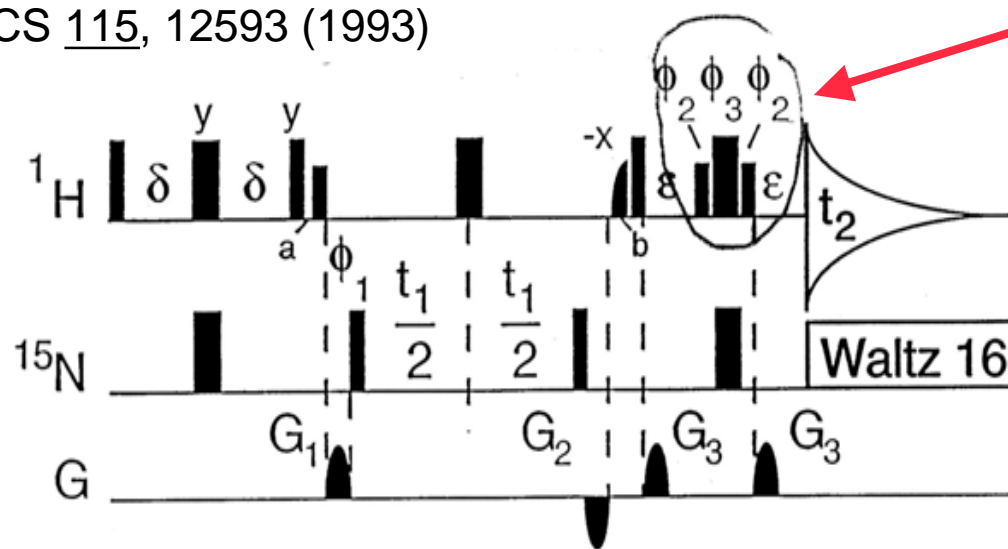
3D ^{13}C -edited NOESY - HSQC

3D ^{13}C – NOESY



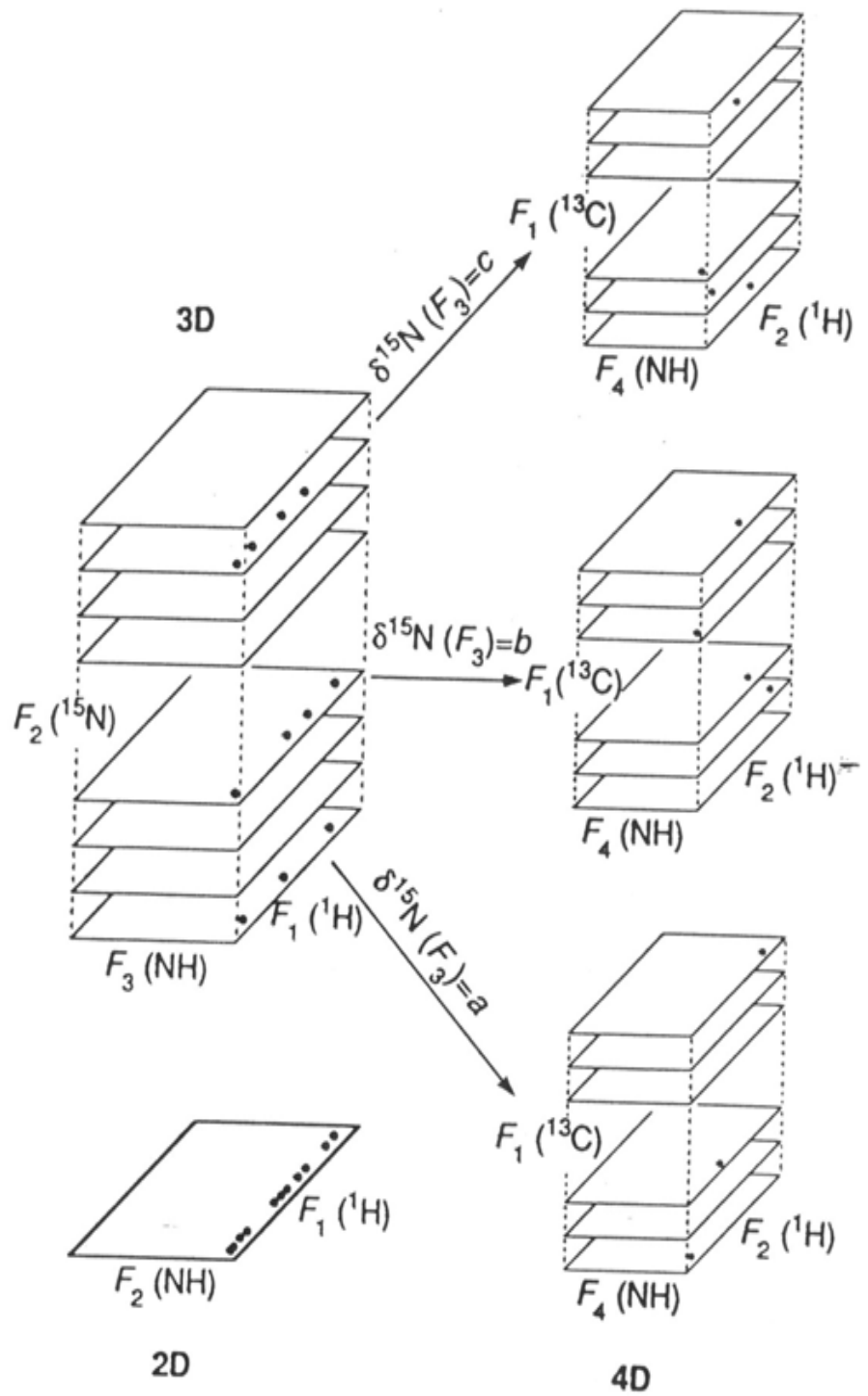
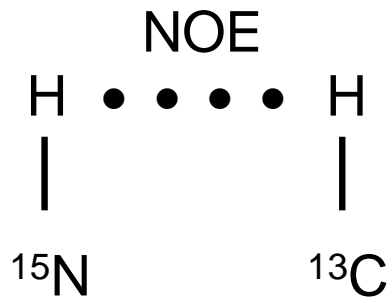
4D ¹³C-, ¹⁵N-separated
NOESY
Kay et al., Science 249, 411
(1990)

JACS 115, 12593 (1993)



"watergate"
Piotto et al.
J. Biomol. NMR 1992

Gradient-enhanced
4D ¹³C/¹⁵N - NOESY:
Muhandiram et al. (1993)
J. Biomol. NMR 3, 463



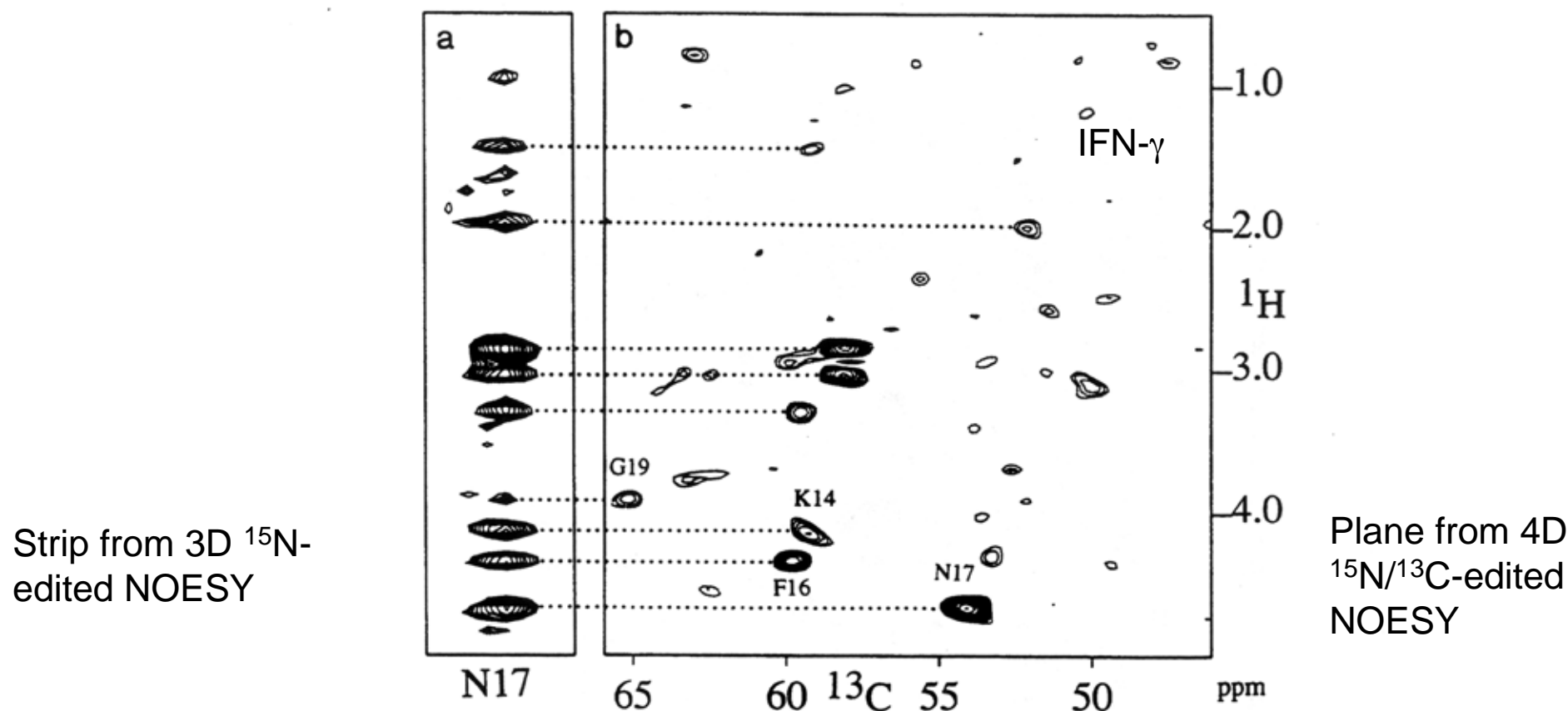


Figure 3. (a) Strip from the ^{15}N -separated 3D NOESY spectrum of interferon- γ displaying the chemical shifts of aliphatic protons that have an NOE with the backbone amide of Asn-17. The strip is actually a narrow vertical band of a 2D cross section, such as shown in Figure 2a. (b) Cross section through the 4D $^{15}\text{N}/^{13}\text{C}$ -separated NOESY spectrum, displaying the chemical shifts of the protons that have an NOE interaction to the amide proton of Asn-17, together with the shifts of the ^{13}C nuclei directly attached to these protons. Broken contours correspond to ^{13}C nuclei in the 46–26 ppm chemical shift range, which have been aliased once in the ^{13}C dimension. Adapted from ref 48.

4D ¹³C-/¹³C-separated NOESY

14 *Biochemistry, Vol. 30, No. 1, 1991*

Accelerated Publications

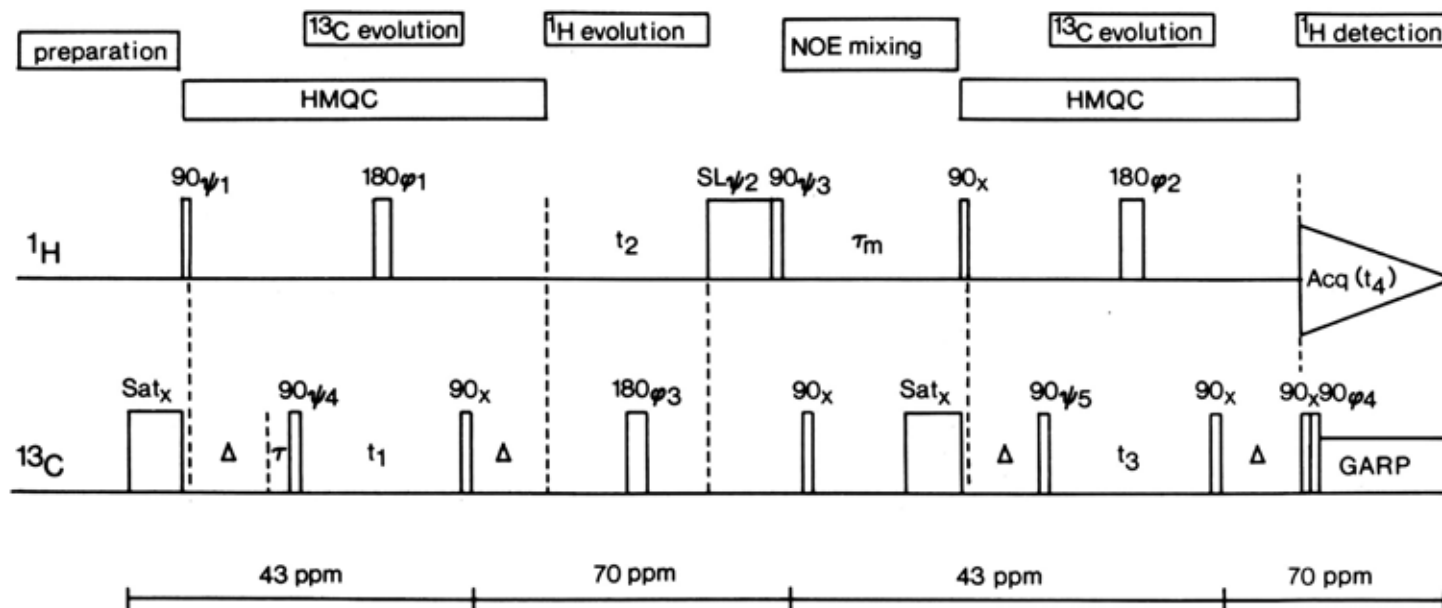


FIGURE 1: Pulse scheme for the 4D ¹³C/¹³C-edited NOESY experiment. The ¹³C 180° pulse is a composite pulse (90_x-180_y-90_x). The eight-step phase cycle is as follows: $\psi_1 = x$; $\psi_2 = -y$; $\psi_3 = x$; $\psi_4 = x, -x$; $\psi_5 = 2(x), 2(-x)$; $\phi_1 = 4(x), 4(y)$; $\phi_2 = 4(x), 4(y)$; $\phi_3 = 2(x), 2(-x)$; $\phi_4 = x, -x$; Receiver = $x, 2(-x), x$. The 1-ms ¹³C saturation pulse (Sat_x) right at the beginning of the sequence prevents magnetization originating on ¹³C spins from being transferred to coupled ¹H spins via a DEPT (Bendall et al., 1981) type mechanism.

Clore et al., *Biochemistry* (1991), 30, 12-18

Zuiderweg et al., *JACS* (1991) 113, 370-372

8 scans, 3-4 days
 8* (C₁) x 64* (H₁) x 8* (C₂) x 256* (H₂)

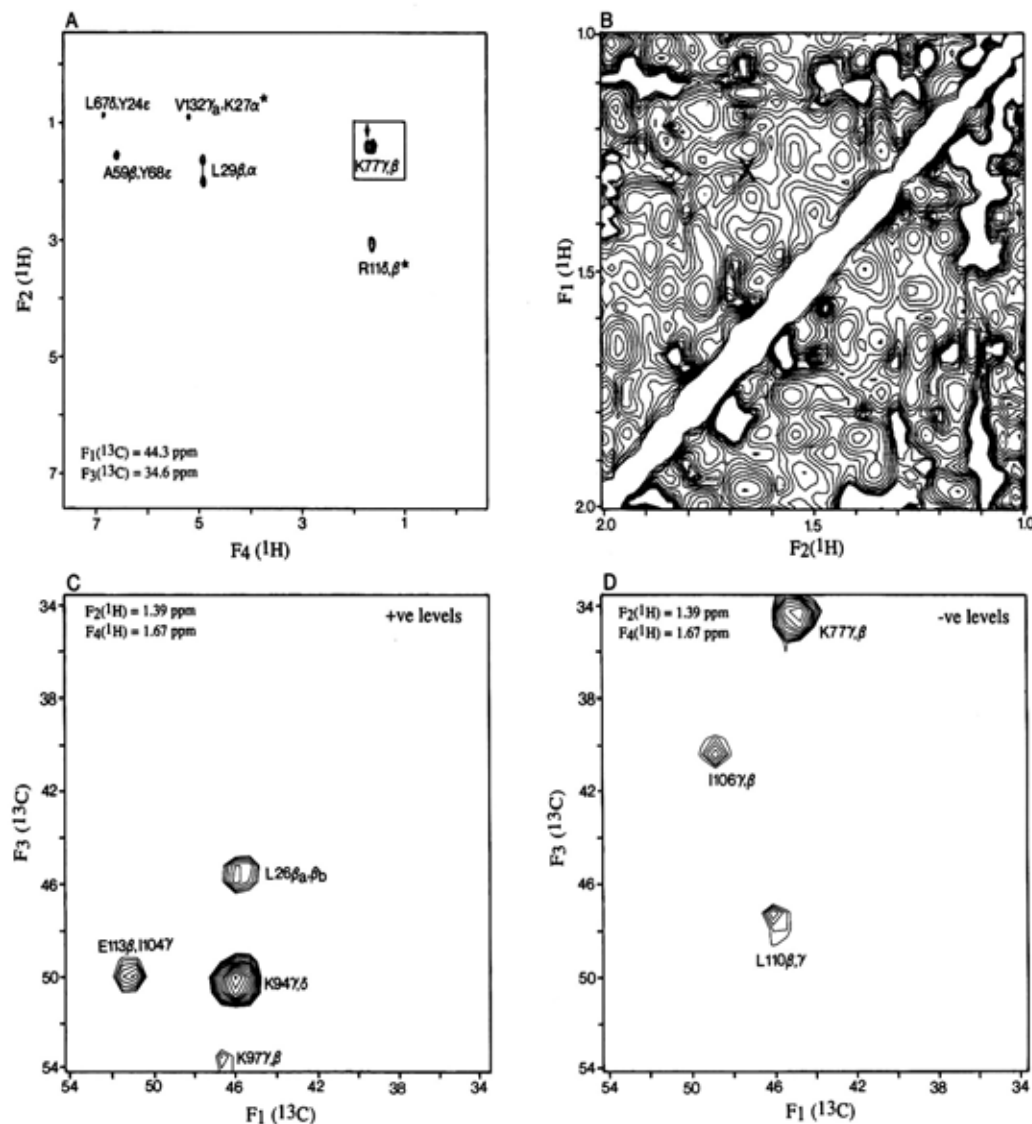


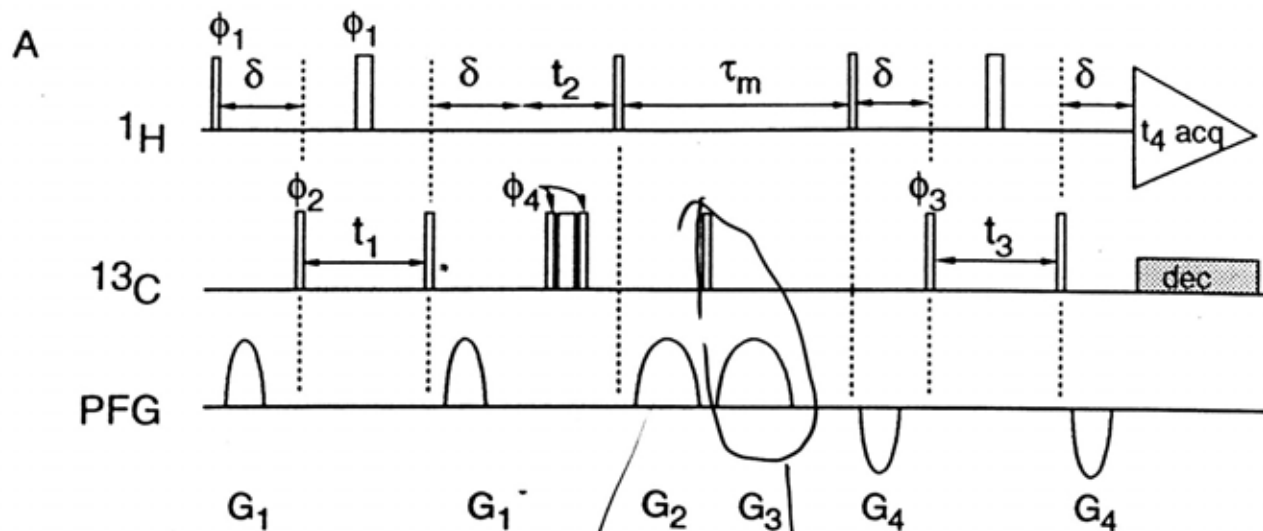
FIGURE 3: Selected $F_2(^1\text{H})-F_4(^1\text{H})$ and $F_1(^{13}\text{C})-F_3(^{13}\text{C})$ planes of the 4D $^{13}\text{C}/^{13}\text{C}$ -edited NOESY spectrum of 1.7 mM uniformly (>95%) $^{13}\text{C}/^{15}\text{N}$ -labeled IL-1 β recorded on a Bruker AM600 spectrometer. (A) $F_2(^1\text{H})-F_4(^1\text{H})$ slice at $\delta F_1(^{13}\text{C}) = 44.3$ ppm and $\delta F_3(^{13}\text{C}) = 34.6$ ppm; (C and D) positive and negative contours of the $F_1(^1\text{H})-F_3(^{13}\text{C})$ plane at $\delta F_2(^1\text{H}) = 1.39$ ppm, $\delta F_4(^1\text{H}) = 1.67$ ppm corresponding to the ^1H chemical shifts of the cross peak between the C^αH and C^βH protons of Lys-77 shown by the arrow in (A); (B) region between 1 and 2 ppm of the 110-ms 2D NOESY spectrum of IL-1 β (with a digital resolution of 6.9 Hz), corresponding to the boxed region shown in (A). [The X marks the ^1H coordinates of the peak indicated by the arrow in (A).] Note that because extensive folding is employed, the ^{13}C chemical shifts are given by $x \pm n\text{SW}$, where x is the ppm value listed in the figure, n is an integer, and SW is the spectral width (20.71 ppm). In (A) there are two positive cross peaks indicated by an asterisk, while the remaining cross peaks are negative. In the peak assignments, the first proton refers to the originating proton, while the second relates to the destination one. It should also be noted that small differences in ^{13}C chemical shifts (up to half a data point ~ 0.4 ppm) with values reported earlier (Clare et al., 1990b) are caused by the software used for peak picking of poorly digitized spectra in the earlier work.

4D Gradient $^{13}\text{C}/^{13}\text{C}$ separated NOESY

Vuister et al., J. Magn. Reson. B 101, 210 (1993)

2 scans!

HMQC - HMQC



HMQC - HSQC

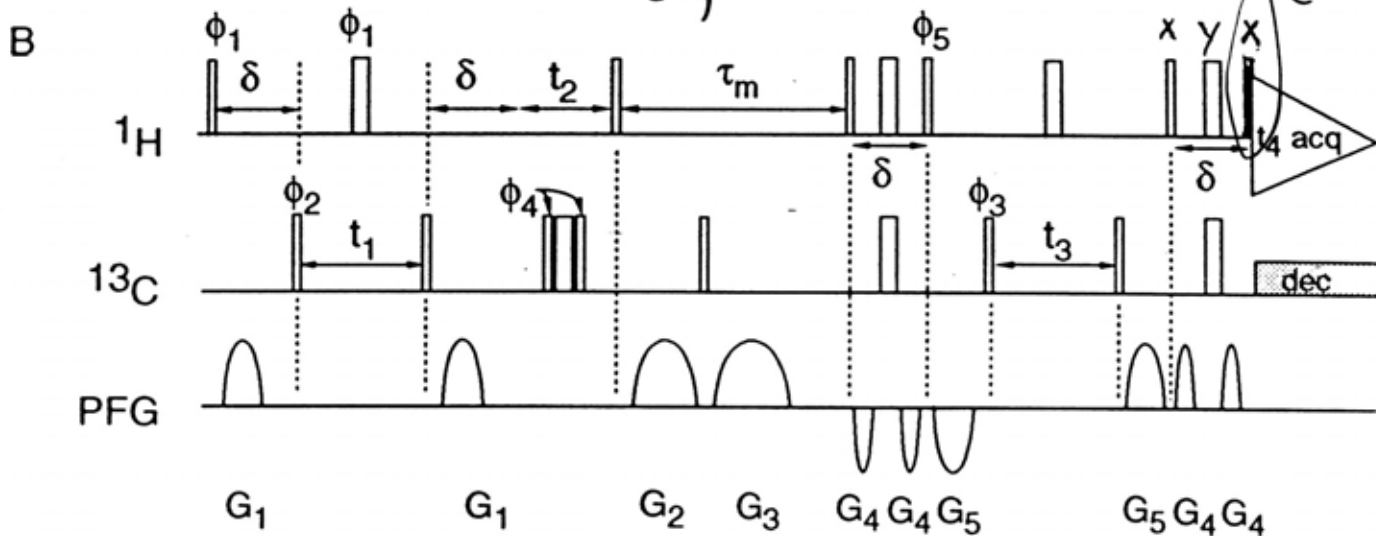
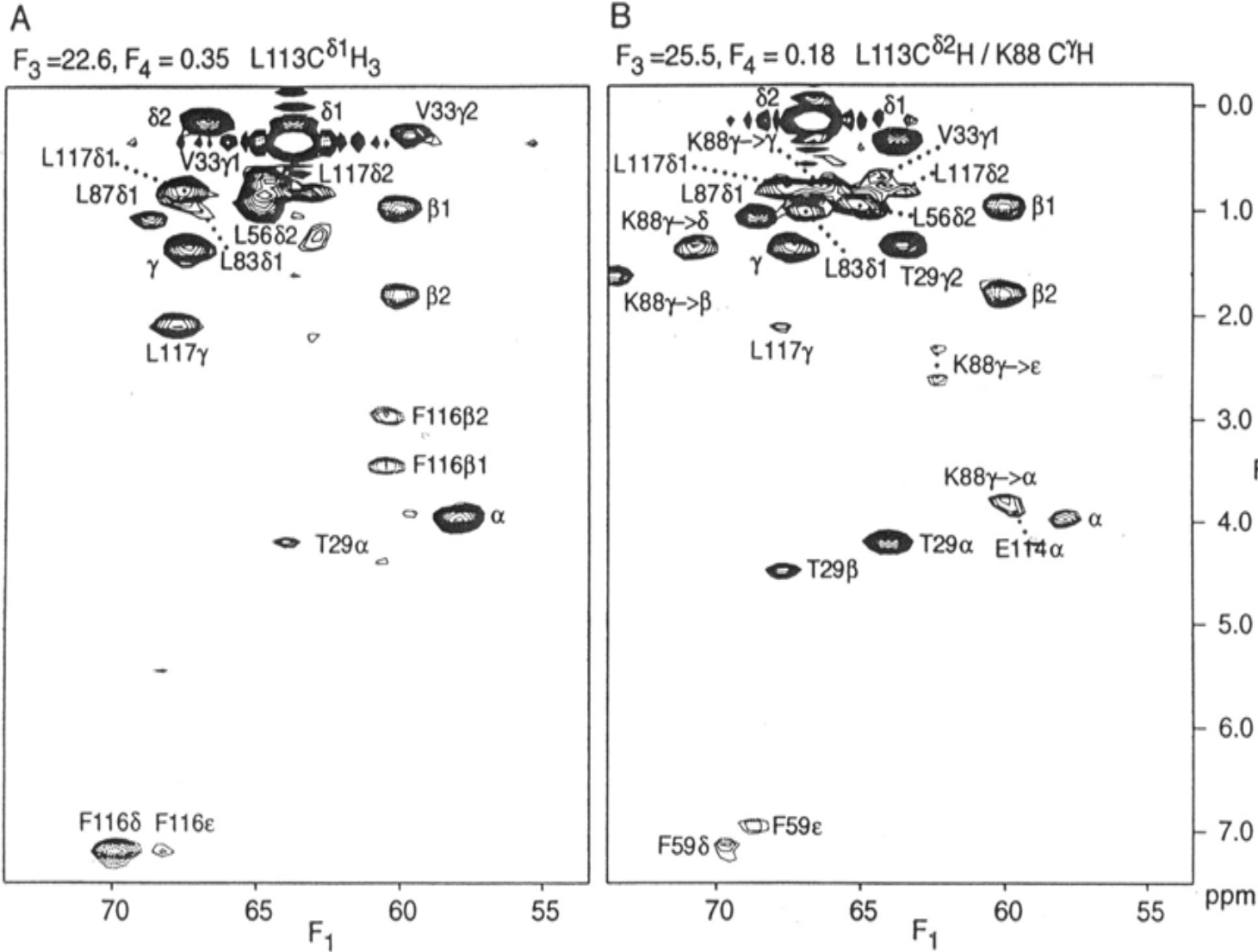


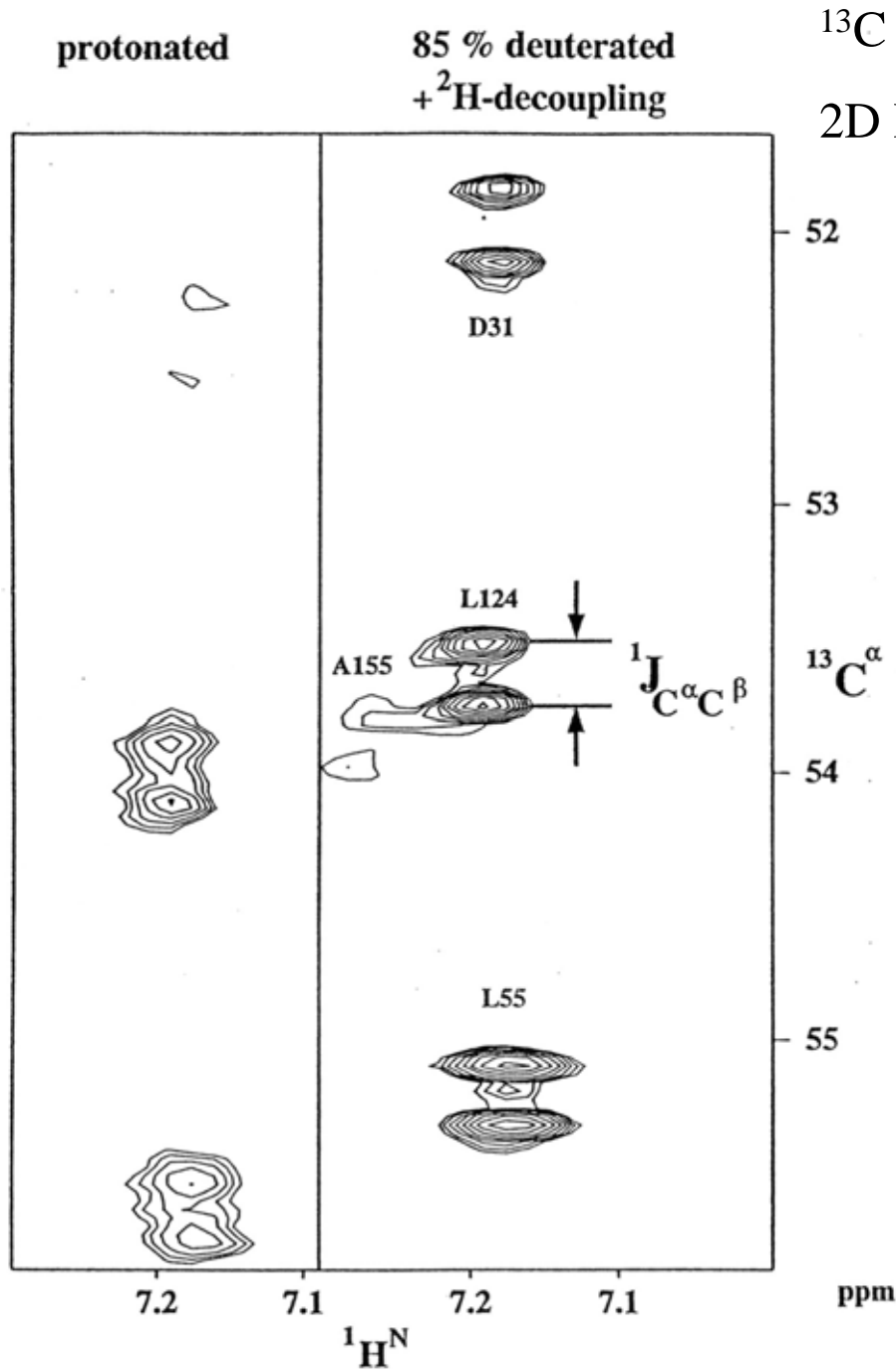
FIG. 1. Pulse schemes for the gradient versions of the 4D $^{13}\text{C}/^{13}\text{C}$ separated HMQC-NOESY-HMQC (A) and HMQC-NOESY-HSQC

COMMUNICATIONS



18* x 64* x 16* x 300*
(4 days)
107 ms mixing
2 scans
zerofilled to
64* x 128* x 64* x 512*
(16 Gbyte)
Reals only: 1 Gbyte

Line narrowing and reduction of spin diffusion by deuteration



¹³C line narrowing by deuteration
2D H(N)CA Calcineurin B 310K

Dipolar relaxation

$$\frac{1}{T_1}, \frac{1}{T_2}, NOE - buildup \propto \frac{\gamma_1^2 \gamma_2^2 S_2 (S_2 + 1)}{r^6}$$

$$\gamma_H / \gamma_D \approx 6.5, \quad S_H = \frac{1}{2}, \quad S_D = 1$$

$$H \rightarrow D: \quad rate \rightarrow rate \frac{8}{3 \cdot 6.5^2} \approx \frac{rate}{16}$$

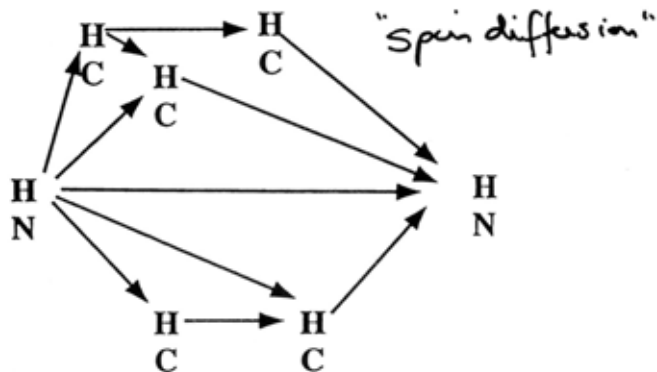
in praxis
≈ 3-4

Multinuclear pulse sequences making use of deuteration:

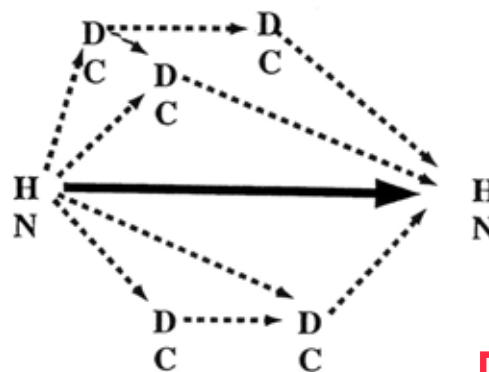
- Grzesiek et al. (1993), JACS, 115, 4369.
- Kushlan & LeMaster (1993), J. Biomol. NMR, 3, 701.
- Yamazaki et al. (1994), JACS, 116, 6464.
- Yamazaki et al. (1994), JACS, 116, 11655.
- Farmer & Venters (1995), JACS, 117, 4187.
- Venters et al. (1995), JACS, 117, 9592.
- Grzesiek et al. (1995), JACS, 117, 9594.
- Venters et al. (1995), J. Biomol. NMR, 5, 339.
- Nietlispach et al. (1996), JACS, 118, 407.
- Shan et al. (1996), JACS, 118, 6570.
- Metzler et al. (1996), JACS, 118, 6800. + ...

+ many
TROSY
sequences

protonated protein:

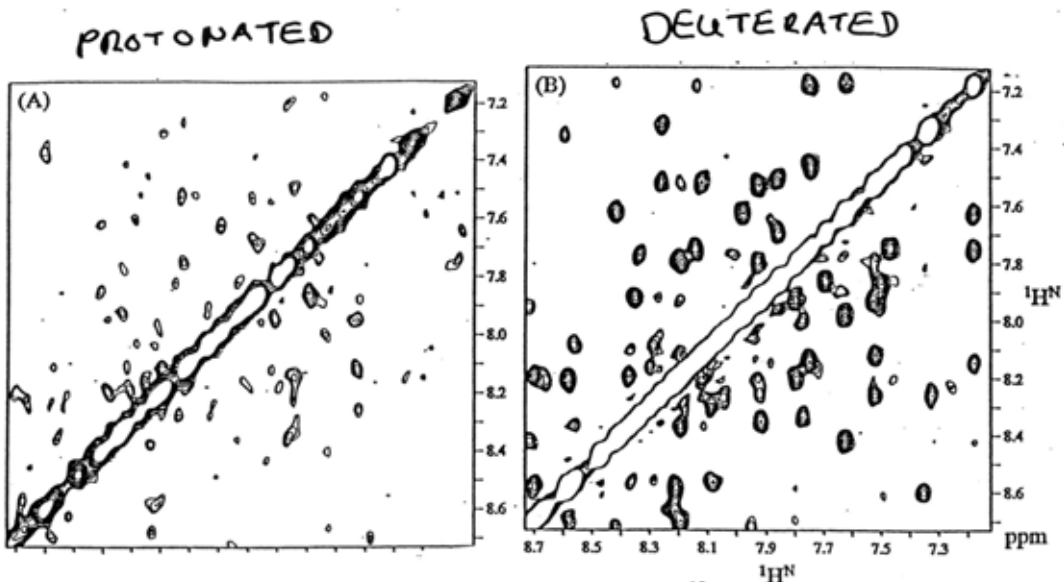


protein deuterated in side chains:



Amide proton to amide proton NOEs

Reduction of spin diffusion by deuteration



Protonated methyl groups on a deuterated background:
 Rosen et al., J Mol Biol 1996, 263:627
 + many more papers from Kay lab

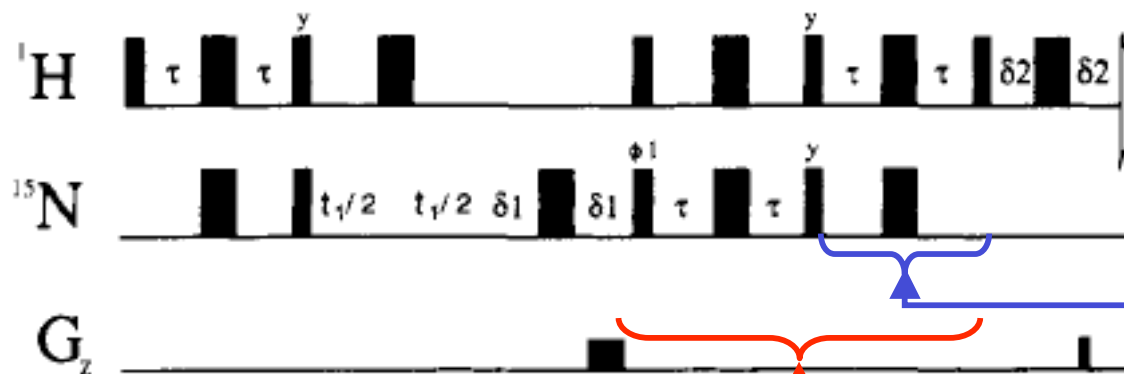
Supplementary Figure 1 Amide region of the ¹⁵N-filtered 2D NOESY spectrum of (A) protonated and (B) perdeuterated HIV-1 nef(39-206), recorded with the scheme of Figure 1, using t₁ = t₃ = 0. Sample concentration: 0.6 mM in a 8 mm sample tube, 35° C, 150 ms NOE mixing. The delay between scans was 1 s for the protonated sample, using 32 scans, and 2.3 s for the perdeuterated sample, using 16 scans. The total acquisition time for each of the 2D spectra was 4.6 h.

JACS 117, 9592
 (1995)
 JACS 117, 9594

4D HNHN NOESY

Sensitivity enhanced scheme: simultaneously record x- and y-component of indirect dimension. Can be used with gradient selection.

10664 *J. Am. Chem. Soc.*, Vol. 114, No. 26, 1992



Gain: $\sqrt{2}$

Cavanagh et al. (1991), *J. Magn. Reson.* 91, 429

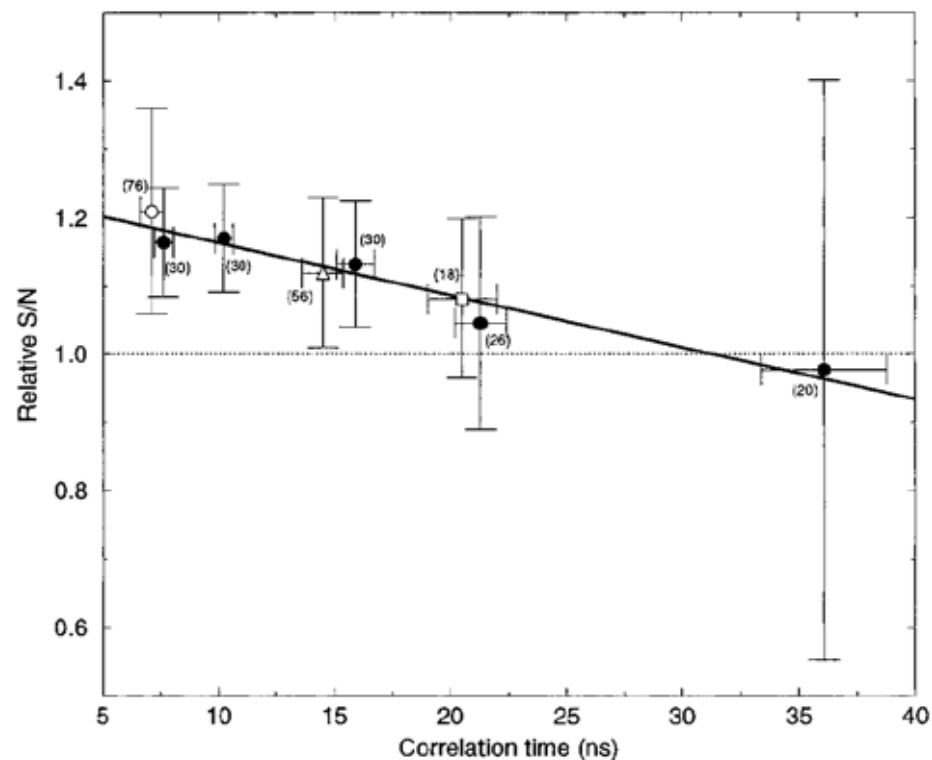
Palmer et al. (1991), *J. Magn. Reson.* 93, 151

Kay et al. (1992), *JACS*, 114, 10663

Shan et al. (1996), *JACS*, 118, 6570

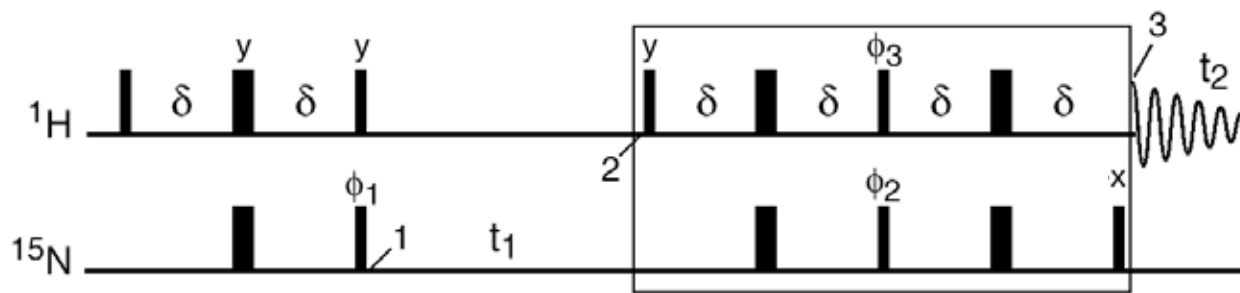
Additional delay: some relaxation losses

Simultaneously transfers $N_x \rightarrow H_y$ and $N_y \rightarrow H_x$

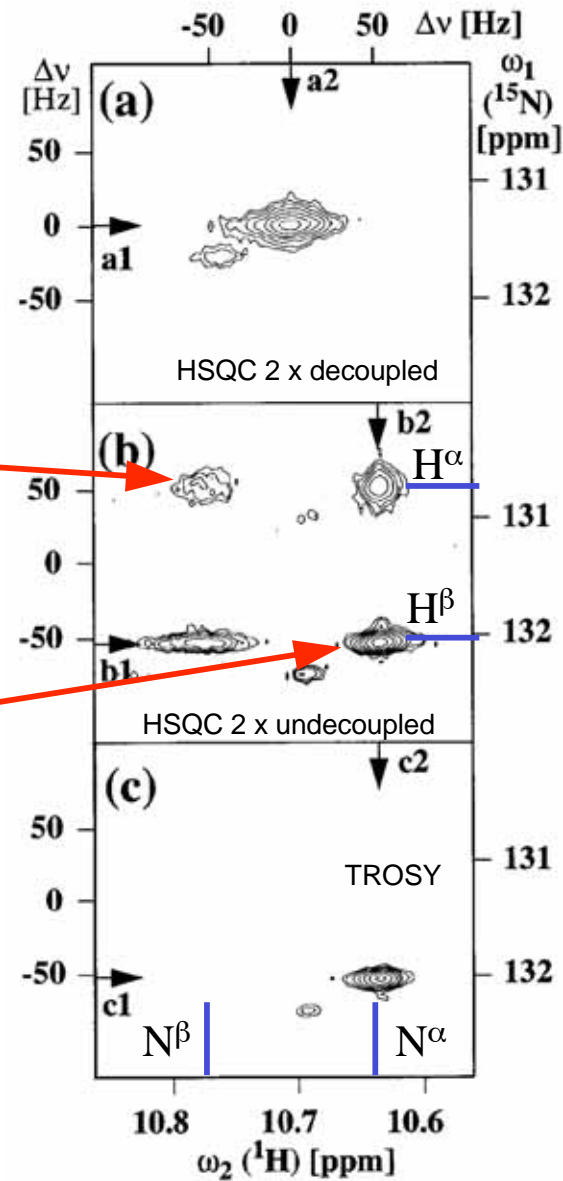


PERVUSHIN, RIEK, WIDER, WÜTHRICH,
PNAS, 1997, 94, 12366

¹⁵N-HSQC-TROSY



Proc. Natl. Acad. Sci. USA 94 (1997)

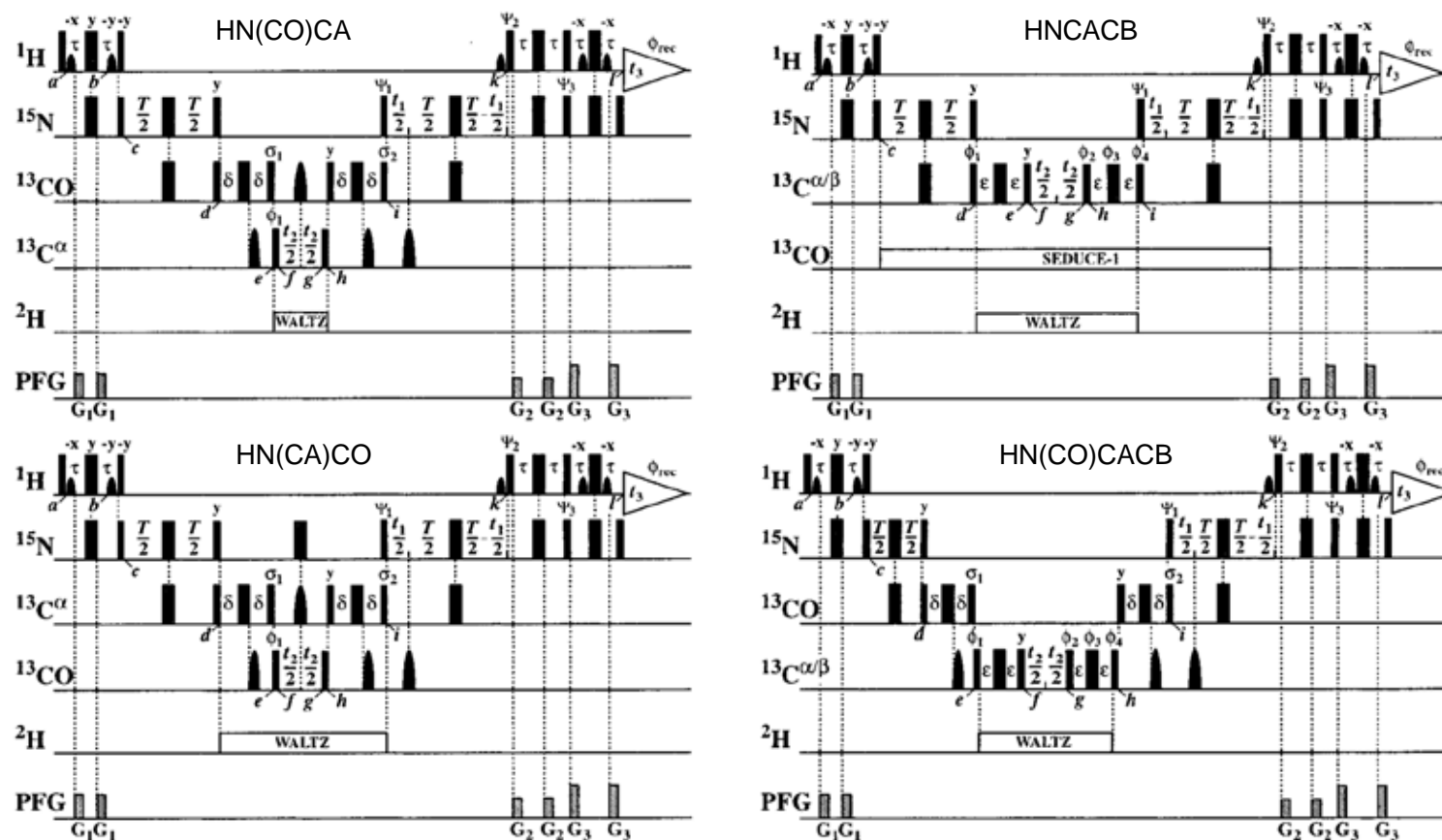


	(2)	TROSY	(3)
(I)	Nx	→	-/+ 2HyNz
(II)	2NxHz	→	+/- Hy
(III)	Ny	φ ₃ = +/-x	-Hx
(IV)	2NyHz	φ ₂ = +/-y	2HxNz
(I+II)	NxHα	→	+/- HyNβ
(I-II)	NxHβ	→	-/+ HyNα
(III+IV)	NyHα	→	-HxNβ
(III-IV)	NyHβ	→	-HxNα

relaxes with rate ~ (c+d)²

relaxes with rate ~ (c-d)²

c: CSA-constant
d: dipolar constant



Salzmann et al., JACS, 1999, 121, 844

Table 1 Sensitivity Gains Obtained with ²H/¹³C/¹⁵N-Labeled Gyrase 23B When Using [¹⁵N,¹H]-TROSY in Triple Resonance Experiments

experiment	enhancement ^a		
	overall	β-sheets	α-helices
[¹⁵ N, ¹ H]-TROSY-HN(CO)CA ^b	2.3	3.1	2.6
[¹⁵ N, ¹ H]-TROSY-HN(CA)CO ^c	3.2	3.9	3.4
[¹⁵ N, ¹ H]-TROSY-HNCACB ^d	2.8	3.4	2.9
[¹⁵ N, ¹ H]-TROSY-HN(CO)CACB ^e	3.1	3.4	3.3

Salzmann et al., PNAS 1998, 95, 13585.
 Pervushin et al., J.Biomol NMR, 1998, 12, 345.
 Pervushin et al., JACS, 1998, 120, 6394.
 Salzmann et al., JACS, 1999, 121, 844.
 Salzmann et al., J Biomol NMR, 1999, 4, 85-8
 Salzmann et al., JACS, 2000, 122(31); 7543-7548: "NMR Assignment and Secondary Structure Determination of an Octameric 110 kDa Protein Using TROSY in Triple Resonance Experiments"
 Yang and Kay, J.Biomol NMR, 1999, 13, 3.
 Yang and Kay, JACS, 1999, 121, 2571.

Transverse Decay Times of $^1\text{H}^{\text{N}}$ -Coupled and -Decoupled ^{15}N Amide Resonances^a

Protein ^c	ν_{H} (MHz)	"TROSY T_2 "			
		$T_{2,\text{df}}^b$ (ms)	$T_{2,\text{uf}}^b$ (ms)	$T_{2,\text{cpd}}^b$ (ms)	$T_{2,180}^b$ (ms)
EIN-N/C/D	800	131	27	51	52
EIN-N/C/D	600	118	33	60	57
EIN-N	800	79	22	52	35
EIN-N	600	72	28	57	39
UBI-N/C/D	800	200	45	74	74
UBI-N/C/D	600	185	55	93	93
UBI-N/C	800	111	40	73	59
UBI-N/C	600	104	46	87	67
FAB-[Y]-N	800	42	12	27	18

loss of ^{15}N -
downfield
component by
proton spin flips for
protonated proteins

Kontaxis et al.
J. Magn. Reson.
143, 184-196 (2000)

^a Reported values are the apparent averaged decay constants measured over a $\tau-180^\circ-\tau$ interval, as described in the text. Random errors, based on duplicate experiments are ca. 4%.

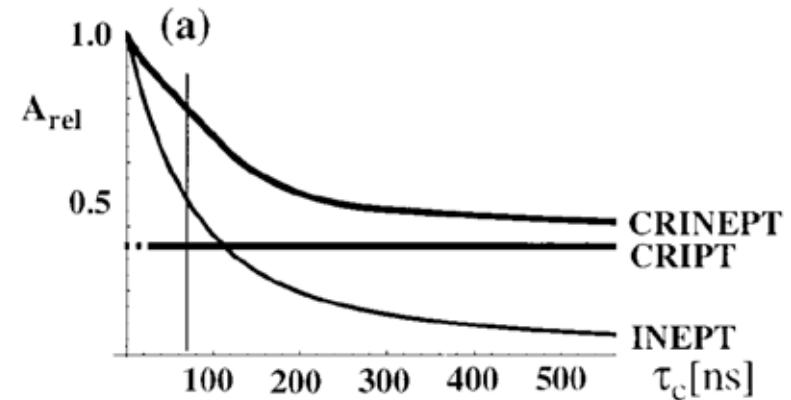
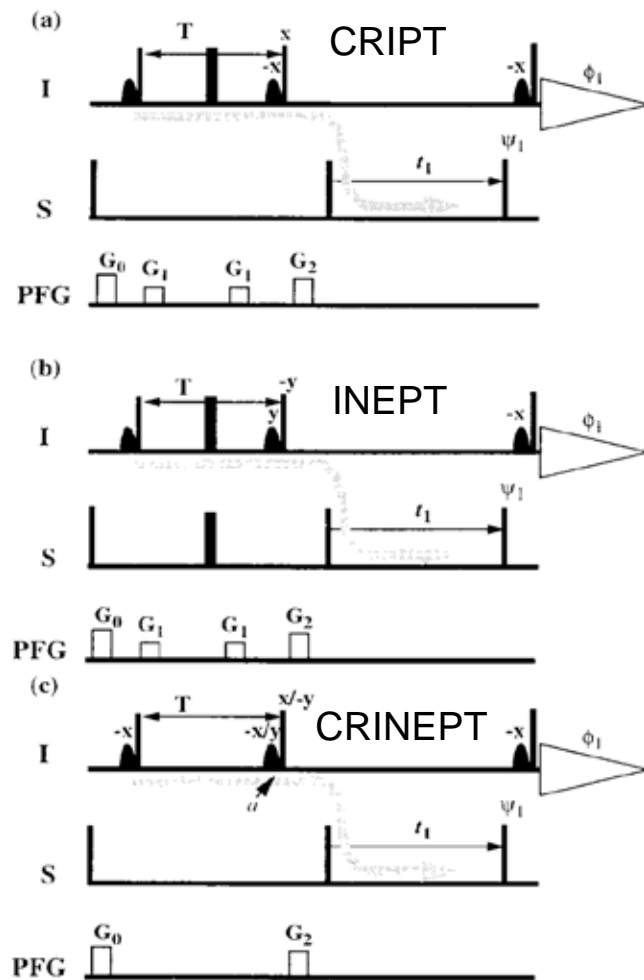
^b Transverse decay constants for the downfield ($T_{2,\text{df}}$) and upfield ($T_{2,\text{uf}}$) ^{15}N doublet components measured using HSQC-TROSY, and for the cpd-decoupled ^{15}N resonance ($T_{2,\text{cpd}}$) and the 180° (^1H) decoupled ^{15}N resonance ($T_{2,180}$).

^c EIN, N-terminal domain of Enzyme 1; UBI, ubiquitin; FAB, Fab fragment of antibody. Characters following the three-letter protein name correspond to the nuclei that were isotopically enriched. For FAB-[Y]-N, only the tyrosine residues are ^{15}N enriched.

H-N Transfer by CRIPT/INEPT

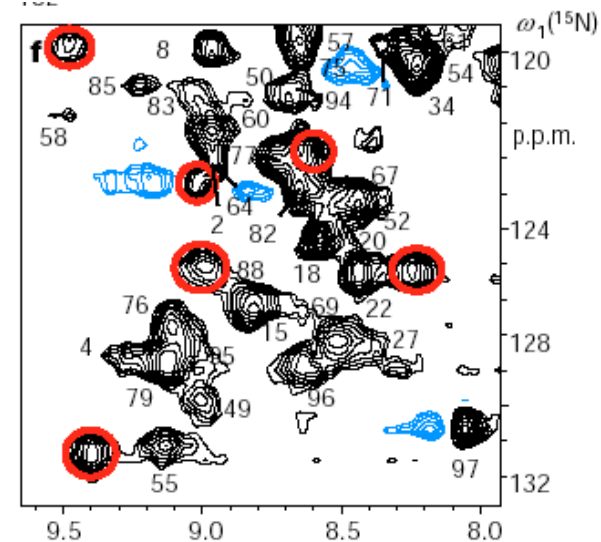
$$H_X = H_X N^\alpha + H_X N^\beta \xrightarrow{\text{relaxation}} H_X N^\alpha = 1/2 H_X + \underline{H_X N_Z}$$

Riek et al., PNAS (1999) 96, 4918;
 Dalvit, J. Magn. Reson. (1992) 97, 645



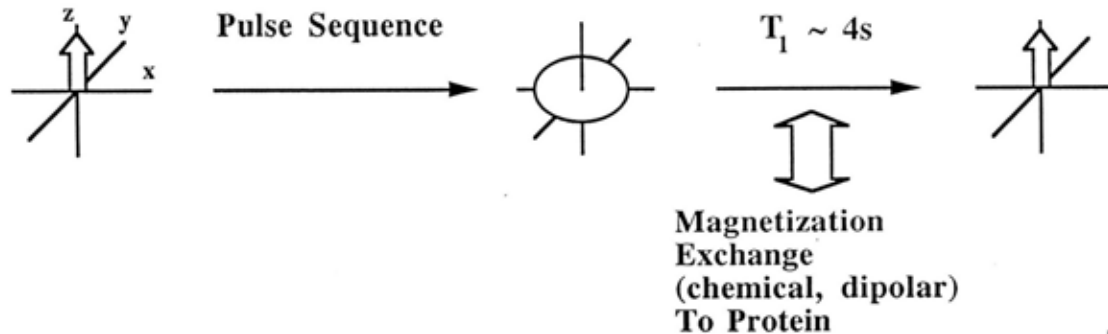
CRIP-TROSY spectrum of GroES bound to GroEL (~900 kDa)

Fiaux et al., Nature 418, (2002), pg.207

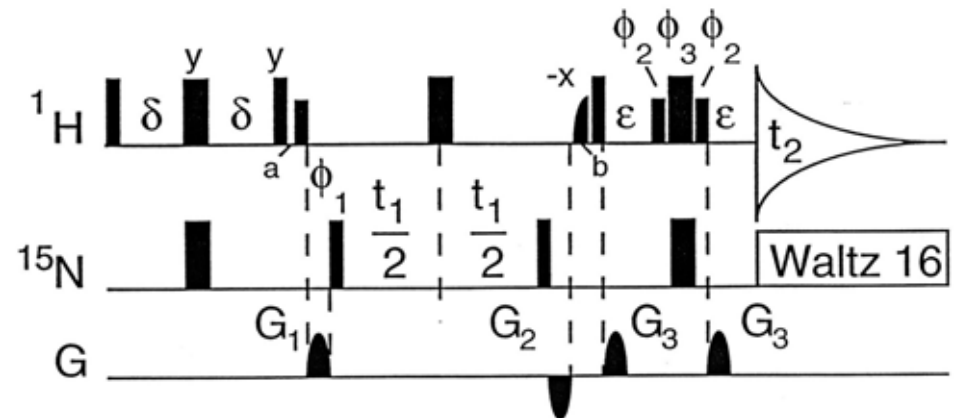
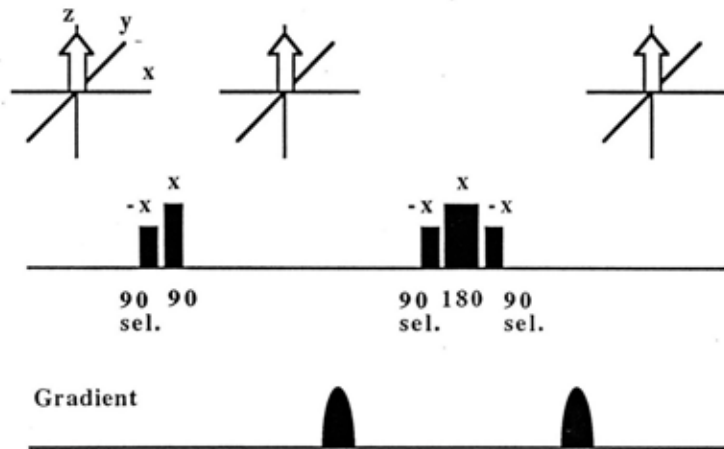


Preservation of exchangeable protein magnetization by WATER FLIP-BACK JACS (1993) 115, 12593

Water scrambling schemes



Water flip back



Water flip-back HSQC

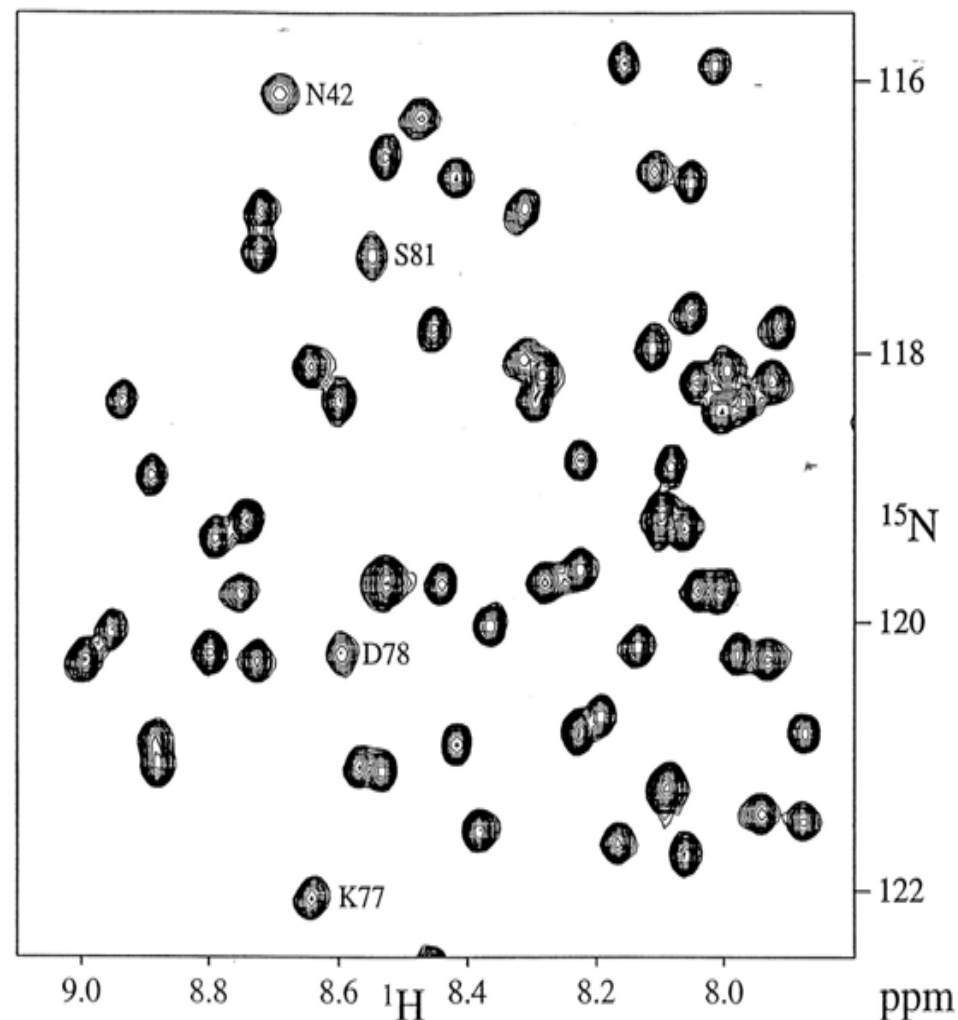
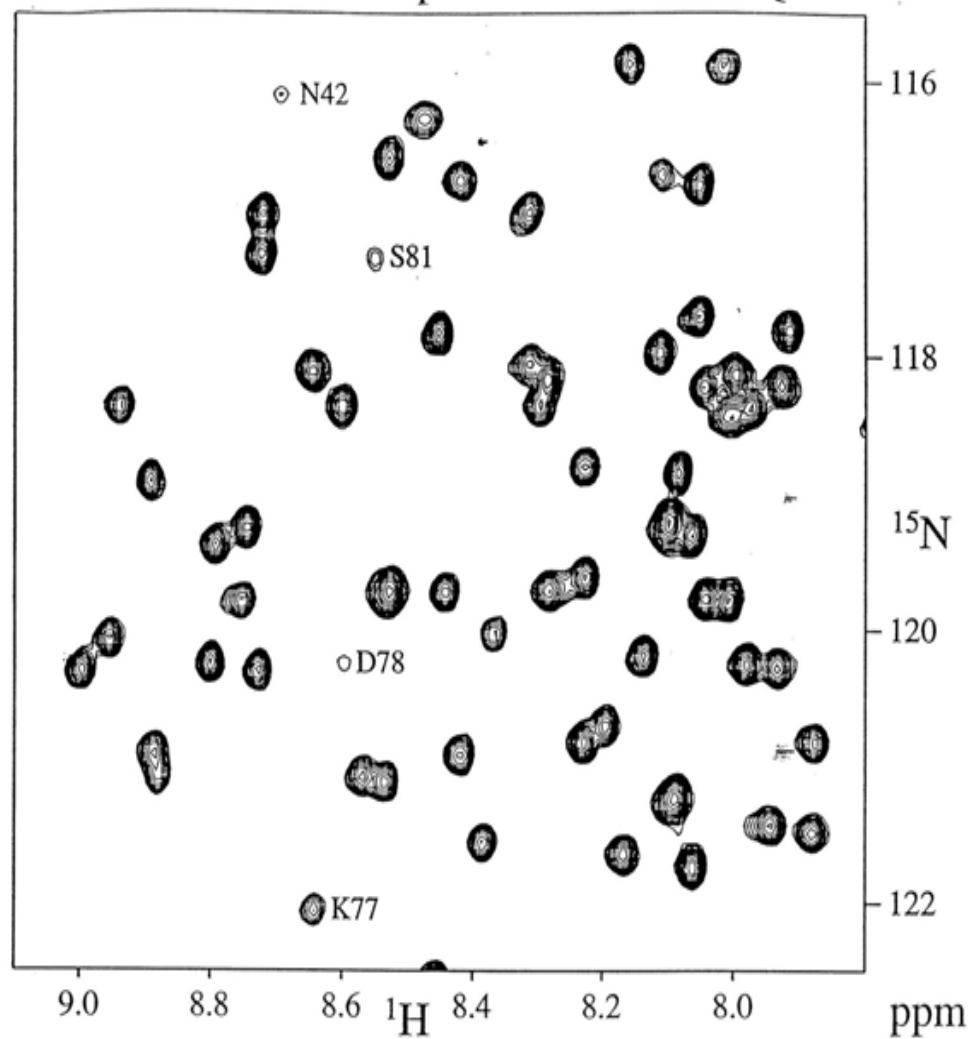
Flip-back can be put into many triple-resonance exps.

Kay et al. 1994, J. Magn. Res. A108:129

Calmodulin + M13 pH 6.6 ^1H - ^{15}N HSQC

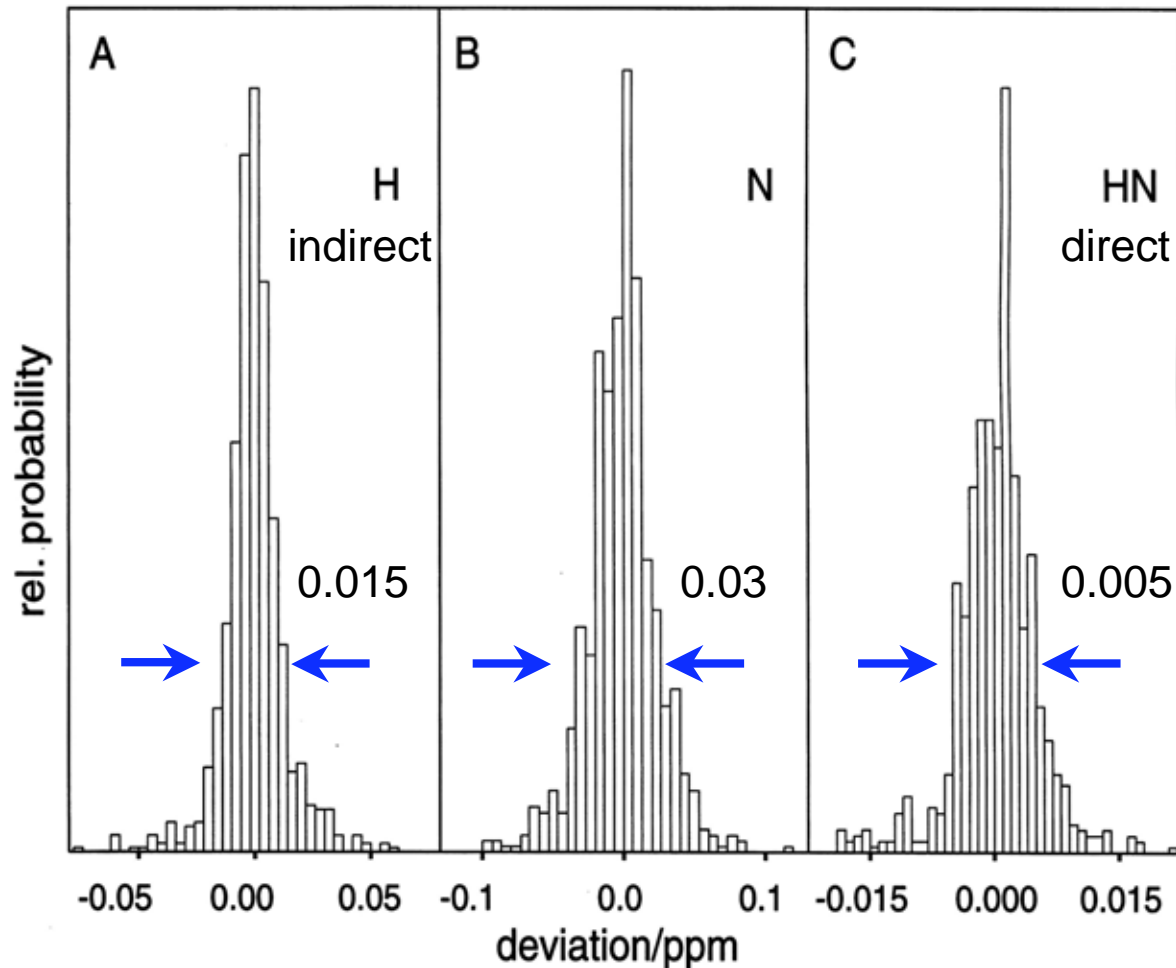
Water scrambling

Water flipback



Standard deviations (reproducibility) of the chemical shift in heteronuclear experiments

^{15}N NOESY NEF, Protein Science, 1997, 6, 1248



Nef empirical:
 deviation (Hz) \sim
 $1/(\text{"lifetime of resonance"} * 25)$

Simulation Kontaxis et al.
 JMR 143, 184-196 (2000):

$$\text{rmsd} = \frac{1}{\text{S/N}} \left(\frac{0.26}{\text{AT}} + 0.067 * R_2 \right)$$

e.g. $R_2 = 1/13$ ms, AT = 55 ms, S/N = 3 : 1
 \Rightarrow rmsd = 3 Hz $\hat{=}$ 0.005 ppm

Fig. 1. Histogram of the relative probability of deviations from the mean frequency of assigned peaks, corresponding to individual nuclei for the ^{15}N -edited NOESY spectrum of NEF $^{\Delta 2-39, \Delta 159-173}$. A: Deviations of the assigned ^1H frequencies in the indirect dimension. B: Same as A, for ^{15}N dimension. C: Same as A for directly detected $^1\text{H}^{\text{N}}$ dimension.

Perpendicular strip plots from 3-D experiments

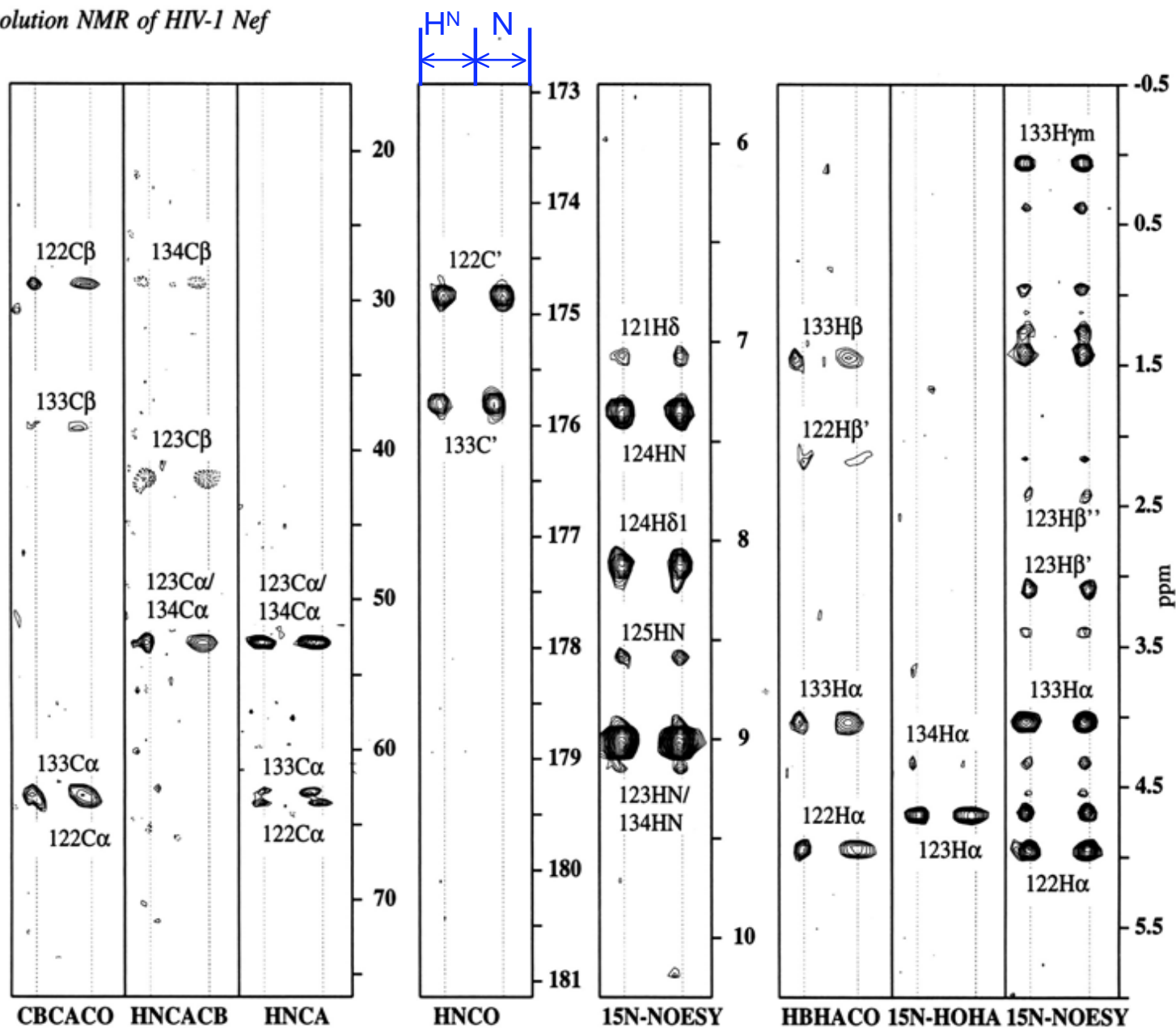


Fig. 2. Orthogonal strip plots (see text) for the backbone assignment experiments extracted from the three-dimensional data cubes at the ^1H - ^{15}N amide frequency pair of D123 of NEF^{D2-39}. Individual experiments are marked at the bottom of each strip. The strip plots have a width of 0.15 ppm in the ^1H dimension (left side of strips), and of 1.2 ppm in the ^{15}N dimension (right side of strips). Vertical axes correspond to $^{13}\text{C}^\alpha/^{13}\text{C}^\beta$ frequencies for CBCA(CO)NH, HNCACB, and HNCA, to $^{13}\text{C}'$ frequencies for HNCO, and to ^1H frequencies for the ^{15}N -edited NOESY, HBHA(CO)NH and ^{15}N -edited HOHAHA experiments, respectively.

How many dimensions does one really need?

Every additional dimension results in:

- sensitivity loss:
 - $1/\sqrt{2}$ for every additional dimension (without Rance/Palmer/Kay trick)
 - loss for additional magnetization transfer (not always): e.g. 3D HNCA and HN(CA)HA vs. 4D HNCAHA, 3D N15-NOESY vs. 4D N15/C13-NOESY
- resolution loss (almost always): e.g. two 3Ds with the same sensitivity, but with much higher resolution can be recorded in the same time as one 4D:

$$4D: \begin{matrix} H\beta & C\beta & 15N & HN \\ 8^* & \times 8^* & \times 32^* & \times TD^* \end{matrix}$$

(* is complex number of points)

$$3D: 64^* \quad \times \quad 32^* \quad \times \quad TD^*$$

$$3D: \quad 64^* \quad \times \quad 32^* \quad \times \quad TD^*$$

More dimensions are useful

- when there is overlap, and the higher dimensionality spectrum is not limited in resolution and sensitivity
 - 4D not useful in CBCACONH-type assignment exps. of smaller proteins
 - 4D useful in CBCACONH-type assignment exps. of very large # residue proteins, e.g. 723-residue Malate Synthase G, Tugarinov et al. J. Am. Chem. Soc.; 2002; 124; 10025.
 - 4D sometimes useful for NOESY experiments, but sensitivity can be a problem

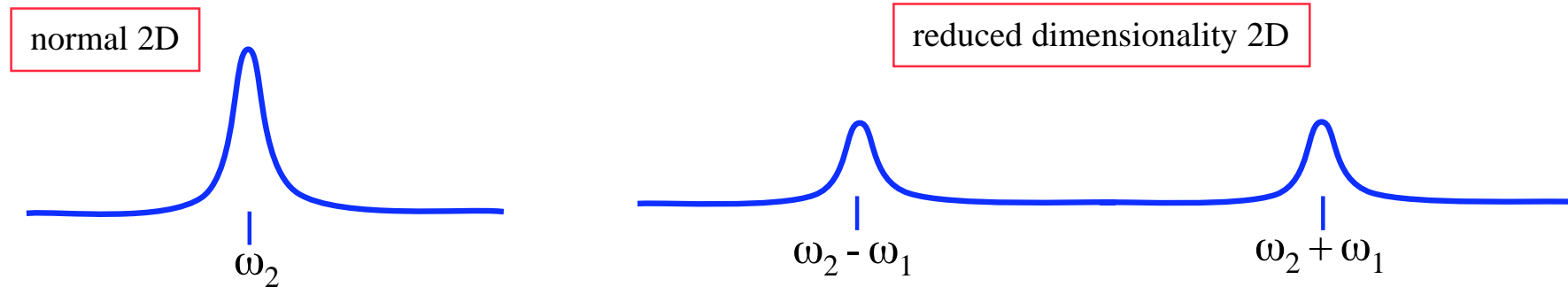
Reduced dimensionality?

Principle:

record $\cos(\omega_1 t_1) * \exp(i \omega_2 t_2) * \exp(i \omega_3 t_3)$, with t_1 and t_2 incremented simultaneously

=>

- 2 dimensions instead of 3
- cosine-modulation gives signals at $\omega_2 \pm \omega_1$ (peaks are split in two)



- signal weaker by factor of 2 compared to normal 2D
- signal weaker by factor of $\sqrt{2}$ compared to normal 3D which records $\exp(i \omega_1 t_1) * \exp(i \omega_2 t_2) * \exp(i \omega_3 t_3)$ and where t_1 and t_2 are incremented independently.

Szyperski et al. J. Am. Chem. Soc. (1993) 115, 9307-9308, ...

G-transform Kim+Szyperski, J. Am. Chem. Soc. (2003) 125, 1385-1393

Experiments for Backbone Assignments and Secondary Structure

Protonated Proteins

experiment	labelling		
	¹⁵ N	¹³ C	S/N
¹⁵ N-separated HOHAHA	+	-	±
¹⁵ N-separated NOESY	+	-	±
HNCO	+	+	++
HNCA	+	+	++ ¹⁾
HCACO	+/-	+	++
HN(CO)CA	+	+	++ ¹⁾
HN(COCA)HA	+	+	++ ¹⁾
CBCA(CO)NH	+	+	+
HBHA(CO)NH	+	+	+
HNCACB/CBCANH	+	+	±
HN(CA)CO	+	+	±
HN(CA)HA	+	+	±

¹⁾ when you are desperate for S/N, and CBCA(CO)NH, HBHA(CO)NH, HNCACB don't work well enough

Deuterated Proteins (H^N reprotated)

experiment	labelling		
	¹⁵ N	¹³ C	S/N
¹⁵ N-separated NOESY	+	-	++
HNCO	+	+	++
HNCA	+	+	++ ¹⁾
HN(CO)CA	+	+	++ ¹⁾
HNCACB	+	+	+
HN(CO)CACB	+	+	+
HN(CA)CO	+	+	++

¹⁾ when you are desperate for S/N, and HNCACB, HN(CO)CACB don't work well enough

NEF, Protein Science, 1997, 6, 1248

Table 2a. *Assignment experiments*^a

Experiment	Sample ^b	Time (h)	Acquisition times (ms)			No. of constraints ^c
HOHAHA15N ^d	1	35	15.4 (H)	39.6 (N)	55.3 (HN)	
HOHAHA12C ^e	4	2	50.4 (H1)	145.1 (H2)		
NOESY12C ^f	4	15	51.0 (H1)	141.3 (H2)		
HNCA ^g	2, 8	33	11.0 (CA)	26.8 (N)	55.3 (HN)	
HNCACB ^h	2, 6	83	7.2 (CACB)	26.8 (N)	55.3 (HN)	
HNCO ⁱ	2	14	49.6 (CO)	26.3 (N)	55.3 (HN)	
HBHACO ^j	2	63	13.0 (HAHB)	19.8 (N)	55.3 (HN)	
CBCACO ^k	2,6,8	62	6.2 (CACB)	19.8 (N)	55.3 (HN)	133
CH3COSY ^l	4	12	12.8 (C1)	25.8 (C-MET)	52.6 (H-MET)	
CH3DIPSI ^m	4	46	6.2 (C)	25.6 (C-MET)	79.8 (H-MET)	

Total time (all exps.) ~ 51 d => 7 structures/year/conventional instrument

Cryoprobe increase in S/N ~ 2 => 28 structures/year/cryoprobe instrument

1. Building a 3D HNCO from scratch:

a) sketch a pulse sequence that achieves the following magnetization transfer steps by INEPT intervals and RF pulses (Grzesiek and Bax, *J. Magn. Reson.* 1992, 96, 432-440):

$H_Z^N \rightarrow -H_Y^N(1) \rightarrow H_X^N N_Z(2) \rightarrow H_Z^N N_Y(3) \rightarrow -H_Z^N N_X C'_Z(4) \rightarrow -H_Z^N N_Z C'_Y(5) \rightarrow -H_Z^N N_X C'_Z(6) \rightarrow -H_Z^N N_Y(7) \rightarrow H_Y^N N_Z(8) \rightarrow -H_X^N(9)$ [acquire H^N /decouple N]

b) determine the "optimal" INEPT transfer times as $0.8/(2J)$ between points 1/2, 3/4, 4/6, 6/7, and 8/9 (see lecture notes for J-couplings)

c) how can a carbonyl evolution period be introduced? Which J-couplings are active during the evolution period? How can they be decoupled?

d) introduce a constant-time nitrogen evolution period in the interval 3/4. Which J-couplings are being reintroduced? How can they be decoupled?

e) introduce a minimal phase cycle, i.e. select for transverse nitrogen magnetization at point 3 and transverse carbonyl at point 5. How can quadrature detection be implemented?

f) calculate the relative intensity of term 9 as compared to term 1 according to the INEPT transfer functions and the T_2 s in the hand-out (neglect longitudinal magnetization).

g) H^N spin flips occur in the 100 ms range and act as a relaxation mechanism between points 3 and 7. A better sequence can be achieved by refocusing the proton magnetization in the interval 3/4 ($H_Z^N N_Y \rightarrow -N_X$), subsequent proton decoupling, and dephasing again to proton antiphase magnetization between points 6 and 7 ($N_X \rightarrow H_Z^N N_Y$). How can this be achieved? What must be done to the phases of the nitrogen pulses?

h) the pulse sequence doesn't contain any water suppression. How can water suppression be achieved? (Messerle et al., *J. Magn. Reson.* 1989, 85, 608-613; Piotto et al., *J. Biomol. NMR*, 1992, 2, 661-665; see at end of exercises)

i) water scrambling attenuates fast exchanging amide protons, if the repetition rate is faster than the T_1 of water (4s). Water flip-back can alleviate this problem (Grzesiek and Bax, *JACS* 1993, 115, 12593-12594; see lecture notes). How can it be implemented in this sequence?

j) how can gradients be used to reject unwanted magnetization pathways? (Bax and Pochapsky, *J. Magn. Reson.* 1992, 99, 638-643; see at end of exercises)

k) how can gradient sensitivity enhancement be added? (see lecture + Kay et al., 1992, *JACS*, 114, 10663)

l) how can the scheme be changed to incorporate TROSY? (see Salzman et al., 1998, *PNAS*, 95, 13585; Loria et al., 1999, *J. Magn. Reson.* 141, 180)

m) determine the initial delays for the ^{15}N - and ^{13}C -dimensions such that the first order phase correction is 0 and -180° degrees, respectively? What would the zero order phase correction be for these cases? (see lecture notes)

n) the one-bond $^1J_{NC}$ coupling is approximately -15 Hz. For hydrogen bonded amides, couplings across hydrogen bonds exist of the type $^3hJ_{NC}$. These couplings are in the range of

-0.2 to -0.9 Hz. How can the HNCO be modified such that the one-bond $^1J_{NC}$ couplings do not lead to transfer, but that the transfer occurs mainly across the hydrogen bonds? (Solution JACS, 1998, 121, 1601).

2. Making an HNCO into an HNCA:

- the HNCA sequence can easily be derived from the HNCO sequence by interchanging the respective frequencies. What else has to be taken into account?
- is the $C^\alpha C^\beta$ J-coupling important?
- what is the efficiency of the HNCA experiment? (refer to HNCO (f)).

3. Product operators and efficiencies for the CBCA(CO)NH:

The hand-out shows the CBCA(CO)NH sequence with parameters (Grzesiek and Bax, 1992, JACS, 114, 6291-6293). Assume a leucine spin system with a $C^\beta C^\gamma$ J-coupling of 35 Hz.

- determine the relevant operator products at points a-g for the first step of the phase cycle.
- calculate the efficiencies for all the INEPT transfers. (Assume no chemical shift evolution, no relaxation).
- take transverse relaxation into account and compare to HNCA and HNCO

4. Bloch Siegert shifts and aliphatic carbon pulses with zero excitation at the carbonyls:

A rectangular RF pulse of duration p and strength ω is applied along the x-axis at an offset δ from the resonance frequency of spin S.

- what is the direction and amplitude of the effective field that S experiences?
- assume $p = \pi/\omega$ (180° pulse on resonance) and that we have S_y magnetization. Choose the strength of the RF field ω such that S goes through one 360° rotation during the duration of the pulse. What is the value of p for $\omega = 2\pi * 150 * (177-56)$ Hz? How do those numbers and formulae change for a 90° or arbitrary flip-angle pulse on resonance?
- during the duration p of the pulse, S precesses faster around the effective field axis than it would in the absence of the RF-field. Calculate the resulting change in phase for S. This is the famous Bloch-Siegert phase shift.

5. Analysis of artifacts in an HCACO (courtesy Rolf Boelens and Geerten Vuister):

In the handout the pulse sequence of the HCACO experiment is shown (Grzesiek and Bax, 1993, J. Magn. Reson. B, 102, 103-106). Using product operators we start at point a with antiphase C^α magnetization $C^\alpha_y H^\alpha_z$.

- assume there is no t_1 evolution, but only active $C^\alpha C'$ and $C^\alpha C^\beta$ J-couplings. Calculate the operators at point b.
- the phase cycle of ϕ_7 selects for coherences containing C'_z at b. Assume $\phi_6 = y$, $\phi_7 = x$ and that the C^α pulses are also active at the C^β frequencies. Calculate the operators at point c.
- evaluate the effect of the $C^\alpha H^\alpha$, $C^\beta H^\beta$, $C^\beta C^\gamma$ J-couplings during t_2 . What multiplet structure does $C^\alpha_y H^\alpha_z C'_y C^\beta_x$ have?
- at point d, the 90° pulses are given with $\phi_9 = y$, $\phi_{10} = x$. Verify that $C^\alpha_y H^\alpha_z C'_y C^\beta_x$ of point c is refocused into observable magnetization during the remainder of the sequence ($\phi_{12} = x$).
- evaluated the effect of setting $\phi_9 = x$, $\phi_{12} = y$.

NOTES

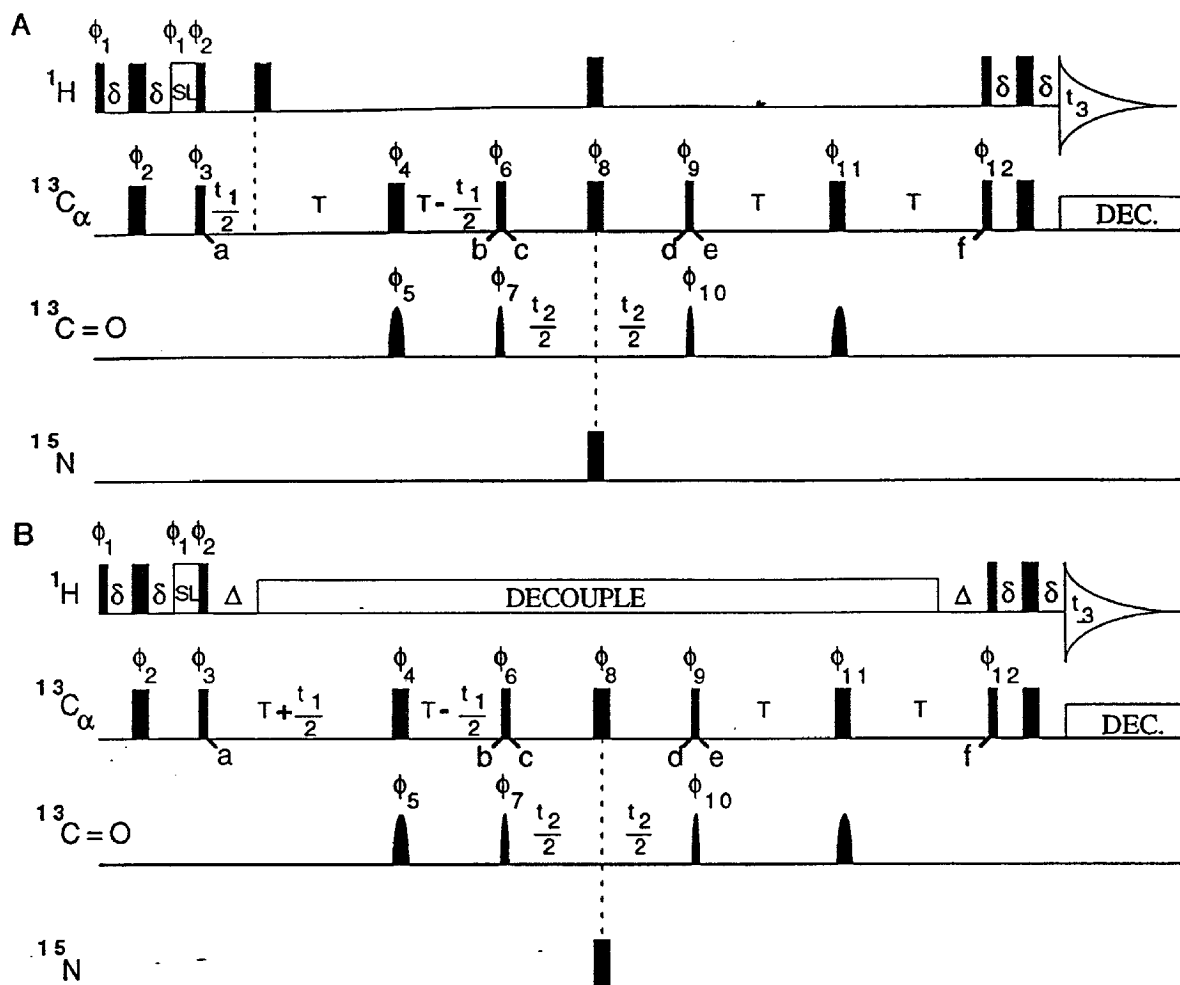


FIG. 1. Pulse schemes of the CT-HCAEO experiment. Narrow and wide pulses correspond to 90° and 180° flip angles, respectively. Pulses for which the phase is not indicated are applied along the x axis. The carrier is set to the HDO frequency for the proton pulses, to 56 ppm for the $^{13}\text{C}\alpha$ pulses, to 177 ppm for the carbonyl pulses, and to 116.5 ppm for the ^{15}N pulses. The power of the 90° and 180° $^{13}\text{C}\alpha$ pulses is adjusted such that they do not excite the ^{13}CO nuclei (i.e., 4.7 and 10.5 kHz RF field for 150.9 MHz ^{13}C frequency, respectively). Carbonyl pulses have a shaped amplitude profile, corresponding to the center lobe of a $\sin x/x$ function and a duration of 245 μs for both the 90° and the 180° pulses. Carbon decoupling during acquisition is achieved using WALTZ-16 modulation with a 3.4 kHz RF field. The proton spin-lock pulse, SL, is applied for a duration of 1.8 ms and serves to suppress the intense HDO resonance. Delay durations are $\delta = 1.5$ ms, $\Delta = 3.3$ ms, and $T = 3.5$ ms. In sequence B, signals from glycine residues are absent for $\Delta = 3.3$ ms. Phase cycling for scheme A is as follows: $\phi_1 = y$; $\phi_2 = x, -x$; $\phi_3 = x$; $\phi_4 = 8(x'), 8(y'), 8(-x'), 8(-y')$; $\phi_5 = 8(x), 8(-x)$; $\phi_6 = 4(y), 4(-y)$; $\phi_7 = x, x, -x, -x$; $\phi_8 = 4(x), 4(-x)$; $\phi_9 = x$; $\phi_{10} = x, -x$; $\phi_{11} = x'$; $\phi_{12} = y$; Receiver = $2(x), 4(-x), 2(x), 2(-x), 4(x), 2(-x)$. For scheme (B), the phase cycling is as above, except for $\phi_6 = 4(x), 4(-x)$ and $\phi_9 = y$. For a pure cosinusoidal t_1 modulation, the phase ϕ_4 needs to be adjusted relative to the phases of the 90° $^{13}\text{C}\alpha$ pulses in order to compensate for Bloch-Siegert-induced phase errors (9) caused by the carbonyl 180° pulses and for phase changes caused by the change in RF power level between the 90° and 180° $^{13}\text{C}\alpha$ pulses. For optimal sensitivity, the phase ϕ_{11} requires the same adjustment. In practice, this amounted to a rotation of 4° on our AMX-600 spectrometer. Quadrature in the t_1 and t_2 domains is obtained by changing the phases ϕ_3 and ϕ_7 , respectively, in the usual States-TPPI manner (14).

Grazesich & Bax J. Magn. Reson. 9, 1993, 102, 103-106.

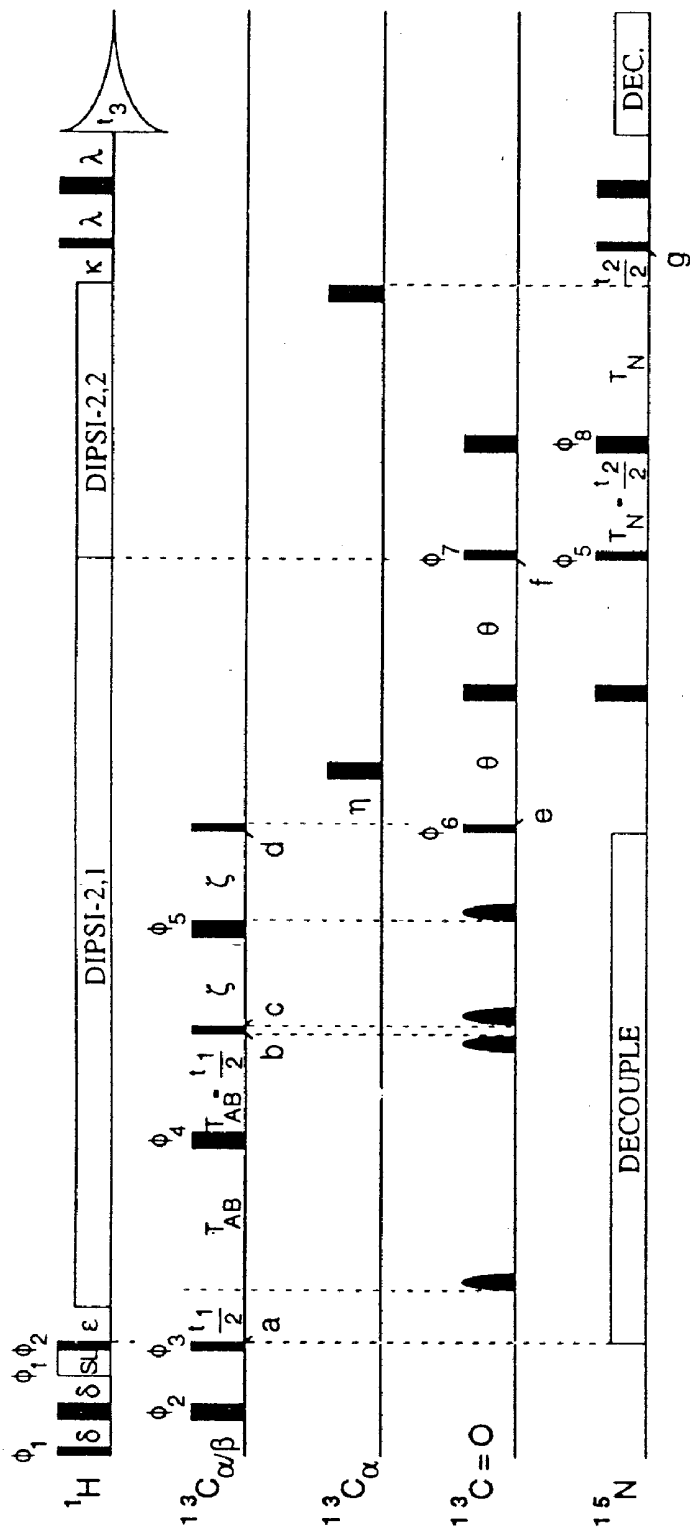
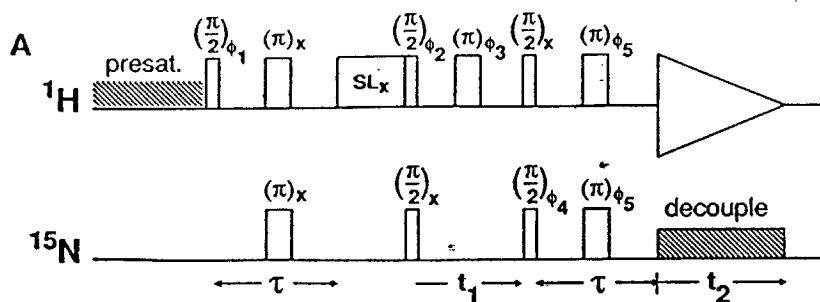


Figure 1. Pulse scheme of the CBCA(CO)NH experiment. Narrow pulses correspond to a 90° flip angle and wider pulses to 180° . Pulses for which no phase is indicated are applied along the x axis. The ^1H carrier is placed at 4.75 ppm until the 90° CO pulse is applied. After this time the ^1H carrier is switched to 8.1 ppm. The $\text{C}_{\alpha/\beta}$ carrier is positioned at 46 ppm and the power of the RF pulses is adjusted to yield zero excitation in the CO region (11.4-kHz RF for the 180° and 5.1-kHz RF for the 90° pulses at 151-MHz ^{13}C frequency). C_{α} pulses are applied at 56 ppm, using an RF field of 10.5 kHz. Rounded carbonyl pulses have a 180° flip angle and have the shape of the center lobe of a $\sin x/x$ function and a duration of 202 μs . The second and third shaped CO pulses serve to compensate the $\text{C}_{\alpha/\beta}$ phase errors caused by Bloch-Siegert effects¹⁰ related to the first and fourth shaped pulse (see text). The rectangular CO pulses are applied using an RF field strength of 4.7 kHz, yielding minimal excitation of the C_{α} resonances. All ^{15}N pulses are applied with the carrier at 117 ppm, using a 6-kHz RF field. ^{15}N decoupling was accomplished using low power (1.5-kHz RF) WALTZ decoupling. ^1H decoupling during the magnetization relay is accomplished with a DIPSI-2 scheme,¹⁸ using a 5.5-kHz RF field. Delay durations are $\delta = 1.5$ ms, $\epsilon = 2.3$ ms, $T_{AB} = 3.3$ ms, $\zeta = 3.7$ ms, $\eta = 11.4$ ms, $T_N = 11.1$ ms, $\kappa = 5.4$ ms, $\lambda = 2.25$ ms. The H_2O resonance was suppressed with the 1.8-ms purge pulse, SL. Phase cycling was as follows: $\phi_1 = y$; $\phi_2 = x, -x$; $\phi_3 = x$; $\phi_4 = 8(x), 8(y), 8(-x), 8(-y)$; $\phi_5 = 4(x), 4(-x)$; $\phi_6 = 2(x), 2(-x)$; $\phi_7 = 51^\circ$ (Bloch-Siegert phase error compensation); $\phi_8 = 8(x), 8(-x)$; Rec. = $x, 2(-x), x, -x, 2(x), 2(-x), 2(x), -x, x, 2(-x), x$. Quadrature in F_1 and F_2 is obtained by altering ϕ_3 and ϕ_5 in the usual manner.²



Messersch et al.

J. Magn. Reson. 1983, 85, 608-613

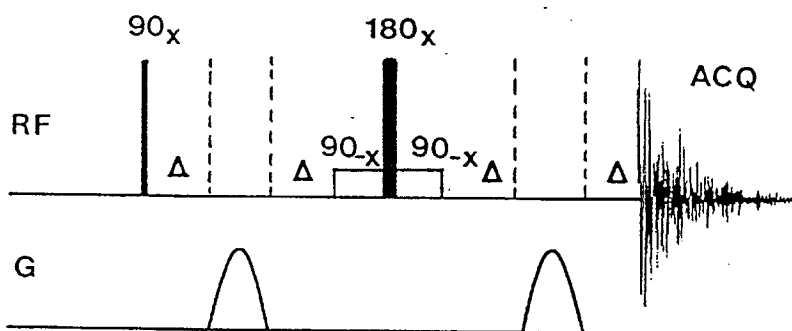


Fig. 1. Pulse scheme for gradient-tailored water suppression. The radiofrequency and field-gradient pulses are shown on separate lines. In addition to a standard non-selective spin-echo pulse pair, two selective 90° pulses with the opposite direction of rotation and two shaped magnetic field gradients are placed symmetrically to the non-selective 180° pulse. Four delays (Δ) are inserted to allow for gradient recovery. For experimental details see Fig. 2.

Pioch et al. J. Biomol NMR. 1992, 2, 661-665

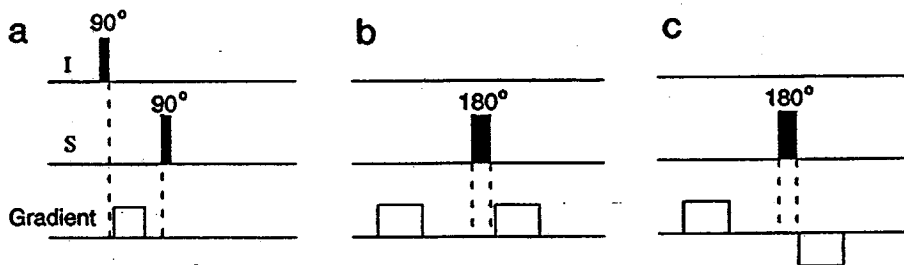
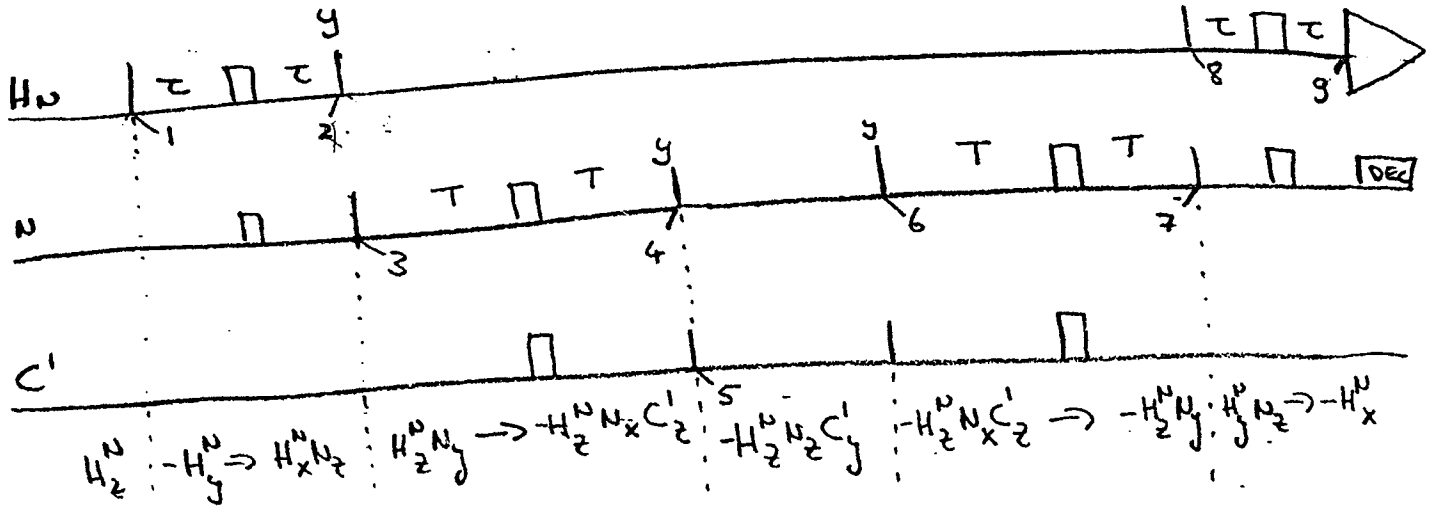
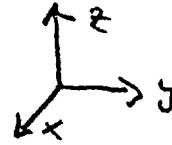


FIG. 1. Examples of different applications of pulsed field gradients in heteronuclear NMR. (a) Selection of an I_2S_z intermediate, (b) selection of transverse S -spin magnetization which is being refocused by a 180° pulse, and (c) elimination of transverse S -spin components caused by an imperfect 180° (S) decoupling pulse.

Bax + Podapsky J. Magn. Reson. 1992, 99, 638-642

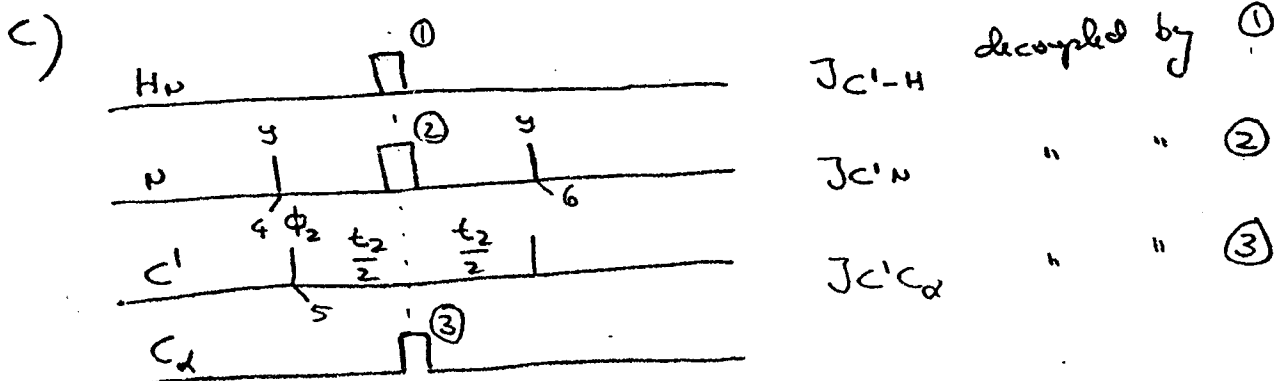
HNC0 a)



$$b) \quad 2\tau = \frac{0.8}{2J_{HN}} = \frac{0.8}{2 \times 33\text{Hz}} = 4.3\text{ms}$$

$$2T = \frac{0.8}{2J_{C'N}} = \frac{0.8}{2.15\text{Hz}} = 26.6\text{ms}$$

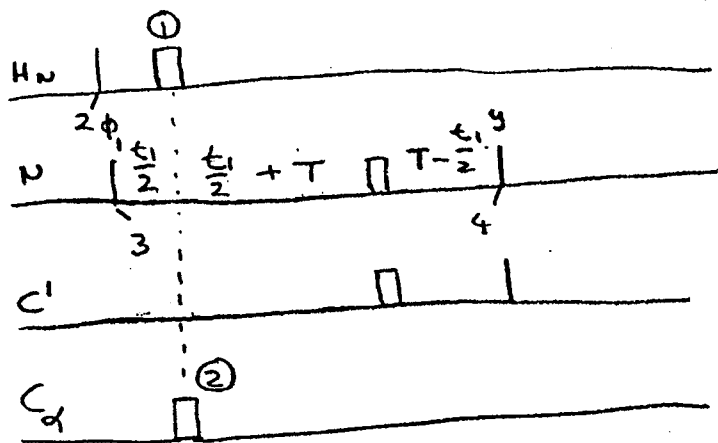
Because of T_2 -relaxation the optimal transfer is slightly shorter than $\frac{1}{2J}$



Solutions to exercises 3, 4-D NMR

(2)

HNCO d)



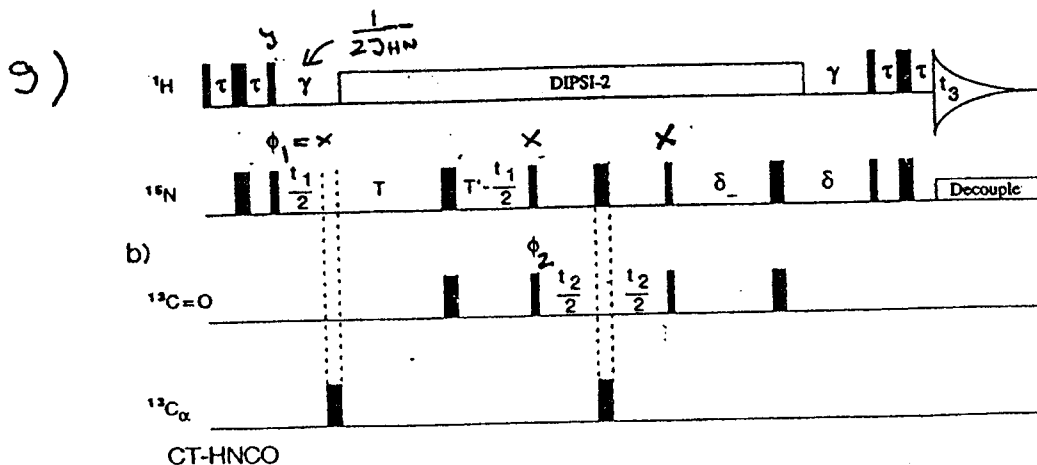
$J_{HN} + J_{NC}$.
They are decoupled by the 180s ① + ②

e) $\phi_1 = x_1 - x$ Receives $x, -x, -x, x$

$\phi_2 = x, x, -x, -x$

$\phi_1 \rightarrow x, y$
 $\phi_2 \rightarrow x, y$ } Quadrature detection { real + imaginary t_1
" " t_2

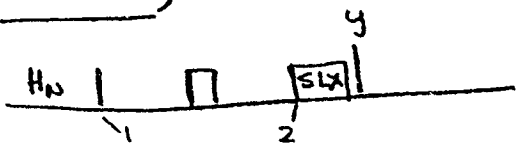
f) $S/N = \exp(-4\tau/T_2(H_N)) \cdot \exp(-4\tau/T_2(N)) \cdot \sin^2(2\pi J_{HN}\tau) \cdot \sin^2(2\pi J_{C'N}\tau)$



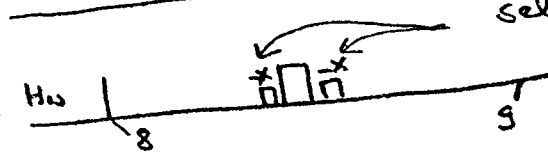
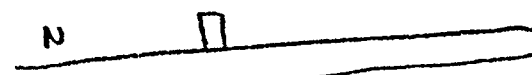
Solutions to exercises 3-, 4-D

(3)

HNCO h)

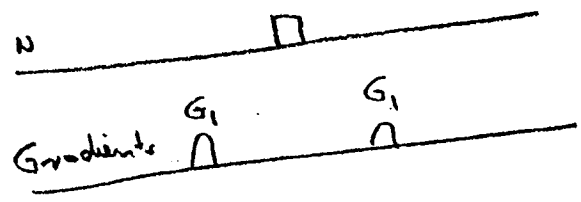


B_1 -field inhomogeneity

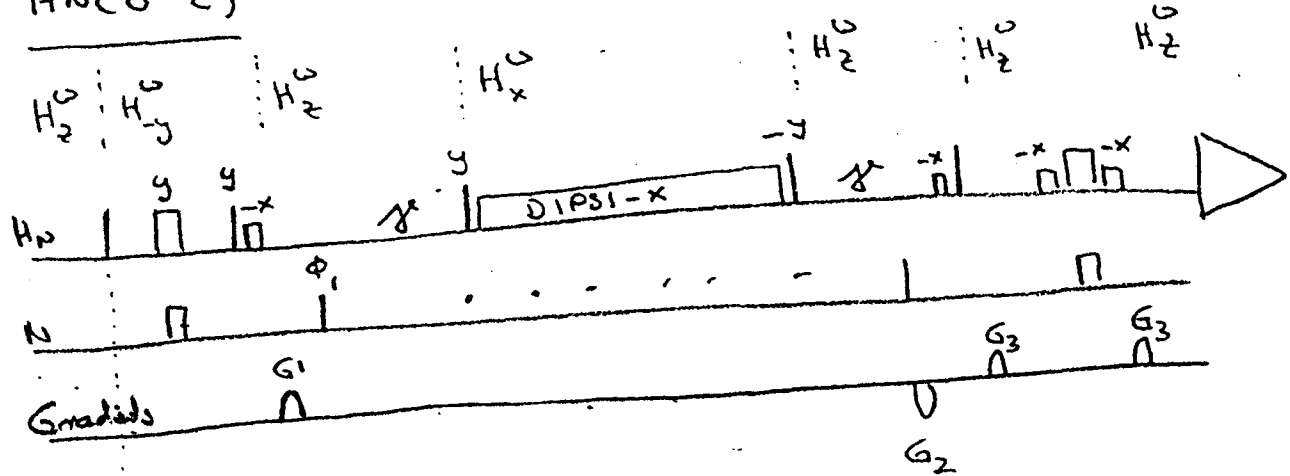


selective 90_x pulses on water

WATERGATE



HNCO i)



$C_x C'$

HNCO j)

see HNCO i) Gradients $G_1 + G_2$

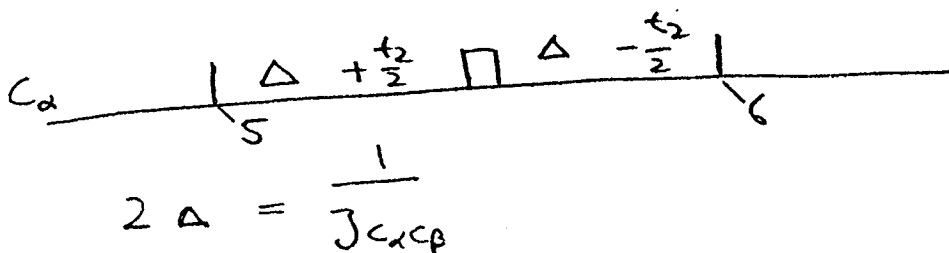
Solutions to Exercises 3-, 4-D

HNCA a) $\sqrt{S/N} \stackrel{1\text{-Bond}}{\sim} \exp(-2T/T_2(N)) \cdot \sin 2\pi \int_{NC\alpha}^1 T \cdot \cos 2\pi \int_{NC\alpha}^2 T$
 $\stackrel{2\text{-Bond}}{\sim} \exp(-2T/T_2(N)) \cdot \sin 2\pi \int_{NC\alpha}^2 T \cdot \cos 2\pi \int_{NC\alpha}^1 T$

$T = 11 \text{ ms}$ is a reasonable compromise

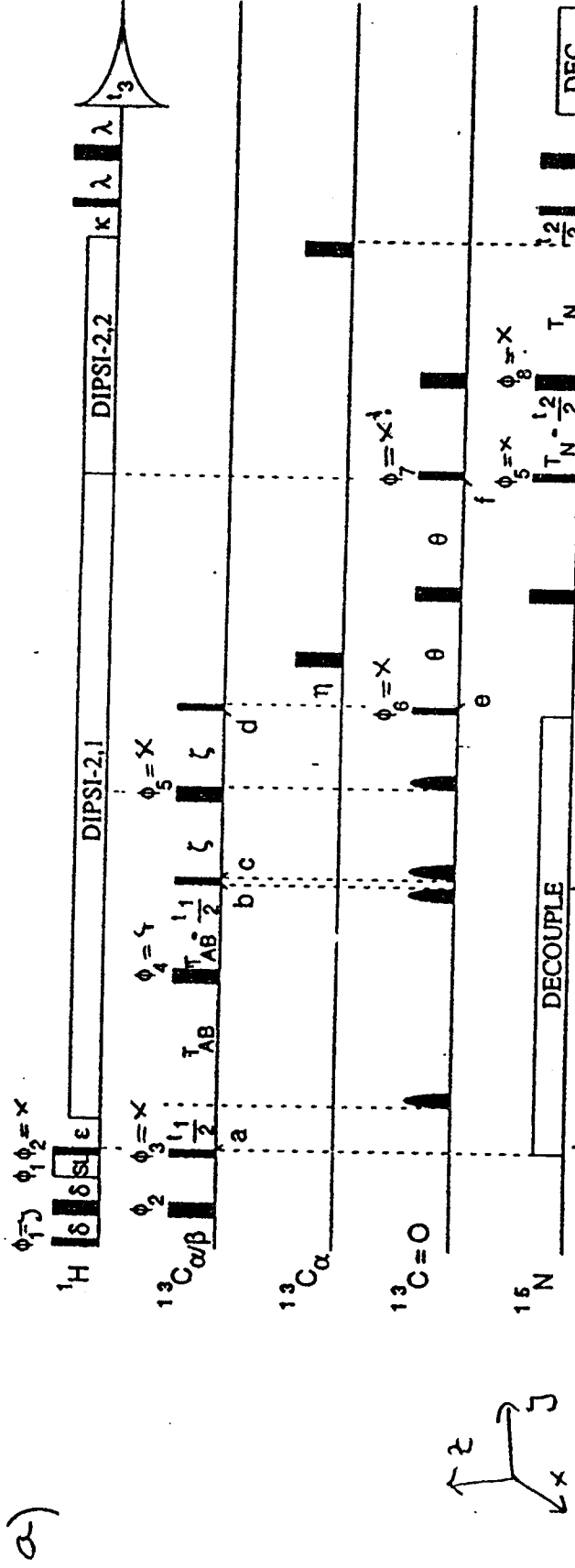
b) Since the $T_2(C\alpha)$ (10-20ms for larger proteins) is comparable to $\frac{1}{2J_{C\alpha C\beta}} = \frac{1}{2 \cdot 35 \text{ Hz}} = 14 \text{ ms}$, it is usually not desirable to collect data in the $C\alpha$ -dimension with large acquisition times than 10-12 ms. In this case $J_{C\alpha C\beta}$ is not really limiting the linewidth

c) $J_{C\alpha C\beta}$ could be decoupled by a selective 180° on $C\beta$, but not for all spin systems (e.g. Ser, Thr, $\delta C\beta = 60-70 \text{ ppm}$)
 Homonuclear $J_{C\alpha C\beta}$ can also be refocused by a constant-time $C\alpha$ -evolution period at the expense of big relaxation losses ($\exp(-2T/T_2(C\alpha))$)!



d) $S/N \stackrel{1\text{-Bond}}{=} \exp(-4T/T_2(HN)) \cdot \exp(-4T/T_2(N)) \cdot \sin^2(2\pi \int_{HN} T) \cdot \sin^2(2\pi \int_{C\alpha N} T) \cos^2(2\pi \int_{C\alpha N} T)$

Solutions to exercises 3-D, 4-D NMR



$$\begin{aligned}
 & C_x \\
 & H_A - C_\beta - H_B \\
 & C_\alpha - C_\beta - C_\gamma \\
 & H_x
 \end{aligned}$$

b)

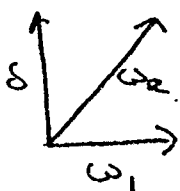
$$\begin{aligned}
 & \sin(2\pi J_{H_A C_\beta} \delta) \cdot \sin(\pi J_{H_B C_\beta} \epsilon) \cdot \cos(\pi J_{H_A C_\beta} \epsilon) \cdot \sin(2\pi J_{C_\alpha C_\beta} T_{AB}) \cdot \cos(2\pi J_{C_\alpha C_\beta} T_{AB}) \\
 & \sin(2\pi J_{C_\alpha C_\beta} \gamma) \cdot \sin(2\pi J_{C_\alpha C_\beta} \delta) \cdot \sin(2\pi J_{C_\alpha C_\beta} \epsilon) \cdot \sin(2\pi J_{C_\alpha C_\beta} \gamma) \cdot \sin(2\pi J_{C_\alpha C_\beta} \delta) \\
 & \sin(2\pi J_{C_\alpha C_\beta} T_N) \cdot \sin(\pi J_{N H_A} x) \cdot \sin(2\pi J_{N H_A} \lambda) \cdot 2K(2\beta - \text{protons})
 \end{aligned}$$

c)

$$\text{EXP} \left(-\frac{2\delta}{T_2(H_A)} - \frac{2T_{AB}}{T_2(C_\beta)} - \frac{2\theta}{T_2(C_\alpha)} - \frac{2T_N}{T_2(N)} - \frac{2\lambda}{T_2(H_B)} \right)$$

$$|S/N \sim \frac{1}{10} \ln CO$$

Aromatic carbon pulses with δ excitation of carbonyl

a)  $\omega_2^2 = \delta^2 + \omega_1^2$

b) $\omega_2 \cdot \tau_p = 2\pi$; $\tau_p = \frac{\varphi}{\omega_1}$

1. $\varphi = 180^\circ \Rightarrow \tau_p = \frac{\pi}{\omega_1}$; $\omega_2 \cdot \frac{\pi}{\omega_1} = 2\pi$

$\omega_2 = 2\omega_1$; $\omega_1^2 + \delta^2 = 4\omega_1^2$; $\omega_1 = \frac{\delta}{\sqrt{3}}$; $\tau_p = \frac{2\pi}{\delta} \cdot \frac{\sqrt{3}}{2}$

$\delta = 2\pi \cdot 150 \text{ MHz} \cdot (177 - 56) \text{ ppm} = 2\pi \cdot 18150 \text{ Hz}$

$\tau_p = \frac{1}{18150 \text{ Hz}} \cdot \frac{\sqrt{3}}{2} = 47.7 \mu\text{s} \hat{=} \omega_1 = 10473 \text{ Hz}$

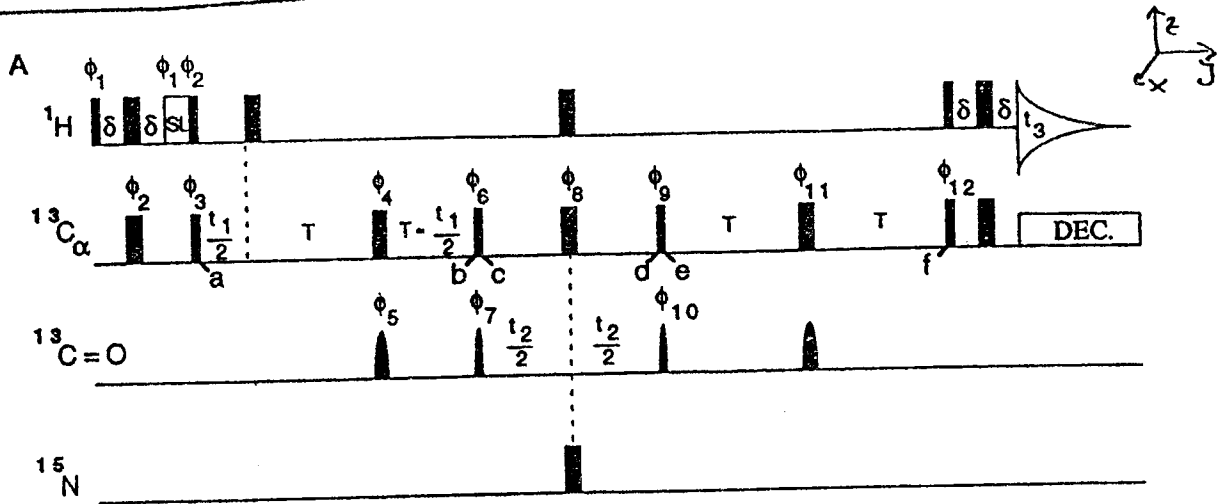
2. $\varphi = \text{arbitrary} \Rightarrow \tau_p = \frac{2\pi}{\delta} \sqrt{1 - \left(\frac{\varphi}{2\pi}\right)^2}$

c) 180° -pulse : phase change $\Delta\varphi = (\omega_2 - \delta)\tau_p$

$\Delta\varphi = \underbrace{\omega_2 \tau_p}_{2\pi} - \delta \tau_p = 2\pi \left(1 - \frac{\sqrt{3}}{2}\right) = 48^\circ$

Solutions to exercises 3, 4-D NMR

(7)



HCACO

$$\begin{aligned}
 a) \ C_y^\alpha H_z^\alpha C_z^i &\rightarrow -C_x^\alpha H_z^\alpha C_z^i \sin(2\pi J_{C\alpha C^i} T) \cdot \cos(2\pi J_{C\alpha C^i} T) \\
 &\quad - C_y^\alpha H_z^\alpha C_z^i C_x^\beta \sin(2\pi J_{C\alpha C^i} T) \cdot \sin(2\pi J_{C\alpha C^i} T) \\
 &\quad + \text{Products not containing } C_z^i \approx \cos(2\pi J_{C\alpha C^i} T)
 \end{aligned}$$

$$\begin{aligned}
 b) \ -C_x^\alpha H_z^\alpha C_z^i &\rightarrow -C_z^\alpha H_z^\alpha C_y^i \\
 -C_y^\alpha H_z^\alpha C_z^i C_x^\beta &\rightarrow C_y^\alpha H_z^\alpha C_y^i C_x^\beta
 \end{aligned}$$

$$c) \ -C_x^\alpha H_z^\alpha C_z^i \xrightarrow{t_2} -C_z^\alpha H_z^\alpha C_y^i \cos(\Omega_{C^i} t_2)$$

$$\begin{aligned}
 C_y^\alpha H_z^\alpha C_z^i C_x^\beta \xrightarrow{t_2} & C_y^\alpha H_z^\alpha C_z^i C_x^\beta \cos(\Omega_{C^i} t_2) \cdot \\
 & \cos(\pi J_{H\alpha C^i} t_2) \cdot \cos(\pi J_{H\beta C^i} t_2) \cdot \cos(\pi J_{C^i C^i} t_2)
 \end{aligned}$$

$n = \# \beta\text{-protons}, m = \# \gamma\text{-carbons}$

HCACO c)

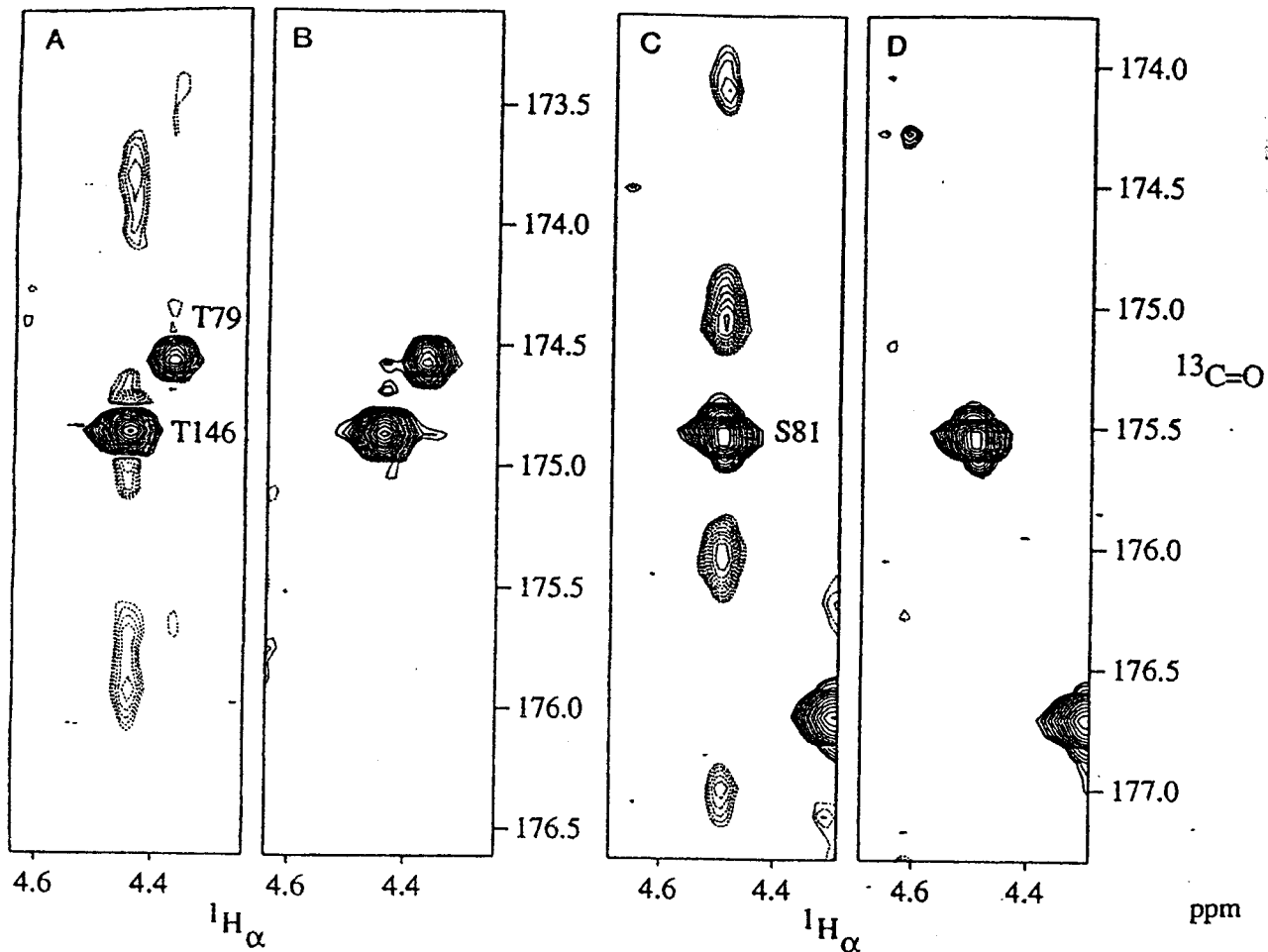
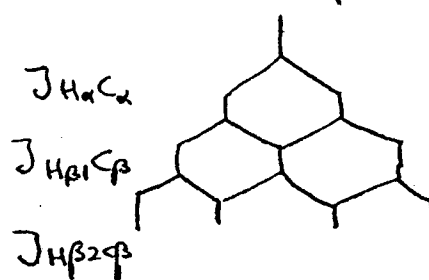
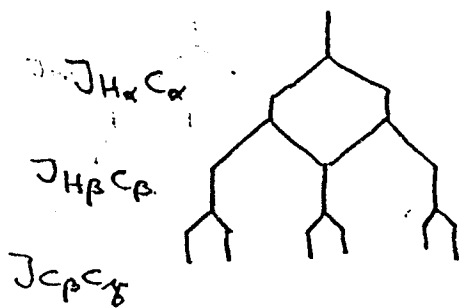
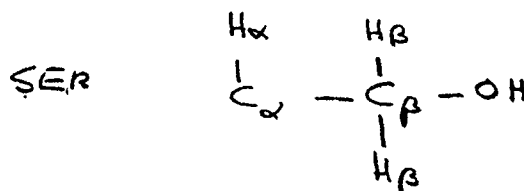
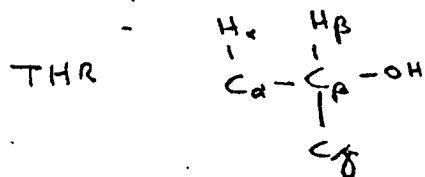


FIG. 2. Small sections of $^1\text{H}-^{13}\text{CO}$ planes of a HCACO spectrum recorded with the pulse scheme in Fig. 1A for the protein calmodulin, taken at a ^{13}C frequency of 62.6 ppm (A, B) and at 59.5 ppm (C, D). Spectra A and C have been recorded with the old phase setting of $\phi_9 = y$ and $\phi_{12} = x$ (see text), whereas spectra B and D have been recorded with $\phi_9 = x$ and $\phi_{12} = y$. Broken contours correspond to negative intensity, associated with the artifactual multiplets discussed in the text.



Solutions to exercises 3-, 4-D NMR

HCACO d)

(1, 2, or 3). At time point d , in the previously described version of the CT-HCACO experiment, the $90^\circ C^\alpha$ pulse, following the t_2 evolution period, was applied along the y axis, giving rise to

$$-C_x^\alpha H_z^\alpha C_y \xrightarrow{90_x^\circ(C'), 90_y^\circ(C^\alpha)} -C_x^\alpha H_z^\alpha C_z' \quad [4a]$$

and

$$C_y^\alpha H_z^\alpha C_x C_x^\beta \xrightarrow{90_x^\circ(C'), 90_y^\circ(C^\alpha, C^\beta)} -C_y^\alpha H_z^\alpha C_z' C_x^\beta \quad [4b]$$

After rephasing of the $^{13}C-^{13}C$ J coupling during the subsequent delay $2T$, between time points e and f , one obtains

$$-C_x^\alpha H_z^\alpha C_z' \xrightarrow{2T} -C_y^\alpha H_z^\alpha \cos(2\pi J_{C\alpha C^\beta} T) \sin(2\pi J_{C\alpha C'} T) \quad [5a]$$

$$-C_y^\alpha H_z^\alpha C_z' C_x^\beta \xrightarrow{2T} C_y^\alpha H_z^\alpha \sin(2\pi J_{C\alpha C^\beta} T) \sin(2\pi J_{C\alpha C'} T). \quad [5b]$$

The $C_y^\alpha H_z^\alpha$ terms on the right-hand side of expressions [5a] and [5b] are converted into observable H^α magnetization

HCACO e)

If the phase $\phi_9 = x$, expression [4] becomes

$$-C_x^\alpha H_z^\alpha C_y \xrightarrow{90_x^\circ(C'), 90_x^\circ(C^\alpha)} C_y^\alpha H_z^\alpha C_z' \quad [6a]$$

$$C_y^\alpha H_z^\alpha C_x C_x^\beta \xrightarrow{90_x^\circ(C'), 90_x^\circ(C^\alpha, C^\beta)} C_z^\alpha H_z^\alpha C_z' C_x^\beta \quad [6b]$$

Apart from a change in phase of the C^α transverse magnetization, which is compensated for by the concomitant phase change of ϕ_{12} , the desired pathway [6a] is not affected and gives rise to a spectrum with the same intensity cross peaks as the pulse scheme with the original phases. As can be seen from [6b], the pathway that gave rise to the spurious multiplet is suppressed by changing the phase ϕ_9 to x ; the $90_x^\circ(C^\alpha, C^\beta)$ pulse now causes a state of $zzzx$ order which cannot be transformed into observable magnetization by the final reverse INEPT scheme, applied at time f .